

This document was prepared in conjunction with work accomplished under Contract No. DE-AC09-96SR18500 with the U. S. Department of Energy.

DISCLAIMER

This report was prepared as an account of work sponsored by an agency of the United States Government. Neither the United States Government nor any agency thereof, nor any of their employees, nor any of their contractors, subcontractors or their employees, makes any warranty, express or implied, or assumes any legal liability or responsibility for the accuracy, completeness, or any third party's use or the results of such use of any information, apparatus, product, or process disclosed, or represents that its use would not infringe privately owned rights. Reference herein to any specific commercial product, process, or service by trade name, trademark, manufacturer, or otherwise, does not necessarily constitute or imply its endorsement, recommendation, or favoring by the United States Government or any agency thereof or its contractors or subcontractors. The views and opinions of authors expressed herein do not necessarily state or reflect those of the United States Government or any agency thereof.

**HANFORD SUPPLEMENTAL TREATMENT:
LITERATURE AND MODELING REVIEW OF SRS HLW
SALT DISSOLUTION AND FRACTIONAL
CRYSTALLIZATION**

A. S. Choi
G. P. Flach
C. J. Martino
J. R. Zamecnik
M. K. Harris
W. R. Wilmarth
T. B. Calloway

September 2004

Waste Treatment Technology Department
Savannah River National Laboratory
Westinghouse Savannah River Company
Savannah River Site
Aiken, SC 29808

Prepared for the U.S. Department of Energy Under Contract Number
DEAC09-96SR18500



DISCLAIMER

This report was prepared by Westinghouse Savannah River Company (WSRC) for the United States Department of Energy under Contract No. DE-AC09-96SR18500 and is an account of work performed under that contract. Neither the United States Department of Energy, nor WSRC, nor any of their employees makes any warranty, expressed or implied, or assumes any legal liability or responsibility for the accuracy, completeness, or usefulness, of any information, apparatus, or product or process disclosed herein or represents that its use will not infringe privately owned rights. Reference herein to any specific commercial product, process, or service by trademark, name, and manufacturer or otherwise does not necessarily constitute or imply endorsement, recommendation, or favoring of same by WSRC or by the United States Government or any agency thereof. The views and opinions of the authors expressed herein do not necessarily state or reflect those of the United States Government or any agency thereof.

Printed in the United States of America

**Prepared For
U.S. Department of Energy**

Key Words:

*Selective Dissolution,
Fractional Crystallization*

Retention: Permanent

**HANFORD SUPPLEMENTAL TREATMENT:
LITERATURE AND MODELING REVIEW OF SRS HLW
SALT DISSOLUTION AND FRACTIONAL
CRYSTALLIZATION**

A. S. Choi
G. P. Flach
C. J. Martino
J. R. Zamecnik
M. K. Harris
W. R. Wilmarth
T. B. Calloway

September 2004

Waste Treatment Technology Department
Savannah River National Laboratory
Westinghouse Savannah River Company
Savannah River Site
Aiken, SC 29808

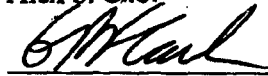


REVIEWS AND APPROVALS

AUTHOR(S):


Chris J. Martino 2-22-2005
Date

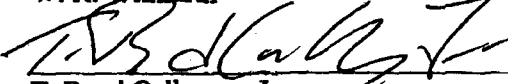

Alex S. Choi 2/10/05
Date


Greg P. Flach 2/22/05
Date

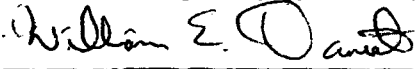

Jack R. Zamecnik 2/16/05
Date


Mary K. Harris 2/22/05
Date

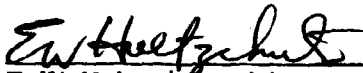

W. R. Wilmarth 2/16/05
Date


T. Bond Calloway, Jr. 2/10/05
Date

TECHNICAL REVIEWERS:


William E. Daniel 2-17-05
Date

APPROVERS


E. W. Holtzschelter, Manager, Immobilization Technology Section 2-22-05
Date


J. C. Griffin, Manager, Waste Processing Technology Section 2/22/05
Date


Kayle Boomer, CH2MHill Hanford Group, Inc. 2/9/05
Date

Table of Contents

1.0	Executive Summary	9
2.0	Introduction/Objectives.....	14
3.0	Selective Dissolution	18
3.1	SRS Salt Waste Dissolution History – Literature Review.....	18
3.1.1	Mechanical Agitation Methods.....	19
3.1.2	Density-Driven Methods.....	19
3.1.3	Issues Encountered During Dissolution.....	20
3.1.4	Selective Dissolution	21
3.2	Update on Selective Retrieval Modeling Activities at SRNL	25
3.2.1	Relationship to Selective Retrieval of Waste from Hanford’s Interim-Stabilized Tanks.....	29
4.0	Fractional Crystallization.....	31
4.1	Fractional Crystallization & Crystal Separation Literature Review	31
4.1.1	Fractional Crystallization.....	31
4.1.2	Separation Processes.....	33
4.2	AP104 Boildown Modeling Evaluation.....	37
4.2.1	Results of ESP Model.....	37
5.0	Appendix A - SRS Salt Waste Dissolution History – Annotated Bibliography	42
5.1	In-Tank Salt Removal.....	42
5.1.1	Tank 10	43
5.1.2	Tank 16 Annulus.....	43
5.1.3	Tank 17	44
5.1.4	Tank 19	44
5.1.5	Tank 20	45
5.1.6	Tank 22	46
5.1.7	Tank 24	46
5.1.8	Tank 33	46
5.1.9	Tank 37	47
5.1.10	Tank 41	47
5.1.11	Tank 49	48
5.2	Laboratory Salt Dissolution Testing and Modeling.....	48
5.2.1	Simulant Dissolution Tests	48
5.2.2	Actual-waste Dissolution Tests.....	52
5.2.3	Salt Dissolution Modeling	54
6.0	Appendix B – Fractional Crystallization & Crystal Separation Literature Review.....	58
6.1	Fractional Crystallization.....	58
6.1.1	Commercial Production of Sodium Nitrate	58
6.1.2	Design of Crystallization Systems	58
6.1.3	Metastability and Kinetically Controlled Crystallization	60
6.1.4	Effects of Impurities and pH on Crystallization	64
6.1.5	Alternative Procedure for Correlating Solubility Data	66
6.1.6	Enhanced and Alternative Crystallization Methods	66
6.1.7	Experimental and Analytical Methods.....	67

6.1.8	Commercial Crystallization Equipment Supplier	68
6.2	Separation Processes.....	69
6.2.1	Separation Method Review – Previous Literature Reviews	69
6.2.2	Conventional Crossflow Filtration.....	69
6.2.3	Centrifugal Filtration (Rotary Microfilter)	70
6.2.4	Novel Crossflow Filters	71
6.2.5	Washing in Crossflow Filtration.....	72
6.2.6	Intensified Filtration.....	72
6.2.7	Crossflow Filtration Modeling.....	73
6.2.8	Dead-End Filters	73
6.2.9	Tubular Filters.....	74
6.2.10	Centrifugal-Discharge Filter	75
6.2.11	Rotary Drum Filters	76
6.2.12	Centrifugal Methods (Perry 1997).....	78
6.2.13	Sedimenting and Filtering Centrifuges	78
6.2.14	Disk Stack Centrifuge.....	79
6.2.15	Peeler Centrifuges.....	80
6.2.16	Pusher Centrifuges	81
6.2.17	Decanter Centrifuges	81
6.2.18	SRNL Centrifuge Tests.....	84
6.3	References for Crystallization/Separation	84
6.3.1	Bibliography of Selected DOE Crossflow Filtration References	88
6.3.2	Bibliography of Selected Publications.....	94
7.0	Appendix C - OLI Modeling for AP104.....	99
7.1	ESP Modeling	99
7.2	Feed Composition	99
7.3	Overview of Model.....	103
7.4	Model Output Files - Bulk Liquid Compositions at Various WVR	106

List of Figures

Figure 1 – Integrated Hanford Waste Treatment Flowsheet – Conceptual Plans including Supplemental Waste Treatment Options.....	15
Figure 2 – Conceptual Selective Dissolution/Fractional Crystallization Flowsheet	16
Figure 3 - Desired Operation of Tank 41 Salt Dissolution Process.....	27
Figure 4 - Strategic Vision for Model Development to Support Selective Retrieval at the SRS.....	28
Figure 5 – Metastable Zone (Mullin 2001).....	31
Figure 6 - Profiles of Predicted and Measured Volume Percent Solids.	40
Figure 7 - Profiles of Predicted and Measured Weight Percent Solids.....	41
Figure 8 – Comparison of Predicted vs. Measured Bulk Density.....	41
Figure 9 – Dissolution of Solidified Synthetic PUREX Waste – Dissolution Rates of 0.1 ft of Saltcake/hr Achieved during Testing	49
Figure 10 – Tank 31H Salt Dissolution Testing – Results Indicate that ¹³⁷ Cs is Removed with Interstitial Liquid	52
Figure 11 – Dissolution Flow-through Testing Using Salt Cake from Tank 3 – ¹³⁷ Cs/Na Concentration as a Function of Dissolved Salt Effluent	54
Figure 12 – Typical Solubility Curves for Two Monotropic Polymorphs or Hydrates (Cardew 1985).....	62
Figure 13-Solubility Curves of Enantiotropes with Metastable Phases (Mullin 2001).	63
Figure 14-Solubilities and Limits of Metastable Zones of an Enantiotropic system.....	64
Figure 15 – SpinTek Filter.....	71
Figure 16 – Enhancement of Flux by Electric Fields	73
Figure 17 – Top Outlet Tubular Filter	75
Figure 18 – Funda Filter	76
Figure 19 – Rotary Filter with Enclosed and Pressure Control Head (BHS Filtration, (Perlmutter 2001)].....	77
Figure 20 – Compartments in Rotary Filter [BHS Filtration, (Perlmutter 2001)]	77
Figure 21 – Compartment Layout in Rotary Filter [BHS filtration, Perlmutter 2001)]	78
Figure 22 – Disk Stack centrifuge Configuration (Alfa-Lavel).....	80
Figure 23 – Peeler Centrifuge	80
Figure 24 – Pusher Centrifuge (Dickenson 1997)	81
Figure 25 – Decanter Centrifuge (Alfa-Lavel 2004a).....	82
Figure 26 – Decanter Centrifuge.....	82
Figure 27 – Screen Bowl Centrifuge	84
Figure 28 – Schematic of AP-104 Semi-Batch Evaporation Model.....	104
Figure 29 – Calculated vs. Measured HNO ₃ Concentrations in Condensate During Batch Distillation of 4M Nitric Acid – Data by P. Ryan ¹⁸	105

List of Tables

Table 1 - Saltcake Dissolution Methods	19
Table 2 - Comparison of the Projected and Actual Salt Solutions during Tank 41 Dissolution (normalized to 6M Na+)	24
Table 3 – Potential Particle Size Distribution Problems in Crystallization Processes – Wibowo 2001	32
Table 4 – Comparison of Separation Techniques	35
Table 5 - Results of AP-104 Supernate Boildown Simulation Using ESP Model	38
Table 6 – SRS Tank Configurations for Selected Salt Waste Tanks which Salt Dissolution Operations Were Conducted.....	42
Table 7 – Tank 19 Salt Batch Compositions	45
Table 8 - Comparison of Density-Driven Techniques.....	51
Table 9 – Selected Data (Bulk Density, Water Content, Porosity and Saturation) for Salt Cake from Tanks 2, 3, 41, 29 and 10	53
Table 10 – Charge Balance Results of BBI AP-104 Supernate Data.	101
Table 11 – Composition of AP-104 Supernate for ESP Model.....	102
Table 12 – Comparison of Halides and Phosphate Levels in Pretreated LAW Feeds and AP-104 Supernate (Normalized to 5.0 M Na)	103

1.0 Executive Summary

In order to accelerate waste treatment and disposal of Hanford tank waste by 2028, the Department of Energy (DOE) and CH2M Hill Hanford Group (CHG), Inc. are evaluating alternative technologies which will be used in conjunction with the Waste Treatment Plant (WTP) to safely pretreat and immobilize the tank waste. Several technologies (Bulk Vitrification and Steam Reforming¹) are currently being evaluated for immobilizing the pretreated waste. Since the WTP does not have sufficient capacity to pretreat all the waste going to supplemental treatment by the 2028 milestone, two technologies (Selective Dissolution² and Fractional Crystallization) are being considered for pretreatment of salt waste.

The scope of this task was to: (1) evaluate the recent Savannah River Site (SRS) Tank 41 dissolution campaign and other literature to provide a more complete understanding of selective dissolution, (2) provide an update on the progress of salt dissolution and modeling activities at SRS, (3) investigate SRS experience and outside literature sources on industrial equipment and experimental results of previous fractional crystallization processes, and (4) evaluate recent Hanford AP104 boildown experiments and modeling results and recommend enhancements to the Environmental Simulation Program (ESP) to improve its predictive capabilities. The following provides the summary of this work and suggested recommendations.

SRS Salt Dissolution & Modeling Update

At SRS, the dissolution of high-level waste salt cake has been necessary for various reasons including tank retirement, tank space, and mitigating salt build-up on equipment. An annotated bibliography is included in Section 5.0 that contains references for salt cake dissolution laboratory experiments and modeling and previous saltcake dissolution operations in the SRS tanks farms.

Salt dissolution has been accomplished at SRS by both mechanical agitation and density-driven methods. Based on solubility differences, selective removal of the more soluble salts during the early dissolution stages is possible. In addition to the solubility differences of the saltcake components, the success of selective dissolution depends greatly on the flow or mixing of interstitial liquid during salt dissolution. Several of the methods, such as the full draining followed by the flow-through dissolution method and the conceptual method of continuous salt mining, should be effective for promoting the

¹ SRNL, through a subcontract with DOE Idaho, is currently evaluating the steam reforming technology using Hanford wastes and simulants. Radioactive testing using Hanford waste is scheduled for early FY05.

² Temporal, spatial and phase variability in species concentration opens the possibility of *selective retrieval* of waste components. As a simple example, selective retrieval of Cs-137 has been accomplished by draining interstitial liquid from a salt tank, leaving behind hard salt and residual amounts of Cs-137 bearing liquid, thus exploiting the variability of Cs-137 with phase. *Selective dissolution* is a special case of *selective retrieval*, in which the more soluble species are retrieved from the tank first (e.g. early batches) followed by the more insoluble species.

selective removal of most of the salts. These density driven methods adequately contact the saltcake with fluid while either promoting the mixing or displacement of the saltcake interstitial liquid. Conversely, the mechanical agitation methods, such as agitation with slurry pumps are not expected to attain optimal selective dissolution. These mechanical methods fully remove regions of the saltcake without contacting the remaining saltcake, which does not allow for the mixing or displacement of the residual interstitial liquid.

At a programmatic level, the SRS and Hanford face similar challenges for selective waste retrieval from salt tanks, including analysis and data needs. However, technologies for salt retrieval are distinctively different. With primary containment being largely intact for SRS salt tanks, retrieval scenarios under consideration tend to involve washing and/or dissolution steps in which the saltcake is in a saturated/flooded condition. In contrast, Hanford envisions retrieval under largely unsaturated conditions to avoid potential leakage from interim-stabilized tanks with compromised or questionable waste containment. SRS retrieval will likely involve batch processing, such as a series of draining and re-flooding steps. Salt retrieval at SRS must be capable of producing 9,000,000 gallons of diluted salt solution per year. Hanford retrieval will likely proceed in a more continuous level controlled manner³, in which saltcake is locally dissolved and retrieved. The effectiveness of such localized dissolution and retrieval schemes will depend on how liquid migrates and mixes between, around, and potentially away from, the injection and extraction points in the presence of chemical dissolution and physical heterogeneity within the salt.

Savannah River National Laboratory (SRNL) recommends that Hanford incorporate the following into the baseline salt waste retrieval program:

- Resources should be focused on identifying candidate selective retrieval processes that are robust. Processes that are relatively insensitive to chemical and physical heterogeneity, fluid property variation with temperature and composition, kinetic rates of dissolution, and unstable transport phenomena (e.g. fingering) should be selected to the extent possible.
- Future retrieval operations in the initial tank(s) should be carefully instrumented to provide insights and lessons learned of generic value to subsequent tanks.
- A coupled dissolution chemistry and porous media transport model would be useful in designing and optimizing an effective selective dissolution strategy, regardless of the specific scenarios under consideration.

Fractional Crystallization/Separation Literature Review

Fractional crystallization processes are operations such as heating, cooling, and solvent addition or removal used to recover two or more of the solutes from a multi-component solution. This literature focuses on sources not previously examined by past reviews.

³ Addition of water to Hanford tanks will have to be controlled to prevent leaks from occurring.

Previous reviews by CHG (Person 2004) are not covered by this review. Additionally, research conducted by CHG personnel (e.g. Herting) is also not covered by this review. Additionally, a major focus of this review is the potential equipment that could be used to separate the crystals from the concentrated supernate. Recommendations from this literature review are discussed below.

Fraction Crystallization/Separation Recommendations

- Rotary drum filtration and the Screen Bowl Decanter, Peeler and Pusher Centrifuges, ranked in order of separation ability (e.g. solid phase with the least free liquid is ranked highest), have promise for future evaluation. The existing centrifuge designs used at Hanford and SRS should also be evaluated.
- The effects of impurities need to be examined since these have (thermodynamically) unpredictable effects on crystallization.
- The effect of crystal particle size on downstream operations plays a key role in the design and operating efficiency of the solids/liquid separation device.
- The effect of seeding the crystallizer (either by addition of inert commercial seeding materials or by process recycle solids) needs to be examined. Seeds can dramatically affect particle size of the product crystals.
- Consultation with commercial industry experts and onsite visits of manufacturers of crystal separation and washing equipment should be completed before selection of equipment for pilot scale testing.
- Kinetically controlled crystallization and metastable phase formation need to be examined if thermodynamic models do not match experimental data.

Evaluation of the AP-104 Boildown Experiment/Modeling

The fractional crystallization process will likely employ the 242-A evaporator to concentrate the salt waste retrieved from the tanks until the evaporator concentrate is fully saturated and precipitates non-radioactive crystals. Models are needed to predict the quantity of solids that will precipitate in the proposed fractional crystallization process. To date, a large difference has existed between the predicted and actual evaporator solids production.

The AP-104 boildown experiment which was carried out in support of Evaporator Campaign 04-02 was modeled using the Environmental Simulation Program (ESP) v6.7. The results of previous ESP modeling on the AP-104 tank waste boildown conducted by the Pacific Northwest National Laboratory (PNNL) personnel were also evaluated. The results of semi-batch evaporator simulation showed that the ESP model correctly predicted most of the solid phases identified at various stages of boildown and somewhat

under predicted the measured bulk solution densities by less than 5%. On the other hand, the volume and mass fractions of solids that were predicted to form were far smaller than the measured data for centrifuged solids by as much as a factor of 23 and 14, respectively, at the end of boildown, which is a clear indication that the ESP model severely under predicted the measured quantity of precipitates that formed.

However, these large discrepancies between predicted and measured quantities of bulk solids can be partially attributed to the inherent nature of the ESP software. The software calculates the physical properties of bulk solids assuming that they form a bone-dry matrix not containing any interstitial liquid. Experimental observations have shown a significant volume expansion can occur depending on the habit and morphology of crystals or gels. These crystals or gels form a relatively small mass of solids that entrain a much larger quantity of liquid. In principle, these physical events, accompanying the phase transformation in multi-electrolyte solutions, cannot be captured properly by the ESP or any other thermodynamic modeling tool.

Despite these shortcomings, the model was still able to produce results that could be of value to the actual evaporator operation. When the under predicted solids fractions were plotted against the waste volume reduction (WVR), the resulting profile looked markedly similar to the measured profile in that both predicted and measured solids fractions increased gradually with increasing WVR of up to 42-45%, where they both began to increase sharply with further increase in the WVR. This suggests that OLI software could be used to predict the point where the solids loading would become excessively high too quickly, resulting in lower evaporator efficiency and a reduced operating margin for recovering from unexpected incidents.

The ESP model can be run with an assumed (or measured) entrainment ratio of interstitial liquid to insoluble solids which would allow accurate prediction of the vol. %. For example, assuming an interstitial liquid volume of 90% for all WVR's, the discrepancy would have been reduced to a factor of 2.3 at 50% WVR or 41 vol. % (model) vs. 93 vol. % (data). At a 95% interstitial liquid volume, the predicted solids fraction would become 82 vol. % which is practically identical to the measured value, considering the uncertainty of the data. This shows how easily model predictions can be made to match the data simply by adjusting the entrainment ratio.

Based on the findings of this modeling work, the following recommendations are made in order to improve the applicability of the ESP software to the salt solution concentration by evaporation:

- Run additional boildown/evaporation cases to further confirm if the ESP model can predict the location of experimentally observed break point(s) in the solids fraction vs. WVR curves.
- Establish commercial partnership with OLI for future database development. Consideration should be given to establishing a DOE EM wide commercial partnership with OLI to pool resources and funding sources.

- Optimize the WTPBASE database using data taken from higher-order systems and fine tune the solubility (or binary interaction) parameters of all major salt species.
- Validate and optimize the NAFPO4 and DIAL double salt databases.
- Measure the composition and density of the liquid phase during boildown/evaporation tests to help close the material balance and to further develop an empirical correlation of the bulk solids porosity as a function of WVR and solids phases.
- Investigate the use of halogen gravimetric instruments or other methods to determine actual weight percent insoluble solids formed during boildown experiments⁴.
- Future work should include measurement of the interstitial liquid volume entrainment as a function of WVR during all boildown studies. This would allow accurate predictions of solids volume predictions from the proposed fractional crystallization process.

⁴ Mettler Toldedo Moisture Analyzer, www.mt.com or equivalent.

2.0 Introduction/Objectives

In May of 2002, the River Protection Project (RPP) at Hanford proposed to accelerate the waste treatment and disposal of Hanford tank waste by 20 or more years by developing supplemental treatment technologies that would be used in conjunction with the Hanford WTP to achieve completion of waste processing by 2028.⁵ Four technologies (Sulfate Removal, Containerized Grout, Bulk Vitrification and Steaming Reforming⁶) were down selected by a group of Hanford DOE, contractors, national labs and independent experts. DOE is currently testing Bulk Vitrification at Hanford and Steam Reforming at INEEL. Figure 1 shows the conceptual integrated flowsheet of Hanford's waste treatment facilities including the supplemental treatment options. DOE commissioned testing programs in three of the four technologies: Containerized Grout, Bulk Vitrification and Steam Reforming. Prior testing of Sulfate Removal was completed in the 1999-2000 timeframe. Since the WTP does not have sufficient capacity to pretreat and vitrify all the waste by the 2028 milestone, two pretreatment technologies (Selective Dissolution and Fractional Crystallization) are being considered for treatment of salt waste.

⁵ Allen, D. I., A. F. Choho, T. M. Brouns and B. M. Mauss. "Recommendation for Supplemental Technologies for the Hanford Project Potential Mission Acceleration", *Proceedings of Waste Management '03*, Tucson, AZ (2003).

⁶ Some Hanford wastes are high in sulfate. The high sulfate wastes limit the waste loading in the WTP LAW glass. Containerized grout uses grout forming additives to form a waste form suitable for shallow land disposal. Bulk vitrification uses common glass forming materials (Hanford dirt, sand...etc.) to form a glass waste form. Large containers of glass waste forms are made and are suitable for shallow land disposal. The Steam Reforming process denitrates the waste in a high temperature fluidized bed. The calcined product is suitable for shallow land disposal. The containerized grout, bulk vitrification and steam reforming process would reduce the waste sent to the WTP vitrification plant.

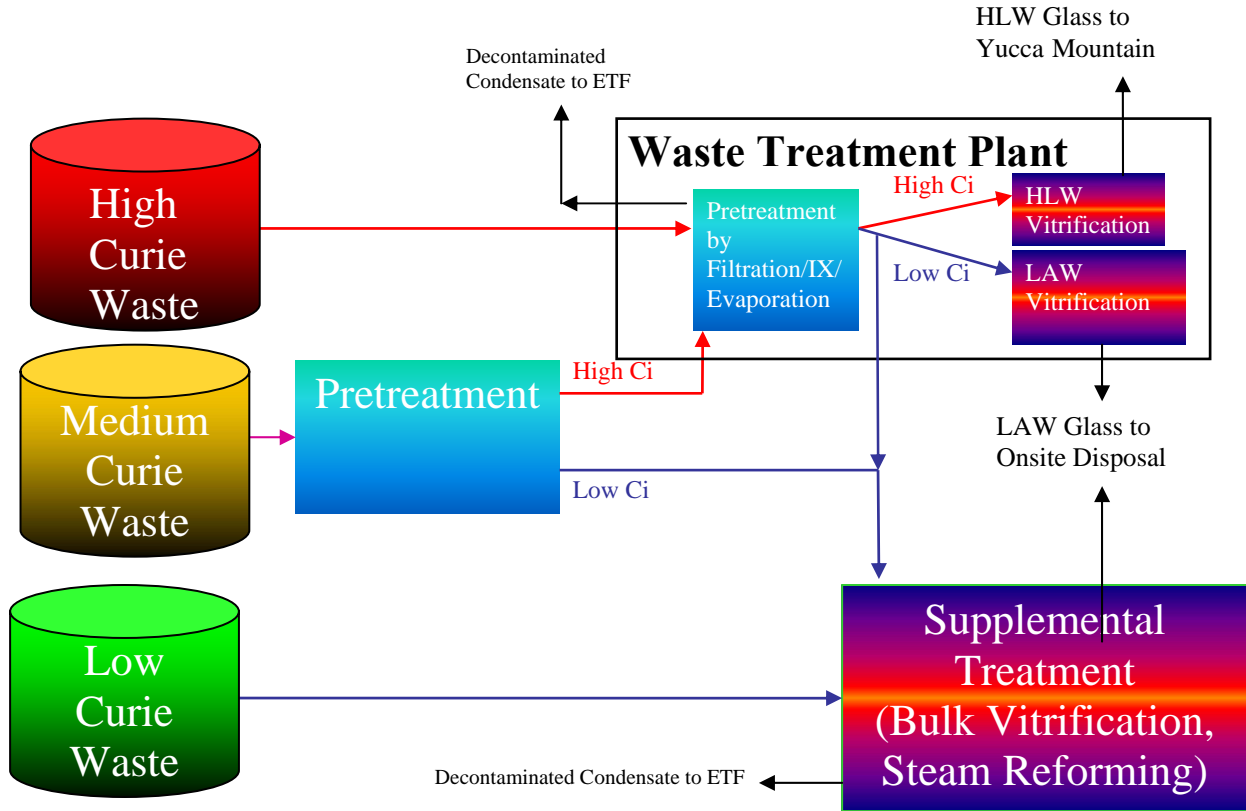


Figure 1 – Integrated Hanford Waste Treatment Flowsheet – Conceptual Plans including Supplemental Waste Treatment Options

The Selective Dissolution process occurs in the tank when water is added to retrieve the salt waste. The cesium, which is primarily in the interstitial liquid, is removed from the tank before the dissolution and removal of the majority of the non-radioactive salts. A gamma monitor on the transfer line detects when the Cs concentration changes and the high activity material can be directed toward the WTP. As more of the tank material is dissolved, the activity level in the waste stream drops and the material could potentially be transferred directly to Supplemental Treatment as shown in Figure 2. During the retrieval of Hanford S-112, high activity spikes were detected on the gamma monitor during initial flushes of salt waste from the tank. Modeling of this phenomenon is needed to understand and propose changes to the process that will prevent spikes in Cs concentration during retrieval and treatment operations. Additionally, modeling could be used to design and optimize the flowsheet for the salt waste pretreatment system.

The fractional crystallization process will likely employ the 242-A evaporator to concentrate the salt waste retrieved from the tanks until the evaporator concentrate is fully saturated and precipitates non-radioactive crystals. The concentrated waste stream can then be separated into a cesium rich stream and a cesium lean stream. The cesium lean stream would be sent to Supplemental Treatment as shown in Figure 2. As an added

benefit sulfate and fluoride, which all have limited solubility in the WTP LAW glass, would be sent to Supplemental Treatment for disposal.

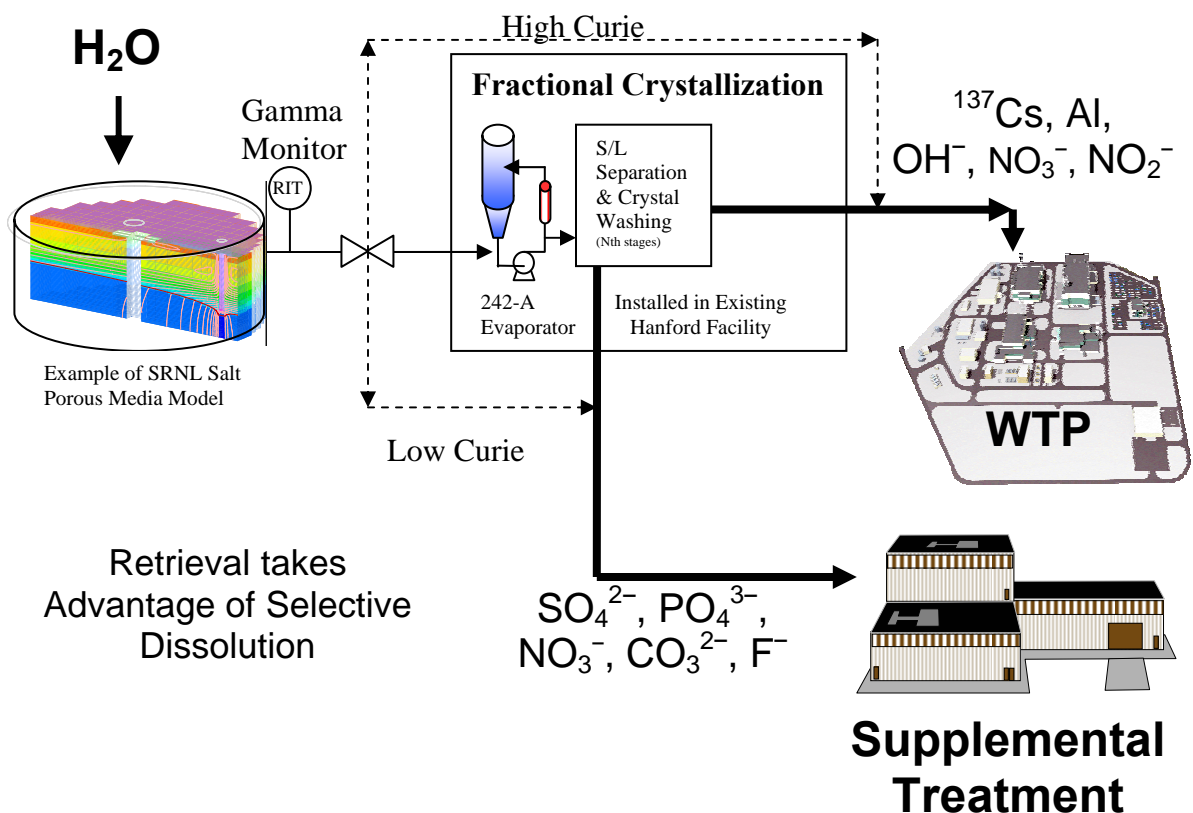


Figure 2 – Conceptual Selective Dissolution/Fractional Crystallization Flowsheet^{7,8}

Currently, Hanford is using OLI System’s Environmental Simulation Program to predict the formation of solids in the evaporator. To date a large difference has existed between the predicted and actual evaporator solids production. The difference between the current thermodynamic model and observed evaporator operations needs to be addressed to successfully evaluate fractional crystallization.

The objectives of this work are:

- Assist CH2M HILL Hanford Group Inc. (CHG) in addressing supplemental treatment issues such as selective dissolution and fractional crystallization,

⁷ Herting, D. L, *Significant Volume Reduction of Tank Waste by Selective Crystallization: 1994 Annual Report*, WHC-SD-WM-TI-643, Hanford Reservation, Richland, WA 29808 (1994).

⁸Herting, D. L, *Fractional Crystallization*, Salt Waste Technical Exchange, CH2MHill Hanford Group, Inc., Richland, WA (2004).

- Evaluate test data from the recent SRS Tank 41 dissolution campaign as well as SRS/public/DOE literature sources that would allow a more complete understanding of selective dissolution,
- Provide an update on the progress of these activities as well as any enhancements that are built into the existing SRS program,
- Evaluate recent Hanford boil-down studies using tank sample AP104 and as well as Hanford OLI modeling results and suggest enhancements to the Environmental Simulation Program (ESP) by OLI[®] that might improve the prediction of the capabilities of the ESP software,
- Investigate SRS experience and literatures sources on industrial equipment, experimental and modeling results of previous fractional crystallization processes for potential application to a Hanford fractional crystallization process.

3.0 Selective Dissolution

3.1 *SRS Salt Waste Dissolution History – Literature Review*

Over the lifetime of the SRS, the dissolution of high-level waste saltcake has been necessary for a variety of reasons. The majority of the large-scale saltcake dissolution activities at SRS before 1990 resulted from the desire to retire the first three generations of waste tanks (Types I, II, and IV). Since 1990, and continuing into the foreseeable future, saltcake dissolution at SRS has been utilized to produce feed material for salt processing (In-Tank Precipitation, Low-Curie Salt, and Salt Waste Processing Facility) with the intention of ultimate disposal. In several cases, the primary driver for saltcake dissolution was the removal of salt to liberate space in a tank so it could be utilized differently (as an evaporator drop tank, a fresh waste receipt tank, a process feed tank, etc.). Additionally, spot dissolution has always been necessary to mitigate buildup on equipment, such as on cooling coils, in the evaporator pots, and in tank annuli.

The annotated bibliography in the Section 5.0 contains summaries of the references for the previous in-tank saltcake dissolution events at SRS. Additionally, it contains information on the past laboratory dissolution and computer modeling efforts. In all cases, dissolution was accomplished by the addition of water or an unsaturated salt solution to a tank containing saltcake. Evident, from several of the references, is the need for efficient salt dissolution methods to facilitate contact of the saltcake with the unsaturated dissolution fluid. Merely adding water to the surface of undrained saltcake is inefficient because the dilute less-dense unsaturated fluid will tend to stratify near the supernate surface and not contact the saltcake. The optimal dissolution technique should ensure good contact between the unsaturated salt solution and the saltcake while avoiding channeling.

SRS has used two general saltcake dissolution schemes, mechanical agitation methods and density-driven methods, to promote contact between the unsaturated dissolution fluid and the saltcake. Table 1 contains a summary of the dissolution methods employed at SRS. Mechanical agitation methods have been used in salt dissolution from Tanks 17, 19, 24, and 49, and from the annulus of Tank 16. Density-driven methods were used for Tanks 10, 33, 37, and 41. Salt dissolution from Tanks 20 and 22 were accomplished by density-driven methods during the early dissolution and then by mechanical agitation methods during the later stages. During these retrieval processes, several factors have been demonstrated to affect the saltcake dissolution behavior, including agitation, temperature, and orientation.

Table 1 - Saltcake Dissolution Methods

Mechanical Agitation Methods	Density-Driven Methods
<i>Deployed in Tank</i>	
<i>Slurry Pump Agitation</i>	Density Gradient
<i>Steam Jet Recirculation</i>	Modified Density Gradient
	Drain-Add-Sit-Remove (DASR)
<i>Modeled or Tested in R&D Program</i>	
<i>Flygt Mixer Agitation</i>	Salt Mining

3.1.1 Mechanical Agitation Methods

Mechanical agitation methods impart flow on regions of the supernatant fluid to mix the fluid and promote contact with the saltcake. Slurry pumps and steam jets have been used in previous dissolution events, and other potential agitation providers, such as Flygt mixers, have been studied and modeled. Mechanical agitation has been shown to work well even near the bottom of the tank where density-driven techniques become less effective.

At SRS, the resuspension and transfer of high level waste (HLW) sludges require the use of slurry pumps. While saltcake dissolution does not absolutely require these pumps, the use of slurry pumps during salt dissolution helps to suspend the layer of insoluble solids that would potentially blind the saltcake surface. Slurry pumps are the optimal method for dissolution of saltcake with alternating layers of sludge and supernate. Slurry pumps, however, are not installed in all tanks and require additional installation time and cost during salt dissolution. For most cases, any time saved during the dissolution period by using slurry pumps is cancelled by the additional preparation time required.

Steam jets have also been used to promote dissolution by both circulating and heating the supernatant liquid. Circulation jets used for Tank 22 dissolution were ideal because of their lack of moving parts and ease of use, but they caused heating of the tank contents to 80 °C to 90°C. This increased the risk of stress corrosion cracking in this tank. The tank does not have cooling capability and approximately two years were required for the tank contents to cool.

3.1.2 Density-Driven Methods

Density driven techniques rely on the continuous replacement of the saturated solution at the salt-liquid interface with lower density unsaturated fluid. Several variations of the density-driven concept have been employed, including the density gradient method, the modified density gradient method, and the Drain-Add-Sit-Remove (DASR) method. Additionally, a continuous salt mining method has been studied experimentally.

The density-driven methods tend to produce level salt dissolution in the tank, with much of the salt dissolved in horizontal slices. The density-driven methods utilize simple equipment, but leave a cake heel in the tank. These methods may be hindered by the presence of insoluble material, which forms a layer on the top of the saltcake.

In the density gradient method, a vertical well is hydraulically mined into the salt and dissolution fluid is added to cover the salt. As the salt dissolves, higher density supernate flows by gravity into the well, causing lower density supernate to dissolve salt from higher elevations. The high density dissolved salt solution is transferred from the bottom of the well using a pump or jet.

The modified density gradient approach is similar to the original density gradient method, but is operated continuously by balancing the water addition with the jetting or pumping out of the concentrated salt solution.

The DASR method begins with draining of a portion of the interstitial liquid. This allows the dissolution to easily flow into the upper regions of the saltcake, enhancing the dissolution rate. Once the saltcake has been covered with dissolution fluid, the DASR method includes a short waiting period and the monitoring of fluid density during removal.

Salt mining is a conceptual method that was tested in the laboratory by Wiersma (1996) but was never applied in the field. Two vertical wells are mined into the saltcake at opposite ends of the tank and dissolution fluid is added to one well. When both wells are full, fluid addition continues while dissolved salt solution is removed from the bottom of the other well. This showed the greatest potential for interstitial liquid displacement due to the flow induced through the saltcake.

3.1.3 Issues Encountered During Dissolution

Concern over several technical and safety issues drive the methods and planning of salt dissolution events at SRS. These issues include nuclear criticality safety, corrosion inhibition, flammability resulting from hydrogen release, and undue stresses caused by perched salt.

Nuclear criticality safety is a concern in tanks that contain greater than critical mass quantities of ^{235}U or other fissile isotopes. Sampling is often required to confirm that adequate neutron poisons and diluents are present throughout the dissolution process to ensure a criticality event is not credible.

Corrosion concerns are often abated by assuring that the dissolution fluid contains adequate corrosion inhibitors. The potential for dissolved salt solutions to be outside of the technical corrosion limits is increased in the later stages of dissolution. The salt dissolution plans usually include visual observation steps to detect masses of salt hanging on the cooling coils. The issue of perched salt is usually mitigated by assuring that these salt masses are covered by the dissolution fluid.

Currently, evaluations that are performed to estimate the hydrogen released from the saltcake during the draining and adding steps place operational limits on in-tank salt dissolution events.

Many of these salt dissolution concerns at SRS should parallel those at Hanford, and the references in the appendix contain information on the strategies for mitigation. Most of the salt dissolution tasks at SRS took place in tanks that did not have known leak sites or took place below the leak sites. At Hanford, the additional issue of minimizing potential release of material from leaks in single shelled tanks should also be considered when dissolving salt. Hanford constraints might impact the ability to deploy some of the dissolution methods used at SRS due to the desire to not have supernatant liquid in contact with tank walls. Additionally, many of the Hanford HLW saltcake tanks have already gone through interim stabilization by the draining and removal of the interstitial liquid and thus have already accomplished the most time consuming portion of the DASR method.

3.1.4 Selective Dissolution

One area in the previous SRS dissolution experience that could benefit the Hanford Site's accelerated program is selective dissolution. Distinguished from dissolution for bulk salt retrieval, selective dissolution accomplishes a separation of materials during in-tank dissolution. Several factors influence the evidence and extent of selective dissolution, including the solubility differences of the salts, the initial tank inventory, the dissolution temperature, and the established flow patterns. There are two main manifestations of selective dissolution during in-tank salt retrieval.

First, and least susceptible to subtleties in flow patterns, is the tendency for less soluble salt components to be concentrated in the residual undissolved heel. As long as the process allows for a rough solid/liquid separation before transfer of the dissolved salt solution, the insoluble sludge materials and low-solubility salts will remain in the tank. Second, and more useful to separation of low-curie and medium-curie waste, is the ability of some dissolution processes to produce solutions with differing compositions. The earliest dissolution stages could be rich in hydroxide, nitrite, cesium-137, while the later stages could be rich in sulfate, carbonate, and some minor components (fluoride and oxalate).

There have been several experimental studies on saltcake simulants and actual-waste saltcake that show the potential for selective dissolution of salt. Wiersma (1996) showed that the solids remaining at several points during simulant dissolution testing differed. At Hanford's 222-S laboratory, Dan Herting has conducted extensive testing on Hanford saltcakes with relation to selective dissolution. While these studies are not reviewed in detail here, they successfully demonstrated selective dissolution on a laboratory scale. Martino and Poirier (2003) dissolved SRS Tank 31 saltcake material in a manner consistent with Herting's methodology. They found that the highly soluble salts that were largely part of the interstitial liquid were removed at the earliest stages of dissolution (most notably hydroxide, nitrite, cesium-137, and technetium-99). In contrast to the Hanford waste, phosphate was also seen to dissolve out of the SRS saltcake in the

early dissolution stages. A portion of the strontium was observed to dissolve in the late dissolution stages, after most of the nitrite, sulfate and carbonate had been removed.

The well-mixed batch contact tests are an idealized representation of selective dissolution that is difficult to relate directly to the full-scale process. The tests incorporate complete mixing of salt with the dissolution medium. The residual undissolved salt heel is not drained of interstitial liquid between dissolution stages. Demonstrational studies on the flow-through dissolution of saltcake samples from Tanks 41, 3, 29, and 10 (Nichols, Martino, McCabe, et al., 2003/2004) provide a less idealized approach to selective dissolution. Still, ^{137}Cs was seen to be removed in greatest quantities from the early stages of these tests. The diverse flow patterns created during these tests affected the results obtained, with each sample achieving different levels of cesium concentration in the initial stages.

Salt chemistry during dissolution at SRS was not a major concern during most of the early retrieval processes. There is, however, dissolution chemistry and residual solid information for the Tank 19 dissolution. Also, some recent analyses provide insight into the solids left behind by the 1979-82 Tank 10 dissolution and the 1996 Tank 41 dissolution. Of the recent dissolution events that have occurred at SRS, adequate selective dissolution information was only collected for the 2003 Tank 41 dissolution. Salt removal from Tanks 37 (Nguyen, 2002) and 49 (Nguyen, 2004) did not include sampling to provide information on selective dissolution.

Over one million gallons of salt was dissolved from Tank 19 in batches using the slurry-pump agitation method. The sample analyses reported for the Tank 19 dissolution (Goslen, 1986) showed that a very similar composition was obtained for all four salt dissolution batches. This suggests that the addition of dissolution fluid to the top of an undrained saltcake, followed by mechanical agitation with slurry pumps is not a good method to produce solutions of varying composition. The soluble components in the residual solid material differed significantly from the initial Tank 19 bulk inventory. In addition to insoluble sludge and zeolite materials, the residual tank heel was rich in sulfate, oxalate, and calcium (note that carbonate was not analyzed).

In the late 1970s's and early 1980's, about 60% of the saltcake was dissolved and removed from Tank 10. Recent analysis of the top 36 inches of Tank 10 saltcake revealed a layer approximately 12 inches below the current saltcake surface that differed significantly from the typical saltcake chemistry. In addition to containing a higher amount of insoluble sludge solids, the solids in this layer were composed of 35% sodium nitrate and 65% mixture of sodium carbonates and sulfates (likely burkeite plus an unidentified sodium carbonate or sodium carbonate sulfate phase). It is likely that the concentration of sodium sulfates and carbonates in a layer near the saltcake surface is a direct result of the previous dissolution events. Similarly, a thin (approximately one inch) layer at the previous (April 2003) surface of Tank 41 was identified as being rich in sodium carbonates and sodium fluoride phosphate double-salt. This material is believed to be the remnant of the 1996 dissolution to produce 7000 gallons of solution.

Tank 41 dissolution performed in 2003 provides the best evidence of the potential for in-tank dissolution to produce solutions of differing compositions. The dissolution, however, was only carried out through the first of several planned dissolution stages. The original plan for Tank 41 was to drain as much of the interstitial liquid from the saltcake as possible and dissolve and transfer only the top portion of the saltcake. This dissolution scheme was designed to minimize the amount of ^{137}Cs transferred out of the tank in the initial dissolution stage. This was to be accomplished by adding water to several locations of the saltcake surface and allowing the liquid to flow over the surface of the saltcake as it would in the modified density gradient dissolution approach. In practice, however, the interstitial liquid draining of the saltcake left the pores unsaturated and altered the solution flow during dissolution from what was expected. As the dissolution water was added to each location, the salt dissolved locally and the dissolved salt solution flowed down through the saltcake. This downward flow of dissolved salt solution washed through undissolved regions of the saltcake and into the pump well. Flow through the unsaturated pores allowed the salt solution to contact a far greater amount of saltcake than just the planned top 100 gallons. As a result, in comparison with the analysis of the top 100 gallons, the first batch of dissolved salt solution was highly concentrated with highly soluble interstitial liquid components.

Table 2 contains information on the expected dissolved salt solution projected from the soluble components in a sample from the top 26 inches (91 gal) of the Tank 41 saltcake (Martino and Nichols, 2003) compared with the actual dissolved salt from after the water addition (Martino, 2003). These are both normalized to 6 M Na^+ , our salt dissolution baseline, though the actual Tank 41 first dissolution batch produced an 8 M Na^+ solution. The components that are thought to be primarily in the interstitial liquid in Tank 41 (hydroxide, nitrite, ^{137}Cs -137, ^{99}Tc , and phosphate) were present in the dissolved salt solution at four-to-seven-times greater quantity than expected from the dissolution plan. Aluminate, another interstitial liquid component, fell outside of this range, likely due to its deficiency in the original saltcake sample. At the same time, other major saltcake components (nitrate and carbonate) were present at only 70 to 75% of their expected levels. The projection was based upon the composition of the saltcake that was to be dissolved, but the actual first batch of dissolved saltcake was highly influenced by other material it flowed through before entering the pump well. As a result, subsequent dissolution batches should be lower in these interstitial liquid components and higher in some of the other salts.

From the observed selective dissolution cases at SRS, use of selective dissolution for cesium-137 separation during in-tank retrieval of salt will require at least a moderate level of mixing or displacement of saltcake interstitial liquid for Hanford salt dissolution. The manner that the DASR technique was implemented in the recent Tank 41 salt dissolution caused flow of saturated fluid through the saltcake and return into the wells, resulting in a supernatant fluid with relatively concentrated ^{137}Cs . While not an effective technique for making Low Curie salt, this method could have been applied to the Hanford salt tanks where high Cs concentrations are desired in the early batches. The concept of continuous salt mining proposed and tested by Wiersma could also prove effective for selective dissolution since it combines dissolution with forced interstitial liquid

displacement. Dissolution methods such as mechanical agitation using slurry pumps are not expected to attain optimal selective dissolution because they fully dissolve and remove portions of the saltcake without contact with the remaining saltcake and interchange with the remaining interstitial liquid. As long as solid/liquid separation is utilized, even the mechanical agitation methods should accomplish some selective dissolution, with the solids remaining in the tank rich in low-solubility salts.

A greater understanding of the physical flow patterns that emerge during salt dissolution is important to the success of some selective dissolution processes. Permeability and flow modeling should be utilized to assist in this flow modeling area, which is difficult to investigate in a meaningful way using waste simulants or small-scale actual-waste samples.

Table 2 - Comparison of the Projected and Actual Salt Solutions during Tank 41 Dissolution (normalized to 6M Na+).

Analyte	Units	Projected Solution	Actual 1 st Batch	Actual / Predicted
Na ⁺	M	6.00E+00	6.00E+00	--
NO ₃ ⁻	M	4.99E+00	3.67E+00	0.74
NO ₂ ⁻	M	2.82E-02	1.78E-01	6.32
OH ⁻	M	1.47E-01	6.32E-01	4.31
AlO ₂ ⁻	M	7.88E-03	4.87E-01	61.74
CO ₃ ²⁻	M	3.50E-01	2.51E-01	0.72
SO ₄ ²⁻	M	1.63E-01	1.77E-01	1.09
PO ₄ ³⁻	M	5.09E-03	2.58E-02	5.08
C ₂ O ₄ ²⁻	M	5.93E-03	1.80E-03	0.30
⁹⁰ Sr	pCi/mL	6.19E+04	2.98E+04	0.48
⁹⁹ Tc	pCi/mL	5.22E+03	3.51E+04	6.72
¹³⁷ Cs	pCi/mL	1.67E+07	7.44E+07	4.44
²³⁸ Pu	pCi/mL	5.02E+05	4.51E+05	0.90

3.2 Update on Selective Retrieval Modeling Activities at SRNL

The composition of liquid residing in and retrieved from a salt tank may vary in time, space and phase (solid vs. liquid) due to a number of chemical and physical phenomena. As a series of three examples, the solubility of a particular anion on an operational time scale is affected by the presence or absence of competing anions, and the kinetic rate of dissolution relative to other anions. Early dissolution batches will be rich in hydroxide, nitrite and cesium, while the later batches will be rich in nitrate, sulfate, carbonate and some minor components. Physical heterogeneity in saltcake properties and discrete locations for flush water addition and salt solution extraction produce a spatially variable composition within salt tanks. Immediately following flush water addition to SRS Tank 41 through tank top risers, a saturated solution rich in hydroxide and ^{137}Cs occupied the relatively undisturbed lower portion of the tank, whereas a partially saturated nitrate solution with lower amounts of hydroxide and ^{137}Cs filled cavities dissolved into the top surface of the saltcake. A species may be present primarily in the liquid or solid phase, or be distributed through both phases, depending on its solubility. In SRS Tank 41, ^{137}Cs is present as a solute while the major ions from a bulk chemistry perspective are present in both the solid and liquid phases.

Temporal, spatial and phase variability in species concentration opens the possibility of *selective retrieval* of waste components. As a simple example, selective retrieval of ^{137}Cs has been accomplished by draining interstitial liquid from a salt tank, leaving behind hard salt and residual amounts of ^{137}Cs bearing liquid, thus exploiting the variability of ^{137}Cs with phase. *Selective dissolution* is a special case of *selective retrieval*, in which the more soluble species are retrieved from the tank first (e.g. early batches) followed by the more insoluble species.

SRNL has developed and/or utilized a variety of models to assess and optimize selective retrieval strategies under consideration for plant deployment. Although typically coupled at tank scale, dissolution chemistry and porous medium transport phenomena have historically been characterized and modeled as separate effects. This approach provides a way to make the analyses functional given the state of modeling capability due to the complexity of coupling the two mediums together.

Dissolution chemistry phenomena have been modeled using OLI System's Environmental Simulation Program (ESP) and Aspen Custom Modeler (ACM). The typical analysis involves estimating the composition of liquid that would be retrieved from various SRS tanks through a batch dissolution process. Analyses of this type implicitly assume that the entire contents of a tank is well-mixed and at chemical equilibrium.

Analysis results are useful in assessing the degree of selective dissolution/retrieval and the impacts on downstream treatment for process selection and optimization. Results may also be used for process control, such as defining the expected density of a saturated solution through time to ensure the retrieval process is making efficient use of flush water. The model databases are calibrated to laboratory experimental data derived from simulants and saltcake samples. Example SRS dissolution chemistry modeling studies include Pike (2001, 2002), Nguyen and Pike (2003) and Nguyen (2004).

Physical phenomena of interest have generally been analyzed using porous media liquid flow and solute transport models that do not account for saltcake dissolution when it occurs and corresponding fluid property variations. The emphasis of such models has been on saltcake washing/interstitial liquid displacement (ILD) scenarios. Here the focus is on the drainage and transport characteristics of saltcake and the spatial distribution of species with respect to discrete retrieval points. The Corps of Engineers performed an early study using the FEMWATER groundwater code that explored the impact of physical heterogeneity on the efficiency of ILD (Staheli and Peters 1998; Brooke, Staheli and Peters, 1999). Subsequently SRNL used the FACT groundwater code to analyze tank drainage scenarios aimed at selective retrieval of ^{137}Cs (Flach 2003, 2004). Historically, characterization efforts have focused on the chemical properties of saltcake. SRNL has recently started analyzing tank process and laboratory experimental data to determine the porous-medium properties of saltcake, such as porosity and permeability. Florida International University (FIU) has recently measured porous medium properties of simulated saltcake.

The current situation of decoupled dissolution chemistry and porous medium transport models significantly limits our ability to accurately predict the behavior of many selective retrieval strategies under consideration at the SRS. Tank 41, at the SRS, is a cogent example, where this “separate effects” approach produced poor predictions of the recent Tank 41 salt dissolution process. Following gravity drainage of interstitial liquid from the tank, a process for dissolving hard salt and retrieving saturated salt solution was developed (See Figure 3).

The operation involved spraying flush water onto saltcake surrounding a salt well, which contained a sump pump for liquid retrieval. The pump was placed above the initial well level. Process plans called for flush water addition until the well level was raised to the pump intake. After that point, retrieval of dissolved salt solution was to be initiated at the same rate as liquid addition.

- *Saturated* liquor enters caisson
- Layer at 275" dissolves slower than overlying salt
- 15gpm to maintain level at 275"
- Minimum of 35 gpm flush water needed to sustain 20 gpm transfer
- >60,000 gallons salt liquor left added to tank by dissolution

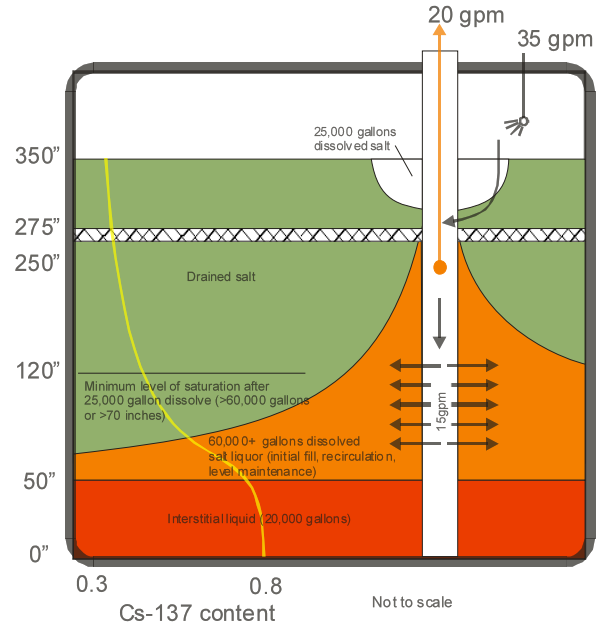


Figure 3 - Desired Operation of Tank 41 Salt Dissolution Process

A porous medium analysis was used to estimate the rate of flush water addition required to raise the well level to the pump intake height. The analysis did not account for the effects of chemical dissolution, namely, decreased viscosity with changing chemical composition, and increased permeability due to changing saltcake morphology. During the actual tank process, water addition at the prescribed rate did not produce a well level noticeably higher than the mean liquid level. The tank was eventually refilled to the original level by flush water addition through multiple risers, leading to several cavities being dissolved into the top surface of the saltcake containing free liquid.

Dissolution chemistry modeling predicted that the ^{137}Cs concentration in a dissolved salt solution would be near the process limits for “low curie salt” at about 0.11 Ci/gal. However, the chemistry analysis did not consider the possibility of salt solution mixing with interstitial liquid residing in saltcake surrounding the dissolved region in the retrieval operation. Because flush water was added through several risers while the saltcake was being re-flooded, considerable mixing occurred due to lateral hydraulic head gradients across the tank. The resulting ^{137}Cs concentration in pools of free liquid, occupying cavities beneath water addition points shortly after tank refill, was about 0.38 Ci/gal, far exceeding the process limits for “low curie salt”.

In both instances, the lack of coupling between dissolution chemistry and porous medium flow led to significant discrepancies between model predictions and reality for Tank 41. In general, the chemical composition of liquid at a location in a salt tank will depend not only on dissolution chemistry, but also on transport of liquid to and from the region of interest. Similarly, fluid transport will depend not only on hydraulic gradients and initial properties, but also changing saltcake morphology and liquid chemical composition as a

result of dissolution. Thus chemistry and mixing/transport phenomena are inherently linked in most salt retrieval scenarios.

SRNL holds the opinion that the greatest improvement to selective retrieval modeling predictions can be achieved by integrating chemistry and porous medium mixing/transport models. As an initial step toward this end point, SRNL has migrated to the STOMP code developed by PNNL for further model development. STOMP is a multi-phase, multi-component porous medium flow and solute transport code, which has been used to model flow in Hanford salt tanks. The multi-component/phase framework of the software enables tracking of solid and liquid phases, and multiple chemical components which may be present as dense or dilute solutes. Currently, SRNL is modifying a version of the code to track multiple brines, while accounting for changes in fluid properties with mixture composition. Of particular interest is the impact of fluid viscosity variations during various retrieval scenarios. Using SRS Tank 41 as an example, the viscosity of dissolved salt solution is roughly 4 times lower than that of the original interstitial fluid and would lead to preferential transport of dissolved salt. Longer-term, SRNL envisions coupling a simplified dissolution chemistry model to STOMP. Figure 4 summarizes the SRNL strategic vision for model development to support selective retrieval process modeling at the SRS.

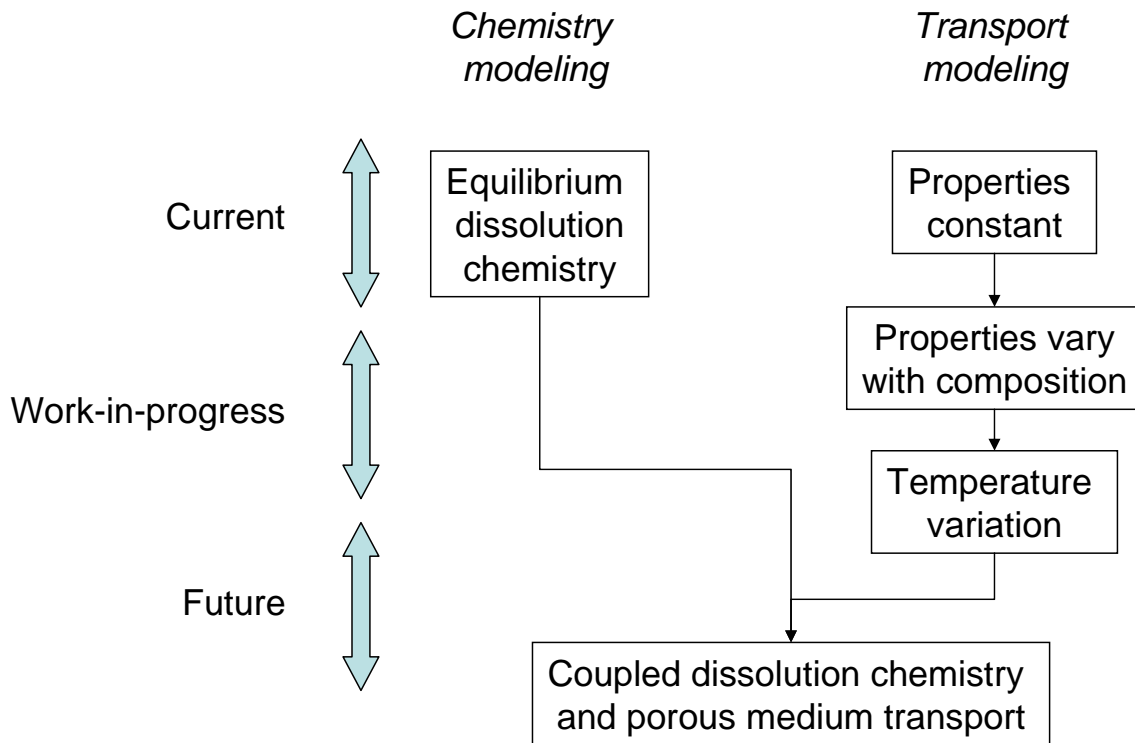


Figure 4 - Strategic Vision for Model Development to Support Selective Retrieval at the SRS

In the coming fiscal year, SRNL anticipates using the variable composition and property version of STOMP to more accurately assess the potential for hydrogen release during flush water addition. Currently, conservative estimates of hydrogen release within a facility safety analysis limit flush water addition to roughly 15 gpm, which comprises a plant operations bottleneck. SRNL also expects to analyze the effectiveness (e.g. "DF") of various saltcake washing scenarios, accounting for physical heterogeneity in permeability and the viscosity contrast between the original interstitial fluid and dissolved salt solution. Prior to these analyses, the model will likely be calibrated to and validated against data from the Tank 41 salt dissolution process in 2003.

The distribution of porosity, permeability, and liquid retention properties is a key input to a porous medium model of mixing within a salt tank. Changes to these properties in the presence of chemical dissolution are also important for some retrieval scenarios. Thus, SRNL is pursuing improved techniques for characterizing the physical heterogeneity within salt tanks to support the level of porous medium modeling envisioned above. A particular thrust is the use of cone penetration testing (CPT) technologies to perform in situ characterization and retrieve samples at depth for both physical and chemical analysis.

3.2.1 Relationship to Selective Retrieval of Waste from Hanford's Interim-Stabilized Tanks

At a programmatic level, the SRS and Hanford face similar challenges for selective waste retrieval from salt tanks, including analysis and data needs. However, technologies for salt retrieval are distinctively different. With primary containment being largely intact for SRS salt tanks, retrieval scenarios under consideration tend to involve washing and/or dissolution steps in which the saltcake is in a saturated/flooded condition. In contrast, Hanford envisions retrieval under largely unsaturated conditions to avoid potential leakage from interim-stabilized tanks with compromised or questionable waste containment. SRS retrieval will likely involve batch processing, such as a series of drainage and re-flood steps. Hanford retrieval will likely proceed in a more continuous level control manner⁹, in which saltcake is locally dissolved and retrieved. Localized dissolution and retrieval will make implementation of selective dissolution strategy more difficult.

The effectiveness of such localized dissolution and retrieval schemes will depend on how liquid migrates and mixes between, around, and potentially away from, the injection and extraction points in the presence of chemical dissolution and physical heterogeneity. Given the inherent challenges of accurately modeling coupled dissolution chemistry and porous media transport, resources should be focused on identifying candidate selective retrieval processes that are robust. Processes that are relatively insensitive to chemical and physical heterogeneity, fluid property variation with temperature and composition,

⁹ Addition of water to Hanford tanks will have to be controlled to prevent leaks from occurring.

kinetic rates of dissolution, and unstable transport phenomena (e.g. fingering) should be selected to the extent feasible.

Nevertheless, SRNL would anticipate that a coupled dissolution chemistry and porous media transport model would be useful in designing and optimizing an effective selective dissolution strategy. The most critical data needed to support such a model may be an estimate of the degree and structure of saltcake physical heterogeneity, both initially and under the influence of subsequent salt dissolution. Experience in subsurface environmental characterization and modeling suggests that the most useful information will come from larger-scale in situ measurements and/or analysis of instrumented tank-scale retrieval processes. SRNL recommends that Hanford give careful consideration to how retrieval operations in the initial tank(s) can be instrumented to provide insights of generic value to subsequent tanks.

4.0 Fractional Crystallization

4.1 Fractional Crystallization & Crystal Separation Literature Review

Fractional crystallization processes are operations such as heating, cooling, solvent addition or removal used to recover two or more of the solutes from a multi-component solution. This literature focuses on sources not previously examined by past reviews. Previous reviews by CHG (Person 2004) are not covered by this review. Additionally, research conducted by CHG personnel (e.g. Herting) is also not covered by this review.

4.1.1 Fractional Crystallization

A detailed review of the literature is presented in Section 1.1. Synopses of several papers by Ng and other authors on crystallization system design are first presented in Section 1.1. Metastability and kinetically controlled crystallization are discussed next in 1.1. Finally, the effects of impurities and pH on crystallization and an interpretation of solubility data are given, followed by a description of several enhanced and alternative crystallization methods.

In crystallization, there is a metastable zone (See Figure 5) above the solubility curve where supersaturation exists. Crystallization in this region is possible, but does not necessarily occur. At the supersolubility limit (the upper bound of the metastable zone), crystallization will occur. The size of this zone is dependent on many factors. Because of this zone, unsaturated solutions cooled or concentrated to the solubility limit do not necessarily crystallize until the supersolubility limit is reached. The apparent solubility is thus higher than the actual value.

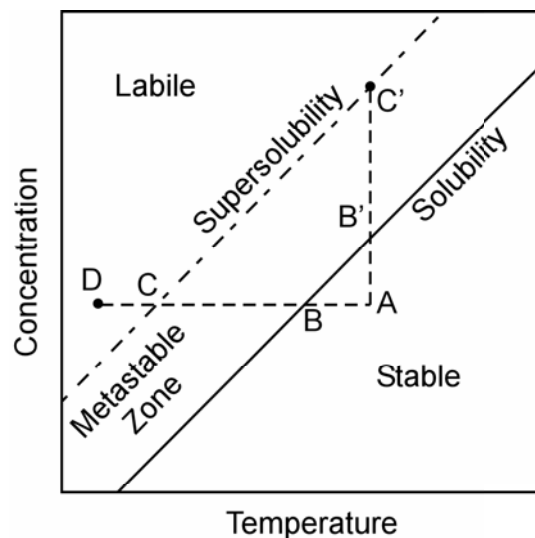


Figure 5 – Metastable Zone (Mullin 2001)

Metastable *phases* are transient solid phases (e.g., crystal structure, hydrate) that are not the thermodynamically most stable at a given set of conditions. Rather, the phase that is formed most quickly (fastest kinetics) is the one that occurs. Metastable phases are always more soluble than the stable phase. Metastable phases that are formed can actually be relatively stable, existing for minutes, hours, or even years. If the thermodynamically most stable phase is not the one produced, the predicted solubility will not match the measured (apparent, or non-equilibrium) value. Such behavior could account for the differences seen between evaporation experiments and thermodynamic predictions using ESP.

The potential particle size distribution problems related to crystallization in down stream processes is highlighted in Table 3. Table 3 points out the need for highly integrated process design and development activities for future crystallization processes.

Table 3 – Potential Particle Size Distribution Problems in Crystallization Processes – Wibowo 2001

Table 1. Potential PSD-Related Problems in Crystallization Downstream Processing

Potential Problems	Possible PSD-Related Sources					Other Possible Sources
	Too Much Fines	PSD Too Wide	PSD Too Narrow	Average Size Too Small	Average Size Too Large	
<i>Filtration</i>						
Batch filtration is too long, or required continuous filter area is too large		✓		✓		The cake is highly compressible. —
Filter system, including the filter medium, is easily clogged	✓					
<i>Washing</i>						
Solvent requirement is too high, leading to expensive recovery cost		✓		✓		The impurity adsorbs strongly on the crystals. The cake is highly compressible
Required washing time is too long, or larger than what is available in a continuous filter		✓		✓		
<i>Recrystallization</i>						
Impurity inclusion level is too high, such that recrystallization is necessary					✓	Crystal growth rate is too fast.
<i>Deliquoring</i>						
Deliquoring time to achieve a specified saturation level is too long, or larger than what is available in a continuous filter		✓		✓		The cake is highly compressible. —
Residual liquid content of the cake is too high	✓		✓			
<i>Drying</i>						
Required drying time is too long and energy consumption is too high		✓		✓		—
Too much dust in the drying system	✓					—
<i>Dissolution</i>						
Dissolution time is too long		✓			✓	—

Important chemical observations about crystallization:

- A metastable zone exists above the solubility of a species where crystallization may not necessarily occur, thus making the solubility appear to be higher than it actually is.

- For some species, metastable phases exist that are thermodynamically less stable than other phases, but are kinetically favored in crystallization.
- Metastable phases can be relatively stable, sometimes existing for very long periods of time.
- Metastable phases are always more soluble than the stable phase at a given set of conditions.
- Impurities can have unpredictable effects on crystallization. Impurities may do nothing; combine or react with the solute or solvent; make the solution supersaturated; or make the solution unsaturated. (For example, Nd⁺³ at 100 ppm totally inhibits the formation of the burkeite phase in the precipitation of sodium carbonate and sodium sulfate.)
- Particle size of the crystals formed can have a large impact on the downstream operating efficiency of the solid/liquid separation devices.

4.1.2 Separation Processes

The major technologies for separation of solids from liquids are filtration (crossflow, dead-end), gravity settling, and centrifuging (which includes centrifugal filtration). Crossflow filtration is the chosen technology used by the Hanford Waste Treatment Plant pretreatment system to separate the HLW solids from the LAW liquid. It is also the technology proposed for use in the SRS Salt Processing Program to remove sludge and monosodium titanate (MST) from dissolved salt.

A comparison of separation processes is shown in Table 4. Note that gravity settling is not compared. Appendix B, Section 6.0 provides a literature review of the solid-liquid separation process equipment.

There is a significant difference between the goals in the referenced reports on crossflow filtration and in the separation required for supplemental treatment by crystallization. In all of the reports found for crossflow filtration, the primary goal was to remove virtually all of the sludge solids from the waste by splitting it into a solids-free liquid and a (somewhat) concentrated slurry stream. For the crystallization process, removal of the liquid from the solid crystals is more important than removal of the solids from the liquid because it is the radioactive Cs in the liquid phase that needs to be removed from the solids. For this separation, carryover of small amounts of crystallized solids into the aqueous Cs-containing stream would be acceptable, whereas for the sludge separation, carryover is unacceptable. Due to this difference, the separation process chosen for crystallization will be considered more efficient if it removes more of the aqueous phase from the solids; i.e., the aqueous phase content of the solids at any step is as low as possible. The major impact of this difference on the selection of the separation process for crystallization is that methods that produce drier solids have an advantage over those producing more dilute solids. Hence, crossflow filtration, which produces a moderately

concentrated solids stream, has a disadvantage compared to dead-end filtration and centrifugation techniques that remove more water.

Crossflow filtration is the most established separation process for handling radioactive waste solids, and centrifugation is used in actinide and low-level radioactive waste processing. Crossflow filtration is very robust and requires relatively low maintenance, but is better for clarifying liquids than producing concentrated solids. Maximum solids concentrations with waste sludge are only around 30%. Washing efficiency in a crossflow filter is also low, with the system behaving as a continuous stirred tank reactor (CSTR).

Dead-end filters, such as tubular, centrifugal, and rotary drum filters all have the potential for recovery of more concentrated solids. The rotary drum filter is very efficient for solids collection and has the added advantage that washing can be performed in the same unit. Moreover, the washing process through the filter cake approaches plug flow, which is the most efficient. Rotary drum filters and solids washing have been used during plutonium processing at the Plutonium Finishing Plant and PUREX Plant at the Hanford Site. Plutonium oxalate was precipitated from a plutonium nitrate solution and the slurry fed to a vacuum rotary drum filter to separate and wash the plutonium oxalate¹⁰.

Applicable centrifuges are either continuous or semi-continuous. The decanter centrifuge, which separates only by sedimentation, can remove particles $<5\mu\text{m}$. Smaller particles can be removed if flocculants are used. The peeler, pusher, and screen bowl decanter centrifuges separate by sedimentation and filtration, so the particle separation is dependent of the filter media. Continuous washing may be done in the pusher and screen bowl types, and semi-continuous washing is done in the peeler. Washing in the screen bowl and peeler also approaches plug flow. The decanter centrifuge is not amenable to washing, with only 50-80% efficiency since it is difficult to contact the solids.

¹⁰ See RHO-MA-116, Addendum I, August 1982, PUREX Technical Manual plutonium Oxide Production & Rework Facilities Section 3.1.2 & 4.1-5 Rockwell Hanford Operations.

Table 4 – Comparison of Separation Techniques

<i>Separation</i>	<i>Sub-Type</i>	<i>Used in Nuclear Applications?</i>	<i>Concentrating Ability (wt% solids)</i>	<i>Clarifying Ability* (filtrate % solids)</i>	<i>Particle Sizes Separated* (µm)</i>	<i>Washing Efficiency (%)</i>	<i>Continuou s Separation</i>	<i>Continuou s Washing</i>	<i>Equipment Size per 10 gpm Feed</i>
<i>Crossflow Filtration</i>	Conventional	yes	low <30%	high <0.1	to submicron	low (CSTR)	yes	yes	>100 ft ² filter area (waste sludge)**
	Rotary	yes	low <30%	high <0.1	to submicron	low (CSTR)	yes	yes	>40 ft ² filter area (waste sludge)**
<i>Dead-End Filtration</i>	Tubular	unknown	Medium	medium-high	>1	unknown, washing difficult	cyclic	cyclic	unknown
	Centrifugal Discharge	yes (power plant water)	medium-high	medium-high	>1	unknown	yes	cyclic	unknown
	Rotary Drum	Yes, at Hanford in Pu Finishing Plant	very high	<1	>1 (>5 typical)	very high	continuous cycles	continuous cycles	25-200 ft ² filter area
<i>Centrifuges</i>	Disk Stack	Probably yes	low	High	0.1-100	not possible	yes	no	unknown
	Peeler	no	high	<1	>10	high	cyclic	cyclic	unknown
	Pusher	no	high	<5	>80	medium	yes	yes	unknown
	Decanter	yes	high	<1	>5 (less with flocculants)	low 50-80%	yes	yes	~40 ft ² footprint
	Screen Bowl Decanter	unknown	high	<1	>10	high	yes	yes	~40 ft ² footprint

Note: Range of crystals formed in Clean Salt tests was 50-190 µm (Herting 1996).

* For filtration based systems, clarifying ability and particle sizes separated depend on the filtering media.

** Filtration area required should be lower for larger particles.

The separation processes examined are ranked below in order of separation efficiency achieved. A solid phase with the least free liquid is ranked highest. The clarity of the removed liquid is not considered in the ranking. This method of ranking is chosen because minimizing the amount of cesium-containing liquid in the solids is most important. Small residual amounts of solids in the removed liquid are not considered detrimental since these solids would carry only a small amount of the salts to the LAW vitrification process. The ability to use these separation methods with radioactive solutions is not considered in the ranking.

1. Rotary Drum Filtration:
Very efficient at removal of large crystals; solids produced have the least liquid; washing in filter unit is possible; washing approaches plug flow, which is most efficient.
2. Screen Bowl Decanter Centrifuge:
Very efficient at removal of large crystals; solids produced have low liquid; washing in unit is possible; washing approaches plug flow, but not as much as the rotary drum filter.
3. Peeler Centrifuge:
Very efficient at removal of large crystals; solids produced have low liquid; washing in unit is possible; washing approaches plug flow; unit operates in a batch cycle.
4. Pusher Centrifuge:
Efficient at removal of large crystals; solids produced have low liquid; washing in unit is possible, but not as efficient as a screen bowl decanter; washing not as close to plug flow; liquid product higher in solids.
5. Decanter Centrifuge:
Efficient at removal of large crystals; solids produced have low liquid; washing in unit is possible, but very inefficient due to poor mixing with cake; has been used in nuclear applications.
6. Centrifugal Discharge Filter:
Similar to screen bowl decanter centrifuge or rotary filter; solids collected are wetter than above methods; some washing in unit possible.
7. Rotary Crossflow Filter:
Poorer ability to concentrate solids (better at clarifying liquid); solids relatively high in liquid; low throughput possible depending on solids; washing very inefficient (CSTR at best).
8. Conventional Crossflow Filter:
Same as rotary, except throughput lower.

9. Tubular Filter:

Not generally used for concentrated solids streams; low solids-handling capacity; solids produced are wet; operation is cyclic.

4.2 AP104 Boildown Modeling Evaluation

The purpose of this work was two-fold: (1) to assess how well the Environmental Simulation Program (ESP) can predict the volume fraction of bulk solids that formed during a recent boildown of the composite AP-104 supernate sample,¹¹ and (2) to determine if any work can be done on the ESP database to improve its predictive capability. The AP-104 boildown experiment which was carried out in support of the Evaporator Campaign 04-02 was modeled using the Environmental Simulation Program ESP v6.7. The private databases, WTPBASE and NAFPO4, were used in conjunction with the software default PUBLIC database to describe the relevant multi-electrolyte equilibria.

4.2.1 Results of ESP Model

The predicted volume and mass fractions of solids in the pot are compared in Table 5 against the measured data at various WVR's. Although one quick glance clearly reveals the trend that the discrepancies between predicted and measured solids fractions are not only large but increase with increasing WVR, direct comparison of the two was only possible at 45 and 50% WVR. This was because within the time limit put on this work the vapor target for each evaporation stage could not be fine tuned to achieve a constant 5% WVR in each stage.

The measured volume percent data for the centrifuge solids were taken directly from Tables 2 and 3 in Reference¹¹, while the weight percent solids data were calculated from the data given in the same tables. For example, at nominal 50% WVR, the weight of centrifuged solids was calculated as the difference between the cone re-gross centrifuged solids only weight and the cone tare weight:

$$20.265 \text{ g} - 6.6236 \text{ g} = 13.6414 \text{ g}$$

The weight of centrifuged liquid was calculated as the difference between the blow-dried cone gross weight and the cone re-gross centrifuged solids only weight:

$$21.846 \text{ g} - 20.265 \text{ g} = 1.581 \text{ g}$$

The weight percent of centrifuged solids is then:

$$13.6414 / (13.6414 + 1.581) (100) = 89.6\%$$

¹¹ Bechtold, D. B., and Cooke, G. A., "Tank 241-AP-104 Liquid Composite Re-Boildown Study for Evaporator Campaign 04-02," Interoffice Memo to T. M. Horner, 7S110-DBB-03-013, CH2M Hill Hanford Group, Inc., Richland, Washington, December 8, 2003.

As shown in Table 5, the model correctly predicted most of the solid phases identified at various WVR's. However, the formation of $NaNO_3$ crystals was not predicted at 45% WVR or 9.6 M Na , although it was identified as one of the major species by x-ray diffraction (XRD). It is not clear whether this discrepancy was due to the over prediction of the $NaNO_3$ solubility or if the detection of $NaNO_3$ by XRD should have been attributed to the precipitation of liquid that dries on the filter during the sample preparation, just as it was at 30 and 40% WVR. At first, it seems that even if the model did over predict the solubility of $NaNO_3$, it would still not be enough to explain the fact that the measured volume and mass fractions of solids were larger than their predicted counterparts by a factor of 23 and 14, respectively.

Table 5 - Results of AP-104 Supernate Boildown Simulation Using ESP Model

% WVR	vol% Solids		wt% Solids		Bulk Density (g/ml)		Solids Phases	
	model	Data (centrifuged)	model	Data (centrifuged)	model	Data	Model	Data
0	0	0	0	0	1.251	1.277	-	-
6	0.08	-	0.21	-	1.275	-	Na ₂ C ₂ O ₄ Na ₇ F(PO ₄) ₂ .19H ₂ O	- -
11	0.11	-	0.27	-	1.289	-	Na ₂ C ₂ O ₄ Na ₇ F(PO ₄) ₂ .19H ₂ O	- -
15	0.14	-	0.32	-	1.303	-	Na ₂ C ₂ O ₄ Na ₇ F(PO ₄) ₂ .19H ₂ O	- -
20	0.16	-	0.38	-	1.319	-	Na ₂ C ₂ O ₄ Na ₇ F(PO ₄) ₂ .19H ₂ O	- -
24	0.18	-	0.42	-	1.336	-	Na ₂ C ₂ O ₄ Na ₇ F(PO ₄) ₂ .19H ₂ O	- -
29	0.21	-	0.46	-	1.354	-	Na ₂ C ₂ O ₄ Na ₇ F(PO ₄) ₂ .19H ₂ O	- -
30	-	3.8	-	5.6	-	1.392	- -	Na ₂ C ₂ O ₄ Na ₇ F(PO ₄) ₂ .19H ₂ O
33	0.2	-	0.46	-	1.374	-	Na ₂ C ₂ O ₄ Na ₇ F(PO ₄) ₂ .19H ₂ O	- -
35	-	10.1	-	10.8	-	1.428	-	not reported
38	0.21	-	0.42	-	1.392	-	Na ₂ C ₂ O ₄ Na ₇ F(PO ₄) ₂ .19H ₂ O	- -
40	-	17.7	-	10	-	1.453	- -	Na ₂ CO ₃ .H ₂ O Na ₇ F(PO ₄) ₂ .19H ₂ O
42	0.4	-	0.8	-	1.411	-	Na ₂ CO ₃ .H ₂ O Na ₂ C ₂ O ₄ Na ₇ F(PO ₄) ₂ .19H ₂ O	- - -
45	1.3	18.1	2.1	14.9	1.424	1.482	- Na ₂ CO ₃ .H ₂ O Na ₂ C ₂ O ₄ Na ₇ F(PO ₄) ₂ .19H ₂ O	NaNO ₃ Na ₂ CO ₃ .H ₂ O Na ₂ C ₂ O ₄ Na ₇ F(PO ₄) ₂ .19H ₂ O
47	1.9	-	3	-	1.434	-	NaNO ₃ Na ₂ CO ₃ .H ₂ O Na ₂ C ₂ O ₄ Na ₇ F(PO ₄) ₂ .19H ₂ O	- - - -
50	4.1	93.4	6.4	89.6	1.458	1.522	NaNO ₃ Na ₂ CO ₃ .H ₂ O Na ₂ C ₂ O ₄ Na ₇ F(PO ₄) ₂ .19H ₂ O	NaNO ₃ Na ₂ CO ₃ .H ₂ O Na ₂ C ₂ O ₄ Na ₇ F(PO ₄) ₂ .19H ₂ O

These large discrepancies between predicted and measured quantities of bulk solids that form during boildown can also be attributed in part to the inherent nature of the ESP software. As shown in the attached model output of pot liquid compositions, the physical properties of bulk solids are calculated by the model based on the assumption that they form a bone-dry matrix not containing any interstitial liquid. On the contrary, experimental observations have shown that depending on the habit and morphology of crystals or gels that are forming, a relatively small mass of solids can entrain a much larger quantity of liquid, thus resulting in a significant volume expansion. For example, during a pretreated AN-107 evaporation study with regulatory organic spikes^{12,8} much of the cloudy liquid was seen to suddenly turn into precipitates just as the solubility limit of NaNO_3 was exceeded at 10.3 M Na. In principle, this sudden expansion of bulk solids volume accompanying the precipitation of major salts cannot be captured properly by the ESP or any other thermodynamic modeling tool.

The under predicted volume and mass fractions of solids were next plotted in Figure 6 and Figure 7, respectively, as a function of WVR along with their measured counterparts. It is shown that both predicted and measured solids fractions increased gradually with increasing WVR of up to 42% and 45% WVR, respectively, where they both began to increase sharply with further increase in the WVR. It is interesting to note that the formation of $\text{Na}_2\text{CO}_3 \cdot \text{H}_2\text{O}$ needles was first predicted at 42% WVR or 9.4 M Na, and the slopes of the predicted solids fraction curves became even steeper when the precipitation of the most abundant salt, NaNO_3 , was first predicted at 47% WVR or 9.8 M Na. Incidentally, the increased slopes of the predicted volume and mass fraction curves at 47% WVR or higher are shown in Figure 6 and Figure 7, respectively, to be identical to those of the measured volume and mass fraction curves at 45% WVR or higher, where the formation of NaNO_3 crystals was also first observed by XRD.

This means that the solids fraction vs. WVR curves for the AP-104 boildown exhibited a rather sharp break point when one or more of the major salt species started to precipitate out. This result is indeed consistent with the observation made earlier during the AN-107 regulatory evaporation test¹²; the precipitation of the most abundant salt, NaNO_3 , at 10.3 M Na was accompanied by a sudden expansion of the bulk solids volume. However, both predicted and measured bulk solution density profiles shown in Figure 8 did not exhibit any break points at all WVR's. Considering the fact that the ESP model successfully predicted most of the solid phases identified at various stages of boildown, this result seems to suggest that the sudden expansion of the bulk solids volume is initiated by the precipitation of one or more of the major salt species; but, much of the volume change may be due to the entrainment of liquid in the solids matrix that forms as a result of the phase transformation.

The significance of Figure 6 and Figure 7 to the actual evaporation operation is that the accurate determination of the break point(s) in the solids fraction vs. WVR curves may help determine the target endpoint for the optimum evaporator performance. For

¹² Saito, H. H., Calloway, T. B., Ferrara, D. M., Choi, A. S., White, T. L., Gibson, Jr., L. V., and Burdette, M. A., "AN-107 (C) Simulant Bench-Scale LAW Evaporation with Organic Regulatory Analysis," WSRC-TR-2000-00486, Westinghouse Savannah River Co., Aiken, South Carolina, December 2000

example, concentrating the AP-104 supernate beyond 45% WVR would not be a good idea, since the solids loading would then become excessively high too quickly so that there would not be much liquid left to decant in the end, and the operational margin for recovering from unexpected incidents would be greatly reduced. In conclusion, although the ESP model would inherently predict too low solids fractions at all WVR's, it may still be possible to determine the optimum evaporation endpoint using the predicted solids fraction profiles coupled with the accurate solubility data for all major salts that can potentially form.

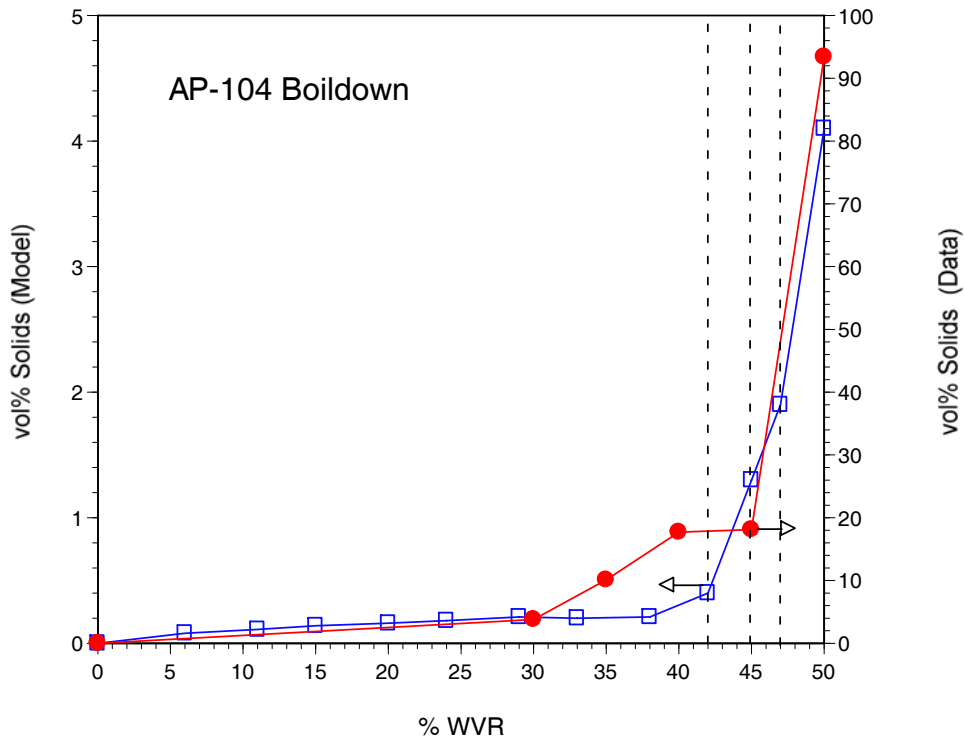


Figure 6 - Profiles of Predicted and Measured Volume Percent Solids.

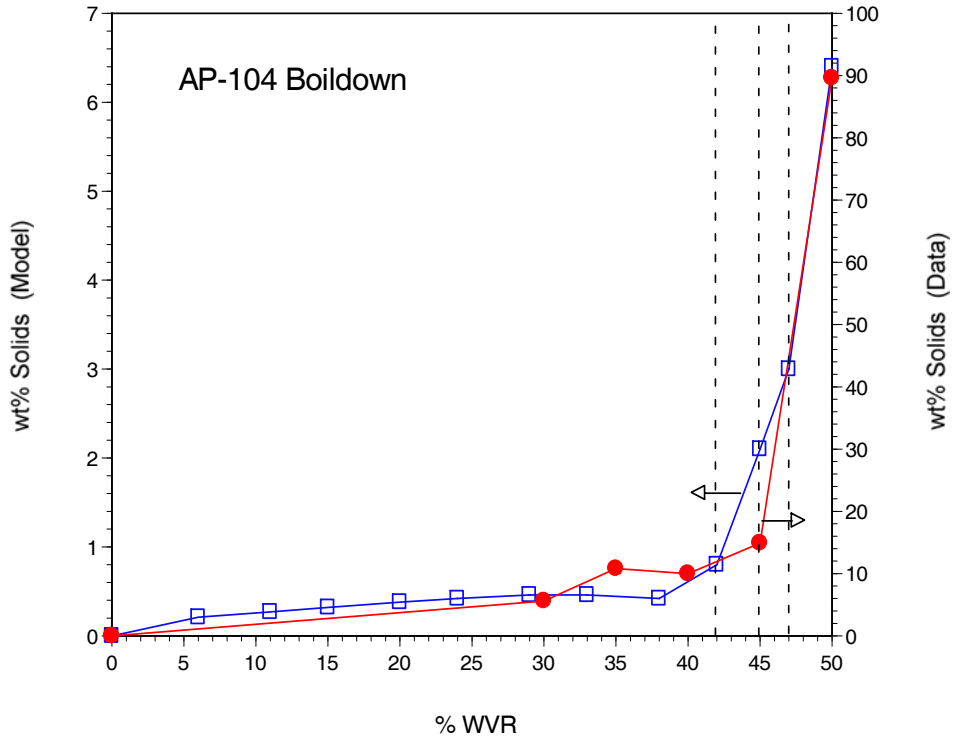


Figure 7 - Profiles of Predicted and Measured Weight Percent Solids

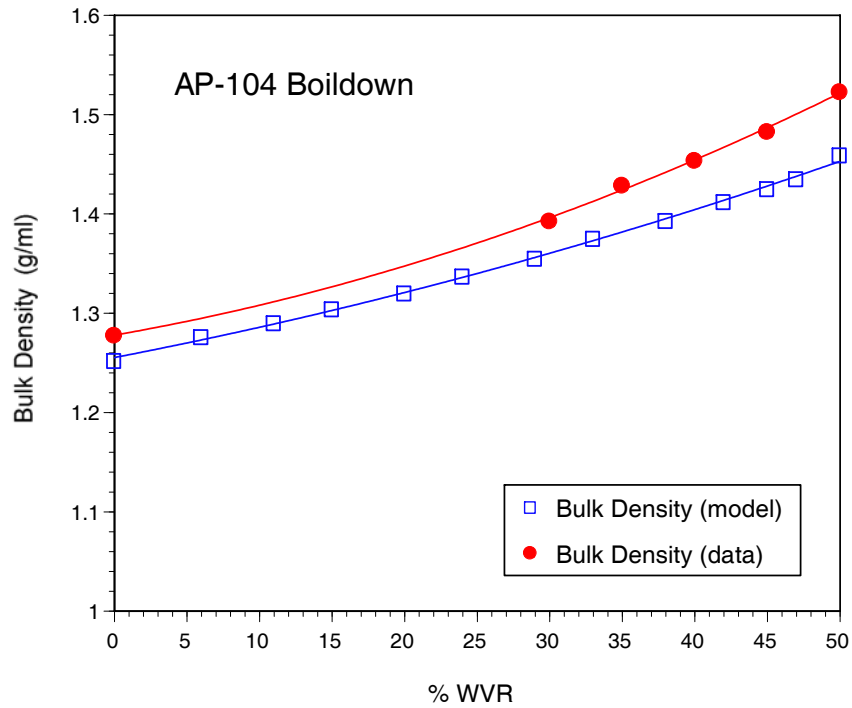


Figure 8 – Comparison of Predicted vs. Measured Bulk Density

5.0 Appendix A - SRS Salt Waste Dissolution History – Annotated Bibliography

5.1 In-Tank Salt Removal

- D. L. Kisler, “Removal of Salt from High-Level Waste Tanks by Density-Driven Circulation or Mechanical Agitation,” DP-1587, January 1981.
- D. E. Morgan, “History of Salt Cake Dissolution at SRS,” HLW-SDT-2002-00060, May 2002.
- D. E. Morgan, “Operational Experience with Salt Disposition,” HLW-SDT-2002-00060, May 2002.

This section outlines the prior documentation of practical operating experience with saltcake dissolution at SRS. The three references given above also provide summary information on in-tank dissolution. They were up-to-date at the time of their writing. The table below contains information on the tank configuration useful in the interpretation of the tank-specific information.

Table 6 – SRS Tank Configurations for Selected Salt Waste Tanks for which Salt Dissolution Operations Were Conducted

Tank Type	I	II	III/IIIA	IV
Salt Dissolution Tanks	10	16 annulus	33, 37, 41, 49	17, 19, 20, 22, 24
Capacity	750 kgal	1.0 Mgal	1.3 Mgal	1.3 Mgal
Vol./Ht. Factor	2710 gal/in	3500 gal/in	3510 gal/in	3540 gal/in
Support	Columns	Center Column	Center Column	Domed Roof
Secondary Containment	Pan	Pan	Full liner	None
Cooling Coils?	Yes	Yes	Yes	No
Stress Relieved?	No	No	Yes	No

5.1.1 Tank 10

- G. H. Street, "Salt Removal from Tank 10 (2-959)", DPSOX-9168, April 9, 1979.
- J. C. Bailey, "Tank 10 Salt Removal Demonstration Details," DPSP-79-17-11, April 11, 1979.
- W. L. West, "Mechanical Assistance for Salt Dissolution by the Density Gradient Technique," memorandum to D. C. Nichols, December 27, 1979.
- W. L. West, "Mechanically Assisted Density Driven Salt Dissolution," memorandum to D. C. Nichols, February 14, 1980.
- G. H. Street, "Salt Removal from Tank 10 (2-959A)", DPSOX-9272, March 31, 1980.
- "Tank 10 Salt Removal Demonstration," Waste Management Technology Teletype, April 25, 1979 – May 29, 1979.
- G. H. Street, "Salt Removal from Tank 10 (2-959B)", DPSOX-9342, December 9, 1980.
- D. L. Kisler, "Removal of Salt from High-Level Waste Tanks by Density-Driven Circulation or Mechanical Agitation," DP-1587, January 1981.
- C. J. Thomas, "Tank 10 Transfer Plan," memorandum to L. E. McCarthy, November 18, 1982.

Tank 10 is a 750 kgal Type I tank in the west portion of H tank farm. Approximately 140 kgal of saltcake was dissolved and removed using the density gradient technique. Initially, the tank contained 500 kgal of saltcake with a thickness of about 200 inches. To enable transfer of dissolved material out of Tank 10, a steam jet was mined into the saltcake to within 95 inches of the tank bottom. The dissolution fluid was dilute low-level waste water from the Receipt Basin for Offsite Fuels (RBOF), which was jetted from Tank 23.

When about 28% of the salt had been dissolved, the specific gravity of the supernate averaged 1.38, the liquid temperature was 50 to 55 °C and the dissolution rate was ~0.43 cm/hr. When about 50% of the salt had been dissolved, the specific gravity of the supernate had decreased to about 1.30 and the dissolution rate had diminished to ~0.30 cm/hr. Visual inspection revealed sludge covering a high mound opposite the location of the transfer jet, which covered about one-third of the cake surface area. Although it was not yet employed in Tank 10 salt removal, it was evident that mechanical agitation was necessary after the density-driven circulation reached a point of diminishing returns. All in all, approximately 300 kgal of salt was removed from Tank 10, leaving 200 kgal remaining today.

An additional issue encountered during Tank 10 salt removal was the discovery of a thin sheet of salt above the liquid level clinging to the cooling coils and columns. The initial dissolution did not add enough fluid to cover the highest regions of salt, causing a portion of the salt to be undercut. Water was added to increase the tank level to above this sheet, resulting in its dissolution and removal.

5.1.2 Tank 16 Annulus

- D. E. Gordon, "Removal of Waste Salt from Annulus of Tank 16," DPSPU-77-272-135, May 16, 1977.
- O. M. Morris and D. E. Gordon, "Tank 16 Annulus Cleaning," memorandum to J. R. Hilley, July 6, 1977.

Tank 16 is a 1 Mgal Type II tank in the west portion of H tank farm. Leakage of the Tank 16 primary tank liner in 1960 left approximately 6000 gallons of waste salt cake residing in the 2-1/2 foot wide annular space between the primary tank and the 5 foot high secondary pan. Dried salt deposits were also adhering to the outer surface of the primary tank at the leak sites. Salt dissolution in the secondary containment commenced in 1977 in order to transfer the dissolved salt material back to primary containment.

Low-heat waste was added to the primary tank as ballast. Water with corrosion inhibiting chemicals (caustic and sodium nitrite) was heated to 75 °C and added to the Tank 16 annulus. Circumferential flow of the dissolution fluid in the annulus was promoted by three steam jets placed at three quadrants of the annulus with discharge nozzles directed clockwise. Once circumferential flow had been established, steam was sprayed into the top of the annulus to dissolve salt deposits on the wall surfaces. Ten hours of steam spray operation have removed an estimated 90% of the salt deposits above the middle weld and 20% below the middle weld. Three transfers of salt solution were made removing an estimated 25,500 pounds (1391 gallons) of salt cake.

5.1.3 Tank 17

H. H. Elder, "Waste Transfer from Tanks Containing Alternate Sludge – Salt Layers," memorandum to J. C. Bailey, August 21, 1980.

K. S. Swigart, "Tank 17F Waste Removal Program," memorandum to J. H. Hershey, September 19, 1983.

K. S. Swigart, "Tank 17F Waste Removal (2-1047)", DPSOX-9672, October 24, 1983.

W. Parish, "Open Technical Issue HLE-TI-93-023: Waste Removal from Mixed Salt/Sludge Tanks (U)," HLW-HLE-94-0399, 1994.

Tank 17 is a 1.3 Mgal Type IV tank located in F tank farm. A mechanical agitation method was utilized because Tank 17 contained layers of salt and sludge. Seven batches of salt/sludge were removed from Tank 17 from June of 1980 to July of 1985. Three slurry pumps and a slurry transfer pump were used. Almost 1,000,000 gallons of layered salt/sludge were removed without significant incidents.

5.1.4 Tank 19

A. Q. Goslen, "Tank 19 Salt Dissolution Test Details," memorandum to E. J. O'Rourke, May 19, 1980.

A. Q. Goslen, "Salt Removal from Tank 19 (2-981)", DPSOX-9292, May 29, 1980.

D. L. Kisler, "Removal of Salt from High-Level Waste Tanks by Density-Driven Circulation or Mechanical Agitation," DP-1587, January 1981.

A. Q. Goslen, "Tank 19 Salt Removal," DPSP-84-17-7, August 1986.

Tank 19 is a 1.3 Mgal Type IV tank in F tank farm. From July 1980 to July, 1981, over one million gallons of radioactive waste salt were removed from Tank 19 in four batches by the mechanical agitation method. About 98% of the salt, and 86% of the radionuclides, were removed. Water and salt volumes, solution temperatures, and equipment performance were monitored during the process. Over 2,300,000 gallons of water was added in four batches, for an overall water/salt volume ratio of 1:2.31. About 13,000 gallons of solid salt, 13,000 gallons of zeolite, and 7,000 gallons of sludge remained in the tank. Equipment performance was adequate, though several failures caused some delays.

During the first two batches, the solution density asymptotically approached the saturation density. Agitation efficiency affected the dissolution rate. The third and fourth batches show this by the sharp changes in the density curves which occurred when a pump was lowered further into the

tank and when a second pump was started. During the first batch, salt dissolved at the expected rate. The actual density was above the calculated value because the solution already contained dissolved salt when agitation began. During the second batch, the salt dissolved more slowly than expected. The cause was less effective agitation. Slightly lower salt solubility may also have reduced the dissolution rate, but for the second batch this effect was small compared with agitation effects. During the last two batches, both agitation and solubility affected dissolution rates. Selective dissolution of the more soluble salts reduced the solubility of the remaining salt. Laboratory sample analyses showed the final solutions of the third and fourth batches to be nearly saturated at relatively low densities. The reduced solubility significantly reduced the dissolution rate. The dissolution rate from the Tank 19 demonstration does not reflect a benefit from the added time and cost of installing and maintaining slurry pumps to dissolve waste salts.

Table 7 – Tank 19 Salt Batch Compositions

	Batch			
	I	II	III	IV
Density	1.38	1.35	1.25	1.23
OH ⁻	1.6M	1.7M	1.8M	1.3M
NO ₂ ⁻	0.1M	0.2M	0.1M	0.1M
NO ₃ ⁻	4.7M	4.5M	3.2M	3.1M
AlO ₂ ⁻	NA	0.4M	0.7M	0.5M
SO ₄ ⁻⁻	NA	0.5M	0.2M	0.3M
CO ₃ ⁻⁻	NA	0.1M	<0.1M	<0.1M

5.1.5 Tank 20

- D. P. Steinmentz, “Tank 20 Salt Removal Details,” memorandum to E. J. O’Rourke, July 27, 1979.
- H. H. Elder, “Salt Removal from Tank 20 (2-970)”, DPSOX-9235, October 31, 1979.
- W. L. West, “Tank 20 Salt Removal Details,” memorandum to E. J. O’Rourke, May 1, 1980.
- W. L. West, “Tank 20 Density Driven Salt Removal,” memorandum to J. H. Hershey, August 30, 1982.
- J. N. Chen, “Tank 20F Salt Removal Test Plans,” memorandum to J. H. Griffin, July 13, 1984.
- J. N. Chen, “Salt Removal from Tank 20F (2-1070)”, DPSOX-9762, September 18, 1984.
- J. N. Chen “Tank 20 Waste Removal Batch #1 Plans, Revision 2,” memorandum to J. E. Herbert, January 23, 1986.
- J. N. Chen, “Batch #3 Inhibited Water Addition to Tank 20, memorandum to S. M. Tom, July 23, 1986.

Tank 20 is a 1.3 Mgal Type IV tank in the F tank farm. Salt was removed in two campaigns, the first in 1980 utilizing the density gradient method and the second in 1986 using mechanical agitation provided by three slurry pumps. Approximately 700 kgal of saltcake was removed by the density gradient technique, but the process was stopped when the salt solution was outside of the technical corrosion limits. The remaining ~350 kgal of salt was removed in three batches with the addition of corrosion inhibited water and mechanical agitation using three slurry pumps.

5.1.6 Tank 22

- H. H. Elder, "Waste Transfer from Tanks Containing Alternate Sludge – Salt Layers," memorandum to J. C. Bailey, August 21, 1980.
- D. L. Kisler, "Removal of Salt From High-Level Waste Tanks by Density-Driven Circulation or Mechanical Agitation," DP-1587, January 1981.
- D. M. Rushin, "Tank 22H Waste Removal (2-1098)", DPSOX 9929, February 6, 1986.
- W. Parish, "Open Technical Issue HLE-TI-93-023: Waste Removal from Mixed Salt/Sludge Tanks (U)," HLW-HLE-94-0399, 1994.

Tank 22 is a 1.3 Mgal Type IV tank in the west portion of H tank farm. Tank 22 was dissolved using two dissolution schemes. First, the density-driven scheme of Drain-Add-Sit-Remove was used from 1971 to 1972 to dissolve ~275 kgal of saltcake. This process utilized a mined well and the addition of dilute low-level RBOF waste from Tank 23. In the later stages of dissolution when the well became too shallow to utilize the DASR method efficiently, the remaining saltcake was dissolved in 1972 to 1973 using mechanical agitation by steam jet recirculation. Due to the lack of cooling capability in the Type IV tanks, the steam jet recirculation method caused heating of the tank contents to 80 °C to 90 °C, which increased the risk of stress corrosion cracking. Approximately two years were required for the tank contents to cool.

5.1.7 Tank 24

- W. L. West, "Tank 24 Salt Dissolution Plan," memorandum to G. M. Johnson, May 13, 1981.
- "Tank 24 to 41 Transfer Plan (Batch 2)" January 21, 1982.
- C. J. Thomas, "Salt Decontamination Demonstration," memorandum to E. J. O'Rourke, February 7, 1983.
- H. H. Elder, "Salt Removal Program (2-996)," DPSOX- 9369, April 27, 1981.
- C. J. Thomas, "Completion of Tank 24 Salt Removal," memorandum to R. W. Wilson, June 27, 1983.

Tank 24 is a 1.3 Mgal Type IV tank in the west portion of H tank farm. Tank 24 salt removal was accomplished from 1981 to 1983 using a method that was based on Tank 19 operating experience. Salt was dissolved using corrosion inhibited water and low-level RBOF waste from Tank 23 and providing mechanical agitation by two slurry pumps. Four to six batches of dissolution fluid were added to remove ~600 kgal of saltcake.

5.1.8 Tank 33

- M. S. Peters, "Tank 33 Salt Removal," memorandum to D. J. Coon, March 15, 1983.

Tank 33 is a 1.3 Mgal Type IIIA tank in F tank farm. Partial salt removal from Tank 33 was conducted in 1982 in order to prepare the tank for fresh high-heat waste receipt service. The objective was to dissolve crystalline salt formations from the tank wall and cooling coils so that maximum cooling from the coils could be attained and that the risk of stresses from fresh waste undercutting the salt would be eliminated. About 100 kgal of salt was removed using the Drain-Add-Sit-Remove technique, with a sit time of 9 days proving adequate. Low-heat waste supernate from Tank 47 was used to dissolve the salt in Tank 33 because of its low density and adequate inhibitor concentration. About 96% (99,000 gallons) of a low self-supporting mound beneath the concentrate inlet riser was removed, and the small mound remaining was not in contact with a cooling coil or the tank wall.

5.1.9 Tank 37

Q. L. Nguyen, "Tank 37 Salt Removal Operating Plan," U-ESR-H-00039, Rev. 3, January 2003.

Tank 37 is a 1.3 Mgal Type III tank in the west portion of H tank farm. In 2002, approximately 200 kgal of salt was dissolved and removed from Tank 37 to enable the use of this tank as a concentrate receipt tank for the 3H-evaporator system. Inhibited water was added to the tank in four batches utilizing the Drain-Add-Sit-Remove technique. A telescoping transfer jet was mined into the salt and a portion of the saltcake interstitial liquid was drained and transferred elsewhere. The partial draining of the salt pres allowed the inhibited water dissolution fluid to flow into the saltcake upon addition. The salt was removed in four batches, the first of which took about 7 months to complete due to facility conflicts. All of the salt dissolution batches reached densities approaching 1.4 at the pump location very quickly. Little sit time was needed, and the density was monitored during transfer. The highest measured hydrogen concentrations in the vapor space were obtained at the end of the transfer cycles, when salt cover was at a minimum. After a transfer was stopped, the hydrogen concentration immediately decreased.

5.1.10 Tank 41

- L. B. Romanowski, "Tank 41 Low Curie Salt Process History and Data Analysis," CBU-SPT-2003-00224, Rev. 0, December 18, 2003.
- C. J. Martino and R. L. Nichols, "Tank 41H Drained Saltcake Core Sample Analysis (HTF-E-03-033 – HTF-E-03-035)," WSRC-TR-2003-00227, Rev. 0, December 16, 2003.
- C. J. Martino, "Tank 41H Dissolved Saltcake Sample (HTF-E-03-91 – 92) Saltstone Waste Acceptance Criteria Analysis," WSRC-TR-2003-00380, Rev. 1, September 22, 2003.
- C. J. Martino, R. L. Nichols, and M. R. Millings, "Tank 41H Post-Dissolution Saltcake Core and Supernate Sample Analysis," WSRC-TR-2004-00165, Rev. 0, April 22, 2004.

Tank 41 is a 1.3 Mgal Type III tank in H tank farm east. In July 1996, approximately 1700 gal of water was added to dissolve salt by the modified density gradient technique. This produced about 7000 gal of potential feed for the In-Tank Precipitation (ITP) process for cesium removal. This solution was not transferred out of Tank 41 due to problems with the ITP process.

A second salt dissolution in support of the Low-Curie Salt (LCS) accelerated salt processing initiative was carried out beginning in 2002. The original plan for Tank 41 combined aspects of the Drain-Add-Sit-Remove and the Modified Density Gradient salt dissolution schemes. The previous dissolved salt supernate was transferred to another tank and the 1.23 Mgal of saltcake was drained of 152 kgal of interstitial liquid. Data from the mining and draining activities and results from the annulus gamma scans all indicate that at least two levels within the saltcake, approximately 260 inches and 200 inches from the tank bottom, may contain saltcake with physical/chemical properties different from the other levels within the tank.

After completing interstitial drainage, approximately 244,000 gallons of flushwater were added back into Tank 41 to dissolve the saltcake. The salt that was dissolved near the saltcake surface passed through a large portion of the remaining saltcake, mixing with interstitial liquid and increasing in cesium concentration. The salt solution resulting from this dissolution activity has not yet been transferred from the tank. Dip samples and annulus gamma scan results show that as the salt solution sits in the tank, the residual interstitial liquid is mixing with the salt solution and

the ^{137}Cs concentration of the bulk liquid is increasing. It is predicted that the ^{137}Cs concentration of the bulk salt solution could get as high as 1.0 Ci/gal.

5.1.11 Tank 49

- L. B. Romanowski, "Path Forward: Tank 49 Salt Water Addition, Salt Dissolution," CBU-SPT-2004-00070, Rev. 0, April 1, 2004.
- L. B. Romanowski, "Tank 49 Salt Removal Scope Document," CBU-SPT-2003-00092, Rev. 1, May 10, 2004.
- E. E. Seufert, "Tank 49 Ready for Actinide Removal Process," CBU-SPT-2004-00148, June 24, 2004.
- Q. L. Nguyen, "Tank 49 Salt Dissolution Evaluation and Data Analysis," CBU-SPT-2004-00173, August 17, 2004.

Tank 49 is a 1.3 Mgal Type III tank in H tank farm east. Tank 49 returned to High Level Waste service in September 2001 following the removal of residual organics (mainly sodium tetraphenylborate) from the In-Tank Precipitation (ITP) process. Tank 49 received approximately 800 kgal of material, mainly warm concentrated supernate from the 3H-evaporator system (Tanks 30, 32) and supernate and drained interstitial liquid from Tank 41. The Tank 49 supernate was transferred to Tank 42 in April 2004 to prepare Tank 49 for use as the feed tank to the Actinide Removal Process (ARP).

After the supernate transfer, approximately 37 kgal of saltcake remained on the tank bottom and on the walls and cooling coils in the lower portion of Tank 49. In order to dissolve this residual salt, 65 kgal of inhibited water was added to the tank and a quad-volute slurry pump was operated for 72 hours. The fluid sat without activity for 60 days, after which the dissolved saltcake solution was transferred to Tank 35 using the telescoping transfer pump installed in Tank 49. The density of the dissolved salt solution was estimated as 1.41 g/mL and approximately 98% of saturation at 30 °C had been obtained. Results from a post-dissolution corrosion sample showed the dissolved salt solution to be 4.8 M NO_3^- , 2.5 M OH^- , and 0.63M NO_2^- . Video inspection showed only a small (270 gal) area of salt remained in the northwest quadrant of the tank.

5.2 Laboratory Salt Dissolution Testing and Modeling

5.2.1 Simulant Dissolution Tests

- C. B. Goodlett, "Concentration of Radioactive Wastes," DP-1135, June 1968.

In order to keep waste storage costs at a minimum, SRS evaporates radioactive wastes from the processing of irradiated fuel elements to reduce the volume to approximately 1/3 of the original liquid. The thrust of this study is testing involving the evaporation of actual and simulated SRS waste. Physical and chemical data is gathered on evaporation cycles for several types of waste. Additionally, the rate of dissolution of synthetic waste crystals was determined to provide basic data for removal of the crystals from the tanks.

During all evaporations, the sodium nitrate, sulfate, and carbonate concentrate predominantly into the crystals while the supernatant liquid is enriched in sodium hydroxide and aluminate. Blocks of granular sodium nitrate waste simulant were prepared and tested to determine the dissolution rate at various temperatures. As seen in the figure below, the dissolution rates attained regularly exceeded 0.1 ft/hr.

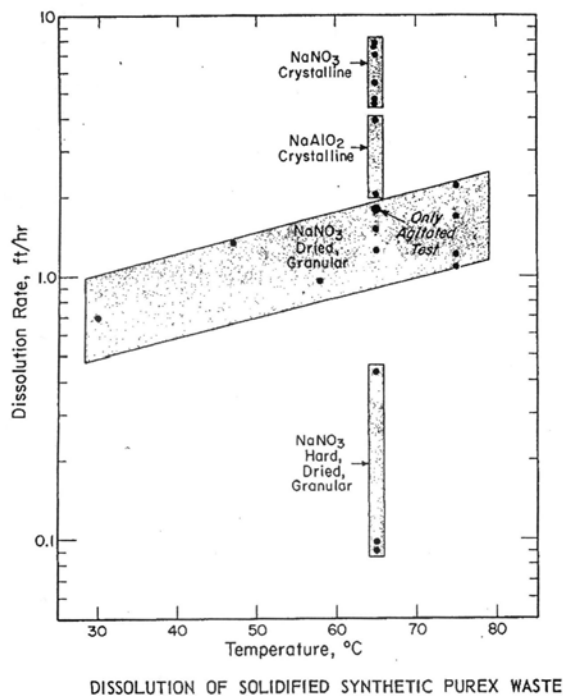


Figure 9 – Dissolution of Solidified Synthetic PUREX Waste – Dissolution Rates of 0.1 ft of Saltcake/hr Achieved during Testing

B. S. Johnson and J. E. Flanders, “Test of Waste Concentrate Coolers – RTA 553-S, Preliminary Results,” memorandum to A. S. Barab, November 9, 1970.

The use of additional bayonet-style coolers to assist in supernate cooling in several tanks at SRS was under investigation. Testing was conducted to study the slat buildup and potential buildup removal methods for these cooling systems. The optimal salt-removal method involved adding a small amount of water (1:1 water:salt volume ratio) via a movable spray ring and applying a mechanical force to knock off parts of the loosened salt. During saltcake simulant testing, the thermal conductivity of the deposits was measured to be slightly greater than 0.5 Btu/hr-ft²-°F/ft.

D. L. Kisler, “Removal of Salt from High-Level Waste Tanks by Density-Driven Circulation of Mechanical Agitation,” DP-1587, January 1981.

This study investigated new concepts for saltcake dissolution that arose from problems with the Tank 22 dissolution. The density gradient technique was initially employed. The steam circulation jets used later in Tank 22 dissolution were ideal for their lack of moving parts and ease of use, but they caused heating of the tank contents to 80 °C to 90°C, which increased the risk of stress corrosion cracking. Bench scale simulation of Tank 19 dissolution was 85-times faster than the in-tank demonstration, corresponding to the ratio of the diameters of the two vessels.

Several tests were performed to highlight the factors that affect the rate of dissolution. A bench-scale experiment showed that vertical-plane dissolution rate (3.05 cm/hr) was significantly higher than the horizontal-plane dissolution rate (0.06 cm/hr). During continuous dissolution using the density gradient technique, the dissolution rate at 40°C was 0.12 cm/hr faster (17% faster) than for an experiment at 20°C. The dissolution rate increase corresponded to a similar solubility increase for nitrate or nitrite over the same temperature range. Agitation was seen to increase the

dissolution rate, but it resulted in a crater with ledges that was visible under the stirrer. Bench-scale tests showed that density-driven circulation dissolved a salt cake almost as fast as simulated steam-jet circulation, but significantly less rapidly than circulation by mechanical agitation.

The density-driven technique has two disadvantages. As the well becomes shallow, approaching a cake heel in the tank, the dissolution rate diminishes to the rate in the horizontal plane. And, if sludge is dispersed to any significant extent (probably several percent) in the salt cake, the sludge will settle out as the salt dissolves and blanket the cake surface, reducing the dissolution rate. Agitation of the liquid above the salt surface by mechanical agitators or centrifugal pumps would overcome the disadvantages of the density-driven technique. Such agitation would suspend the sludge and would minimize salt concentration gradients, thereby eliminating dissolution inhibition at the cake surface-liquid interface. Agitation should be sufficient to accomplish this objective, but it should not be so vigorous as to erode salt from the cake. Salt cake erosion increases the risk of undercutting the cake surface. Undercutting occurs in a heterogeneous cake because of the presence of salts with different solubilities.

B. V. Churnetski, "Bench Scale Simulation of Waste Removal in Tanks Containing Alternating Layers of Salt and Sludge," DPST-81-366, April 7, 1981.

Four and twelve-liter beaker tests were conducted on simulants of Tank 17 saltcake waste with alternating layers of salt and sludge. The tests dissolved salt by adding water and mixing with blade agitators to simulate the operation of three slurry pumps. When the specific gravity of the centrifuged supernate had reached 1.3 to 1.4 g/mL, the sludge was allowed to settle and the rich salt supernate was removed. The tests showed a projected time requirement of 6 to 9 months for the in-tank dissolution process, with the settling of the simulated sludge constituting a considerable percentage of the total time requirement. Undercutting was noted in all tests, likely due to insufficient agitation outside of the cleaning radius of the agitator. The dissolution rates of the layered salt/sludge simulations were more than 50% lower than the rates of salt-only simulations.

B. V. Churnetski, "Bench Scale Simulation of Salt Removal in Tank 24H," DPST-81-652, September 9, 1981.

A twelve liter simulant test was performed to assist in salt removal from Tank 24. The wet saltcake precipitated from simulated Tank 24 solution had a specific gravity of 1.938. The time requirement for the dissolution with the agitation of two slurry pumps was shown to be between 3 and 4.5 months. This report contains characterization information for actual-waste saltcake samples from Tank 19F and Tank 24H.

B. J. Wiersma, "Recommendations for the Use of Inhibited Water During Phase I Salt Dissolution in Tank 41," WSRC-TR-96-0085, January, 1996.

B. J. Wiersma, "An investigation of Density Driven Salt Dissolution Techniques," WSRC-TR-96-0160, August 1996.

B. J. Wiersma and W. R. Parish, "Laboratory Simulation of Salt Dissolution during Waste Removal (U)," WSRC-MS-96, 0674, March 1997.

A set of laboratory experiments was performed on three foot-long rectangular troughs of non-radioactive saltcake simulants to compare several potential saltcake dissolution methods. The three methods investigated were all in the density gradient class of dissolution methods, where no supernatant fluid agitation is applied. These included the following methods: Drain-Add-Sit-Remove, Modified Density Gradient, and Continuous Salt Mining. The focus of this work was the evaluation of these methods versus the corrosion technical standards. Through analysis of the

residual solids, these investigators noted that the hydroxide and nitrite are removed in the early stages of dissolution. The solids remaining after nearly complete dissolution have greatly reduced sodium nitrate, as it is removed throughout the dissolution, but a higher percentage composition of the di- and tri-valent anions carbonate, sulfate, phosphate, and oxalate.

A comparison between the three dissolution techniques reveals several key observations of the dissolution process that impact the efficiency and cost of operations. The Drain-Add-Sit-Remove method did the best job of retaining interstitial liquid within the saltcake while removing saltcake in small horizontal slices, but salt dissolution was observed to be a very rapid process as salt solutions with densities between 1.38 and 1.4 g/mL were frequently obtained. The optimal dissolution technique should ensure good contact between the unsaturated salt solution and the saltcake while avoiding channeling and short circuiting. When all dissolution processes neared the bottom of the trough, the salt solution densities removed had lower densities, leading to a recommendation for slower transfer rates for the late stages of dissolution.

Table 8 - Comparison of Density-Driven Techniques

<u>Drain-Add-Sit-Remove</u>	<u>Modified Density Gradient</u>	<u>Continuous Salt Mining</u>
1) Retains interstitial liquid the best.	1) Displaces interstitial liquid faster than DASR.	1) Displaces interstitial liquid the fastest.
2) Produces a level profile.	2) Produces a level profile.	2) Produces a level profile.
3) Need to adjust transfer jet level.	3) Transfer jet is fixed near the bottom of the tank.	3) Transfer jet is fixed near the bottom of the tank.
4) Remove liquid as soon as it reaches the pump site.	4) Needs to be drawn down slowly to prevent "short-circuiting".	4) Needs to be drawn down slowly to prevent "short-circuiting".
5) Insolubles: Slow removal: No localization and minimal entrainment. Medium removal: Localization at shallow jet depths. Pluggage of removal jet. No localization at deeper jet depths. Significant entrainment of salt crystals and insolubles. Fast removal: No localization at deeper jet depths. Largest amount of entrainment of salt crystals and insolubles.	5) Insolubles: No localization and minimal entrainment.	5) Insolubles: No localization and minimal entrainment.
6) Removes saltcake in small horizontal slices.	6) Removes salt solution from the bottom.	6) Removes salt solution from the bottom.
7) More likely to gas pumps.	7) Should not gas pumps.	7) Should not gas pumps.
8) Do not begin removal until liquid covers the saltcake.	8) Need to stop removal when liquid reaches the top of the saltcake.	8) Maintain liquid level above saltcake by adjusting the addition and removal rates.

C. J. Martino, M. R. Poirier, and N. E. Gregory, "Saltcake Dissolution Simulant Tests," WSRC-TR-2002-00387, Revision 0, December 11, 2002.

Small-scale (15 to 50 mL) dissolution equilibrium tests were performed on surrogate waste representing typical saltcake at the Savannah River and Hanford Sites. The primary objectives of this study were to gain a better understanding of the solid-liquid equilibrium of simulated-waste saltcakes and chemistry of the dissolved salt solutions. These tests were performed in preparation for similar dissolution tests with actual-waste saltcakes. Two types of tests (single-wash and multiple-wash) were performed at two temperatures (25 °C and 50 °C) for each saltcake simulant. The compositions of the supernatant fluids are provided for both types of dissolution tests, and profiles of the elution of each salt component are provided for the multiple-wash tests.

For both salt waste surrogates, dissolution of the soluble components was achieved at less than a 2:1 mass ratio of inhibited water to saltcake during multiple-wash tests. Dissolution of the Hanford S-112 simulant resulted in a relatively large weight percentage of residual insoluble material (4.2 wt. %), which was identified as a mixture of Al(OH)₃ phases (bayerite and gibbsite).

The profiles for the relative elution of anions from saltcake during dissolution exhibit distinctions that are dependent upon the dissolution temperature and the initial saltcake composition.

5.2.2 Actual-waste Dissolution Tests

C. J. Martino and M. R. Poirier, "Tank 31H Saltcake Dissolution Tests, WSRC-TR-2002-00388, Rev. 0, February 27, 2003.

Two multiple-wash dissolution tests were performed on Tank 31H actual-waste saltcake. The tests contacted 60 g of saltcake with a series of ten small aliquots of dissolution fluid (7 to 45 g). The dissolution fluid was different for the two tests, either inhibited water or an actual-waste 5.2 M Na⁺ solution. Dissolution of Tank 31H saltcake with inhibited water was accomplished with an approximately 1:1 cumulative mass ratio of diluent to salt. Dissolution of Tank 31H saltcake with 5.2 M Na⁺ solution remained incomplete after a 3.3:1 cumulative mass ratio of diluent to salt.

The dissolved salt supernates were characterized and profiles were created for the removal of individual components during the Tank 31H salt dissolution tests. Several general categories were used to describe the compounds that dissolve similarly during saltcake dissolution. Hydroxide, cesium, nitrite, and aluminate are eluted during the earliest stages of salt dissolution. Due to its low concentration in the saltcake sample, phosphate is also removed in the early stages of dissolution relative to the sodium and nitrate. Of the major saltcake components, carbonate and sulfate were removed during the latest dissolution stages. Several of the minor components, including strontium, were only partially dissolved during the tests. As seen in the figure below, ¹³⁷Cs was removed with the interstitial liquid and a portion of the Sr-90 late in the dissolution process during dissolution with inhibited water.

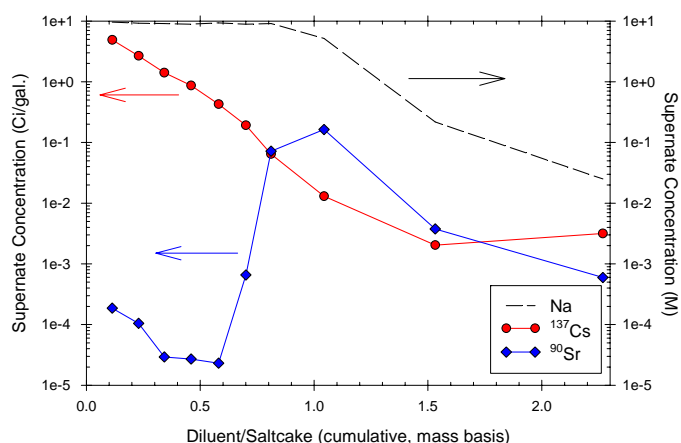


Figure 10 – Tank 31H Salt Dissolution Testing – Results Indicate that ¹³⁷Cs is Removed with Interstitial Liquid

The residual insoluble solid material from the dissolution of Tank 31H saltcake with inhibited water was 87 wt % gibbsite and bayerite and 7 wt % hematite, while the material from the less-complete dissolution with the 5.2 M Na⁺ solution was primarily sodium salts of carbonate and sulfate.

R. L. Nichols and C. J. Martino, "Hydraulic Properties of Saltcake Samples from Tank 41H (U)," WSRC-TR-2003-00543, Rev. 0, January 2004.

- C. J. Martino, R. L. Nichols, D. J. McCabe, M. R. Millings, and M. E. Denham, "Tanks 3F and 2F Saltcake Core and Supernate Sample Analysis", WSRC-TR-2004-00131, Rev. 0, April 13, 2004.
- C. J. Martino, R. L. Nichols, D. J. McCabe, and M. R. Millings, "Tank 10H Saltcake Core Sample Analysis", WSRC-TR-2004-00164, Rev. 0, April 19, 2004.
- C. J. Martino, D. J. McCabe, and R. L. Nichols, "Tank 29H Saltcake Core and Supernate Sample Analysis", WSRC-TR-2004-00130, Rev. 0, April 6, 2004.

A characterization program was carried out from April of 2003 through April 2004. Saltcake and supernate samples from six tanks were pulled to determine select physical, chemical, and radiological properties. The table below contains density, porosity, and saturation information for several of the samples. Additionally permeability was measured on samples from Tanks 41H and 10H. The hydraulic conductivities measured for samples from Tanks 41H and 10H are and 1.5E-5 cm/s and 4.2E-4 cm/s, respectively.

Table 9 – Selected Data (Bulk Density, Water Content, Porosity and Saturation) for Salt Cake from Tanks 2, 3, 41, 29 and 10

Tank	Sample ID	Sample Interval (ft)	Bulk Density (g/cm ³)	Water Content θ_w (wt %)	Porosity ϕ (vol %)	Saturation S (vol %)
10H	HTF-609	0-1	2.03	9.9 ± 0.2	28	94
	HTF-610	1-2	2.17	12.8 ± 0.5	38	> 100
	HTF-611	2-3	1.98	4.4 ± 0.04	21	55
	HTF-610	1-2	2.17	8.6 ^b	26	97
	HTF-611	2-3	1.98	7.2 ^b	26	74
	29H	T29H-B6-1	0-1	2.13	21	nd
2F	T2F-1-1	0-1	2.04	6.2 ± 0.6	23	77
3F	T3F-1-3	1-2	2.07	5.1 ± 2.6	19	76
41H	HTF-E-03-034	1-2	1.92 ^a	3.2 ^a	22	34

Interstitial liquid extraction followed by flow-through dissolution was performed on samples from Tanks 41H, 3F, 29H, and 10H. Water was introduced to the top of the sample contained in a 1" diameter tube and allowed to gravity drain through the sample and into a collection vessel. A series of sub-samples of the dissolved salt effluent were taken over the period of the dissolution process.

Previous centrifuge-tube batch dissolution tests on Tank 31H saltcake showed that individual salt components could be more or less concentrated at different stages of total saltcake dissolution. Similar is true for the flow-through dissolution of drained saltcake, though the separation was not as extreme as it was for the complete mixing conditions of Tank 31H batch contact tests. It was clear that the components partitioned to the interstitial liquid (nitrite, hydroxide, aluminate, and cesium-137) were also contained in the effluent from the first stages of dissolution in much greater quantities than from ensuing stages of dissolution. The primary components of the solid saltcake lattice, the nitrate, carbonate, and sulfate, were contained in the effluent in roughly constant quantities during the major period of saltcake dissolution. The ¹³⁷Cs concentration decreased throughout the flow-through dissolution tests. This decline in ¹³⁷Cs was significantly faster than the decline in sodium as the test proceeded. This is illustrated in the figure below for the flow-through dissolution test using 59 g of salt from Tank 3F.

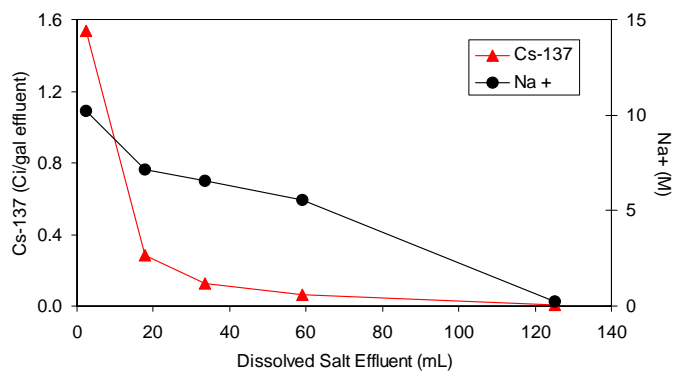


Figure 11 – Dissolution Flow-through Testing Using Salt Cake from Tank 3 – ¹³⁷Cs/Na Concentration as a Function of Dissolved Salt Effluent

Several issues were encountered in the flow-through dissolution tests. For the tank 10H test, the flow through the sample was relatively fast, not allowing for enough contact time between the dissolution fluid and the saltcake. Also, channeling may have occurred as the test proceeded and the bed of salt became progressively smaller. These phenomena caused the ¹³⁷Cs separation over the course of the test to be not as extreme as that noted for Tank 3F. During the flow-through dissolution of the Tank 29H sample, which contained ~13 wt% Al, significant gibbsite and bayerite were formed during testing such that flow through the salt plug was difficult to attain.

5.2.3 Salt Dissolution Modeling

K. Staheli, J. F. Peters, “Interstitial Fluid Displacement for Preferential Recovery of Cesium from Saltcake, U.S. Army Corps of Engineers, Technical Report GL-98-3, April 1998.

J. N. Brooke, K. Staheli, and J. F. Peters, “Hydrological Methods can Separate Cesium from Nuclear Waste Saltcake,” WSRC-TR-99-00358, July 1999.

The interstitial fluid displacement (IFD) process for separating cesium from saltcake was modeled and discussed. Chemical theory and data indicate that none, or very little of the cesium is contained in the saltcake crystal structure. Similar logic applies to potassium and sodium hydroxide, other chemicals important to waste processing. Laboratory and field data demonstrate that saltcake is usually porous, permeable, and dissolves rapidly. Hydrologic modeling of liquid flow through porous saltcake suggests that the cesium, potassium, and sodium hydroxide can be separated at high recovery and low volume using IFD.

Hydrologic modeling showed that the mass of ¹³⁷Cs in the tank could be reduced by pumping or draining the interstitial fluid. Finite element simulations were performed with two homogeneous media and two heterogeneous media. Variability in the saltcake permeability is as important as the mean permeability value because the success of cesium removal depends on the uniform movement of interstitial fluid.

Three methods for cesium removal were investigated: draining only, draining followed by pumping interstitial fluid, and draining followed by controlled saltcake flooding through recharge wells. During draining, cesium removal was limited by the residual saturation in the media. Both the draining and pumping methods were susceptible to localized flow patterns caused by heterogeneities. Controlled flooding through recharge was more efficient in moving water into dead zones and improving the cesium recovery.

- K. C. Kwon, "Tank 29 Temperature during Salt Removal Operation (U)," WSRC-TR-94-0477, October 1994.
- K. C. Kwon, "Tank 41 content Temperature during Salt Removal Operations (U)," WSRC-TR-95-0089, March 1995.
- K. C. Kwon, " Tank 25F Mixed Waste Thermal Analysis During Salt Removal Batch Process with Cooling Coils Off," HLW-CSTE-97-0067, October 1, 1997.
- K. C. Kwon and M. R. Poirier, "Tank 37H Salt Removal Batch Process and Salt Dissolution Mixing Study," WSRC-TR-2001-00277, Rev. 0, July 17, 2001.

A heat transport model (HLWE Tank Cool Program) was developed for SRS Type IIIA tanks. In a series of studies, this model applies different salt dissolution schemes in different tanks. The model includes such components as radiolytic heat generation and losses during endothermic dissolution and evaporation. The model includes the heat transport through the saltcake, supernate, and vapor space, cooling coils, purge gas, walls, concrete, and soil.

For example, the model was used to determine the expected temperature ranges during Tank 25 salt dissolution in the event of the loss of cooling. The maximum liquid waste temperature occurred during the fourteenth and final dissolution batch. The study showed that even if three slurry pumps are operated continuously during the dissolution, the tank temperature would not challenge the 70 °C temperature limit.

The most ambitious use of this model was the comparison of four salt dissolution techniques with the goal of removing 50 inches of salt from Tank 37. The study included cases where water was added as a layer at the top of the saltcake with no agitation; where water was added with Flygt mixer agitation; where water was added with slurry pump agitation; and where water was added using the modified density gradient method. Three dissolution temperatures were included (25 °C, 50 °C, and 75 °C) and the dissolution rates and process times were tabulated. All methods except the no agitation method resulted in the removal of 50 inches of saltcake within an overall time of less than six months. Dissolution at 25 °C using the agitation provided by the Flygt mixers and slurry pumps was marginally faster than that of the modified density gradient method, but the additional time involved for installation of the mixing equipment makes the total processing times the same for the three methods.

- B. J. Wiersma, "Description of the Material Balance Model and Spreadsheet for Salt Dissolution," WSRC-TR-94-0481, October 12, 1994.
- Q. L. Nguyen and J. A. Pike, "Tank 41 Low Curie Salt (LCS) 1st Salt Dissolution Batch Analysis," WSRC-TR-2003-00191, Rev. 0, June 3, 2003.

Spreadsheet models have been used to determine various important factors during saltcake dissolution at SRS. These models are useful in estimating the amount of corrosion inhibitors necessary in the dissolution fluid in order to maintain dissolved saltcake chemistry within the tank technical corrosion limits. They have also been used to forecast the potential activity in dissolved salt solutions that are sent on to subsequent processes. These spreadsheet models are updated when new information becomes available on the properties of the material in the salt tank in question.

J. A. Pike, "Tank 37 Salt Dissolution Flowsheet Basis," WSRC-TR-2001-00599, Rev. 0, December 11, 2001.

J. A. Pike, "Tank 41 Salt Dissolution Flowsheet Modeling," WSRC-TR-2002-00209, Rev. 0, May 23, 2002.

Aspen Custom Modeler™ has been utilized to determine the batch characteristics for saltcake dissolution in Tanks 37 and 41. Aspen Properties Plus™ provided the means to estimate the equilibrium chemical properties during dissolution. Cases were run to provide input to the operational plan and were a basis for dissolution batch expectations. Additionally, the dissolution model was compared with historical data from Tank 10 dissolution.

G. P. Flach, "Porous Medium Analysis of Tank 41 Drain Operations (U)," WSRC-TR-2003-00080, Rev. 0, 2003.

G. P. Flach, "Porous Medium Analysis of Interstitial Liquid Removal from Tank 41 and Tank 3," WSRC-TR-2003-00533, Rev. 0, February 2004.

During Tank 41 draining to produce feed acceptable for the Low-Curie Salt process, the first of these studies analyzed the drainage to better understand the interstitial liquid level profile across the tank, and the liquid saturation profile from tank bottom to top. A static gravity-equilibrium analysis of the well level before and after net removal of 113,000 gallons of liquid indicates the drainable water content of Tank 41 saltcake is in the range of 13-18 volume percent, with a best-estimate of 14%. A semi-empirical analysis of dynamic liquid levels during pumping suggests that mean tank level can be related to well level and pumping rate under pseudo-steady flow conditions (slow transients). The correlation appears to be reasonably accurate at predicting the equilibrium liquid level after 2-3 weeks of downtime.

In the second study, a numerical model of porous medium flow was developed for Tank 41 using a modified version of the finite-element FACT code. The numerical modeling approach can readily accommodate differences in geometry and fluid properties between tanks. Intrinsic permeability for Tank 41 was estimated with the numerical model by comparing actual to simulated well liquid level in response to known pumping rates. Intrinsic permeability is a physical property of a porous media and not dependent on the interstitial fluid. Based on numerical modeling, the average intrinsic permeability of the saltcake in Tanks 41 and 3 appears to lie in the range of 25 to 50 Darcy. A best-estimate is 37 Darcy. A similar finite-element model was developed for Tank 3, and used to assess the benefit of installing an additional salt well. Little benefit is predicted for a 45 day operational window. Drainage data for the lower 160 in. of saltcake, suggest that the saltcake in Tanks 41 and 3 share the same porous medium properties.

Q. L. Nguyen, "Potential Gibbsite and Other Dominant Solids Formation during Tank 41 Salt Dissolution," WSRC-TR-2004-00391, Rev. 0, July 22, 2004.

Dissolving Tank 41 salt cake using Flush Water (FW) has the potential of increasing gibbsite [Al(OH)₃] and other dominant solids formation. This report uses the lab results from a salt core sample as input streams for OLI™ Water Analyzer and Environmental Simulation Program (ESP) thermodynamic modeling calculations. The model predicts that dissolving Tank 41 salt cake level to approximately 77 inches would require eight dissolution batches and approximately 1.64 million gallons of FW with both the salt cake and dissolution fluid assumed at 25 °C.

The total solids remaining after eight dissolution batches are predicted to be approximately 21.7 wt% of the initial total mass. The most dominant solid, sodium nitrate (NaNO₃) composes the

highest percentage of 90.9 wt% of the total solids remaining. The gibbsite is the second dominant solid at 8.99wt%. The rest of the other solids are 0.11wt%. The mass of gibbsite is predicted to be approximately 125,511 kg, which composes greater than 99.0wt% of total solids remaining if NaNO₃ solid is excluded. This mass of gibbsite when converted to a volume would amount to a layer height of around 6.5 inches. Based on the compositions employed, and assuming some distribution of the aluminum within Tank 41, it does not appear that this layer would likely form across the entire tank. The mass of the gibbsite formation is small (< 1.5 wt. %) compared to the total mass in the tank. Gibbsite would not significantly impact the earlier dissolution batches (1st, 2nd, and 3rd), but may impact the later batches. It should be anticipated that some localized regions with high amount of gibbsite could be formed during the dissolution process. Depending on the volume, these regions could slow down the dissolution and percolation rates, which may impact the tank operation/retrieval schedules.

The results from alternative studies using three dissolution fluids at different caustic levels, 3.85wt% (1.0M), 7.5wt% (2.0M), and 10.72wt% (3.0M), indicate that increasing caustic level in the dissolution fluid would dissolve the gibbsite while decreasing the dissolution of other salts. Using higher caustic concentrations would require a longer operating window and generate more liquid waste.

Temperature exhibits a significant impact on most solids dissolution. A large increase in most of the solids remaining in the tank is found with a decrease in temperature. Based on solubility equilibrium, increasing tank temperature would significantly speed up the dissolution process.

6.0 Appendix B – Fractional Crystallization & Crystal Separation Literature Review

This appendix is divided into two sections. The first part contains literature on fractional crystallization, and the second part separation processes. Each of these sections is subdivided into specific subject areas.

6.1 Fractional Crystallization

The review of fractional crystallization performed by CHG (Person 2004) covered numerous articles on fractional crystallization design, specific chemical systems, solubilities, comparisons with thermodynamic calculations, and crystallization systems and crystallizers. These previously reviewed publications are not covered in this current document, except for selected references; the reader is referred to the CHG review.

6.1.1 Commercial Production of Sodium Nitrate

Sodium nitrate is produced in Chile from an ore. The nitrate is purified from the ore by a countercurrent leaching process maintained at 40°C. The nitrate is crystallized by cooling crystallization from solution by lowering the temperature to 8-12°C. The nitrate is of sufficient purity that no recrystallization is needed. Separation of the crystallized sodium nitrate is performed by continuous centrifuging (Kroschwitz 1998). Separations of sodium nitrate crystals in industry are also done by rotary filtration (Dickenson 1997).

6.1.2 Design of Crystallization Systems

The CHG review covered a number of papers on the design of fractional crystallization systems. Several references were made to papers by K. M. Ng and co-authors. Additional papers by Ng are summarized below. Additional references are given in Section 1.1.

A procedure for synthesizing crystallization-based separation processes is presented by (Wibowo 2000). In an evolutionary manner and without being restricted to a particular crystallization technique, flowsheet alternatives are generated to meet the separation objectives for a given system. This is achieved by recognizing the fact that four basic crystallization-related movements in composition space are sufficient to represent a variety of crystallization processes. Suitable movements are selected based on relevant features of the phase diagram to construct feasible flow sheets. The procedure consists of six steps. First, separation objectives are defined. Second, a separation core structure is generated. Third, the separation sequence and unit operations are selected, followed by adding other units to the structure for proper plant operations. Fifth, appropriate crystallizer type is selected. Finally, economic evaluation and feasibility checks are performed for the generated alternatives. Rules are provided to aid decision-making at each step.

The authors also provided some useful definitions of different types of crystallization. In *fractional crystallization*, operations such as heating, cooling, solvent addition or removal are used to recover two or more of the solutes from a multi-component solution. Instead of the solute, if the solvent is recovered by cooling, the process is referred to as *freeze crystallization*. In *extractive crystallization*, an extraneous solvent is added to assist the separation of a multi-component mixture; only cooling crystallizers are used in such processes. A more general technique is the addition of an extraneous component, which may be a gas, a liquid, a supercritical fluid, or a solid, to effect separations and is referred to as *salting-out*, *drowning-out*, *solventing-out*, or *dilution crystallization*. The use of a hydrotrope, which significantly affects the solubility of one or more of the solutes, also falls into this category. In *adductive crystallization*, the added component reacts with one of the components to form an adduct which can easily be separated from the mixture. Finally, solid crystals can be produced as the result of a chemical reaction between the components. This technique is known as *reactive crystallization*.

The effect of the crystallization process on the downstream processing steps and methods to alleviate problems is described by Wibowo 2001. A systematic procedure is developed for designing an integrated crystallization system by considering the interaction between crystallization and downstream processing. Potential problems related to unit operations such as filtration, washing, dewatering, recrystallization, and drying are anticipated and resolved by determining an operating policy and configuration for the crystallizer as well as the downstream units. The approach can be applied to both batch and continuous crystallizers. First, the possible impacts of particle-size distribution (PSD) on the downstream processing units are identified. This forms the basis for determining a target PSD in the second step. Third, possible means by which the desired PSD can be achieved are selected. Fourth, the alternatives thus generated are evaluated and compared to identify the best design. Heuristics are provided along the way to guide the decision making. Shortcut equipment models are used to compare the performance of the alternatives. Several example applications are also given. Table 3 provides a summary of the potential problems related to particle size distribution. A table of relevant equations for analyzing crystallization downstream processes are also given (not shown here).

Techniques described in (Wibowo 2001) are applied to an existing industrial crystallization process by (Cesar 1999). A systematic method is presented for improving the recovery of the desirable product in an existing fractional crystallization process. Solid-liquid-phase behaviors and techniques relevant to product recovery are discussed. Retrofit targets are identified through an analysis of the phase diagram of the mixture under consideration. Conceptual design techniques consisting of heat and mass balances, heuristics, and short-cut unit models are used to determine the necessary changes in flow sheet structure and equipment design in order to meet the retrofit objective. The method is illustrated with an adipic acid plant.

The synthesis of the processing steps upstream and downstream of the crystallization step, including the destinations of solvent, mother liquor, wash liquids, etc. are discussed by Chang 1998. A systematic procedure is developed to synthesize the processing system

upstream and downstream of a crystallizer. In a step-by-step manner, the procedure guides the user to generate alternative flow sheets for treating a given crystallizer effluent. It consists of five steps. The required unit operations are determined by comparing the product specifications (production rate, product purity, and others) with the crystallizer effluent characteristics (occlusions, inclusions, crystal size, and others). Secondly, the destinations of the reaction solvent, mother liquor, wash liquid, recrystallization solvent, and drowning-out solvent are assigned. Third, the solvent recovery system is considered to recover the solvents and unconverted reactants and to remove the impurity from the system. Fourth, alternatives for enhancing process performance are identified. Final short-cut models are used to screen process alternatives. Rules and heuristics are provided for each step, and examples for illustrating this procedure are presented.

A method is presented to synthesize process flow sheets for separations of mixtures by fractional crystallization by Cisternas 1998. Using equilibrium data for a candidate set of potential operating point temperatures, a network flow model is constructed to represent the set of potential separation flowsheet structures that can result. By employing specified approaches to multiple saturation point conditions, linear network constraints are obtained. Solution of the network flow model shows the optimal mass flow pattern between the candidate equilibrium states, and from this the corresponding process flowsheet is readily deduced. The method as presented is generally applicable to problems with two salts and one or more solvents, including systems forming one or more multiple salts or hydrates. Situations having multiple feeds and multi-component products are also included. Several salt separation examples are given which demonstrate the method's application and show some of the types of coupled cycles that are obtained as solutions.

Example applications are crystallization of KCl from sylvinit (KCl, NaCl), separation of Na_2CO_3 and Na_2SO_4 from mixtures and from burkeite ($\text{Na}_2\text{CO}_3 \cdot 2\text{Na}_2\text{SO}_4$), and MgSO_4 and Na_2SO_4 from astrakanite ($\text{MgSO}_4 \cdot \text{Na}_2\text{SO}_4 \cdot 4\text{H}_2\text{O}$).

Development of heat-integrated evaporation and crystallization networks using the heat-induced separation network (HISEN) concept is described by Parthasarathy (Parthasarathy 2001a; Parthasarathy 2001b). Interpretation of high-dimensional (multi-component) phase diagrams are described by Ng and coworkers (Samant 2001; Wibowo 2002).

6.1.3 Metastability and Kinetically Controlled Crystallization

The following statement is from the CHG Statement of Work:

“The ESP model predictions of solids formation in the Hanford evaporator has differed significantly from the actual solids formation measured. The difference between the current thermodynamic model and observed evaporator operations need to be addressed to successfully evaluate fractional crystallization.”

The following discussion of metastable zones and metastable phases may be applicable to the modeling of evaporator operations.

Crystallization occurs due to supersaturation of a species in the solution. Supersaturation can be achieved by (Myerson 2002):

1. Temperature change.
2. Evaporation of solvent.
3. Chemical reaction
4. Changing the solvent composition.

A supersaturated solution has what is called a metastable *zone*. The metastable zone, shown in Figure 5, is the area above a solubility curve (vs. temperature, pressure, solvent composition) where the solution is supersaturated, but spontaneous crystallization is improbable (Mullin 2001). In the stable zone, the solution is unsaturated, and crystallization is not possible. Above the dotted line, or supersolubility curve, spontaneous crystallization is probable; this zone has been called the labile zone. The width of the metastable zone can depend on the thermal history of the solution, the presence of seed crystals, vessel surface characteristics, and agitation. Note that the solution can be relatively stable within the metastable zone.

In a crystallization by evaporation, the solubility would appear to be higher than actual if a significant degree of supersaturation had to be reached before crystallization would occur, as shown by the line A B' C' in Figure 5. Cooling crystallization can give similar results (line ABCD); exceeding the supersolubility may even occur here.

The Ostwald Law of Stages states that an unstable (supersaturated) system does not necessarily transform into the most thermodynamically stable state, but into one which most closely resembles its own, i.e., into another transient state whose formation from the original is accompanied by the smallest loss of energy. This transient state is called a metastable *phase* (Nývlt 1995; Mullin 2001). Figure 12 shows such a transition, where the metastable phase 1 is formed before the stable phase 2 is formed when the composition is moved downward from x_i . Note that monotropic means these two phases do not exist at equilibrium at any conditions, i.e., one phase is always the most stable; polymorph means that these phases are different crystal structures (such as calcium carbonate as calcite, aragonite, or vaterite); different hydrates could be $\text{Na}_2\text{SO}_4 \cdot 7\text{H}_2\text{O}$ and $\text{Na}_2\text{SO}_4 \cdot 10\text{H}_2\text{O}$.

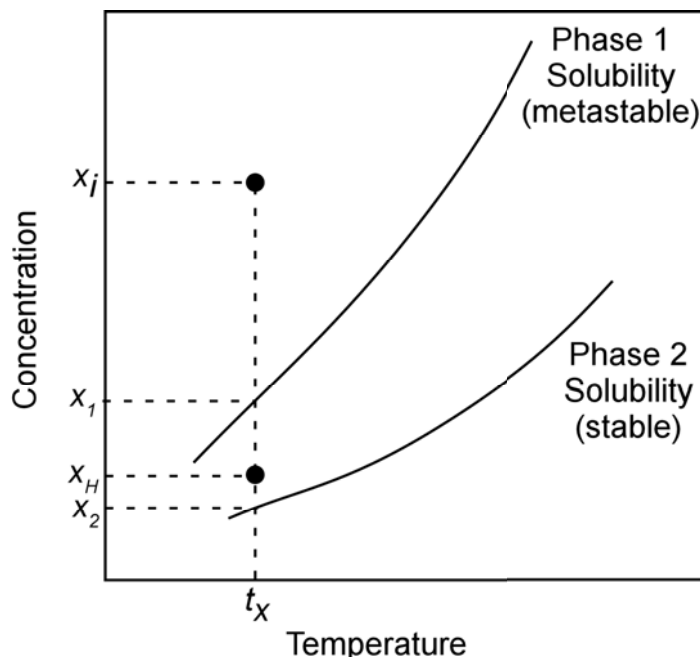


Figure 12 – Typical Solubility Curves for Two Monotropic Polymorphs or Hydrates (Cardew 1985)

The following describes the transformations shown in Figure 12 (Cardew 1985). A solution at point x_i is supersaturated with respect to both the metastable phase 1 and the thermodynamically favored phase 2. The Ostwald Law of Stages indicates that phase 1 will precipitate before phase 2. Actually, since the solution is supersaturated with respect to both phases, phase 2 may also precipitate initially. Once the solution composition has reached x_1 , phase 1 will begin to dissolve and phase 2 will continue to precipitate until thermodynamic equilibrium is reached. The time it takes to reach equilibrium depends on the rates of phase 1 dissolution and of phase 2 formation. The authors present a mathematical model for the formation of the metastable phase and subsequent transformation to the stable phase. They give the extreme example of the solid-phase transformation of metastable diamond to stable graphite, where the slow rate of diamond decomposition governs. Several systems identified with metastable phases were calcium carbonate, sodium sulfate, and potassium nitrate.

This example shows that the metastable phase 1 could be long lived. Thermodynamics would predict formation of phase 2, but none or very little may be formed. Moreover, since the solubility of phase 1 is greater, the molar amount of material crystallized would be less than predicted by thermodynamics.

Another way to state the Ostwald law is: If more than one reaction is thermodynamically possible, the resulting reaction is not necessarily the one that is thermodynamically most likely, but the one with the fastest rate (kinetics) (Mullin 2001). Also, the more stable phase at a given set of conditions always has the lowest solubility, as shown in . For enantiotropic phases (two or more phases that are stable at different temperatures, see),

phases 1 and 2 will exist together at the transition temperature T where the solubility curves cross.

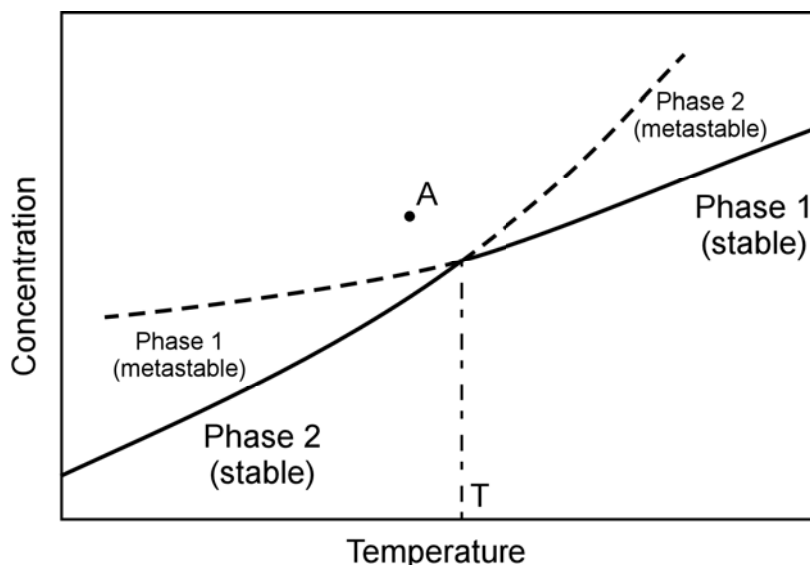


Figure 13-Solubility Curves of Enantiotropes with Metastable Phases (Mullin 2001).

If the metastable phases 1 and 2 are as shown, a solution supersaturated with respect to both phases 1 and 2 at point A may crystallize out phase 1 before phase 2 even though phase 2 is thermodynamically most stable.

A further example of this type of behavior with metastable zones shown is given in . A supersaturated solution at point A will preferentially crystallize to the metastable phase 2 until point B is reached. At this point, spontaneous transformation of phase 2 to phase 1 may occur (depending on the kinetics) since the solution composition is above the metastable zone for phase 1. Crystallization of phase 1 will also occur at point A. A solution below point B will only crystallize phase 1. A solution with composition between F and G is saturated with respect to the metastable phase 2, but is in the metastable zone for phase 1, so the transformation from phase 2 to phase 1 may be kinetically unlikely even though phase 1 is more stable. The authors state this time could be hours, days, or even years (Nývlt 1997; Nordhoff 1999). Nývlt also discusses these types of transformations (Nývlt 1997). Therefore, a metastable phase may be the only phase present in some situations; the thermodynamically stable phase may not be present.

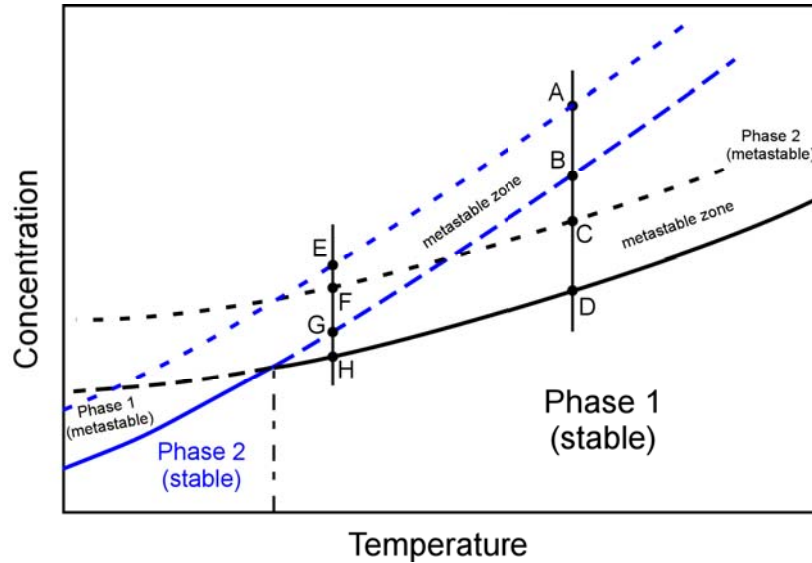


Figure 14-Solubilities and Limits of Metastable Zones of an Enantiotropic system

An example of metastable phases in an actual application is the formation of burkeite (Shi 2001). The burkeite compositions found in experiments at 115°C differed from the compositions expected by interpolating previous equilibrium data at 100°C and 150°C. This difference was explained as the result of this study measuring crystal compositions that were controlled by kinetics rather than equilibrium. The authors concluded the deciding factor was the relative nucleation and crystal growth rates of the stable and metastable phases.

The existence of metastable zones can have a significant effect on predictions of crystallization. Compositions in the metastable zone may or may not result in crystallization, so the apparent solubility of a particular species can depend on the process conditions. Formation of metastable phases can result in differences between actual behavior and thermodynamic predictions. A relatively stable metastable phase may be formed, and since the metastable phase is always more soluble than the more stable phase, the amount crystallized would be less than predicted thermodynamically. This formation of metastable states may be an important factor in the differences between the results of the ESP model of the evaporator and the actual experimental results.

6.1.4 Effects of Impurities and pH on Crystallization

If a third component C is added to a binary solution of solute A solute and solvent B, one of four things may happen (Mullin 2001):

1. Nothing (relatively rare).
2. C may combine or react with A or B to form a complex or compound.
3. C may make the solution supersaturated with respect to A (“salting-out”).
4. The solution may become unsaturated with respect to A (“salting-in”).

Potassium sulfate, once dissolved, has been reported to not recrystallize from aqueous solutions containing traces of Cr^{+3} or Fe^{+3} ; nucleation is apparently prevented. The solubility of K_2SO_4 with ppm levels of Cr^{+3} is significantly lower than without, so the apparent solubility measured by adding K_2SO_4 to the ppm Cr^{+3} solution is lower than the actual solubility. A supersaturated solution of the same, when cooled, will give a higher solubility than the true equilibrium value because the Cr^{+3} species in solution adsorb on the depositing K_2SO_4 crystals, retard their growth, and prevent complete desupersaturation of the solution. Summarizing, the *measured* solubility of K_2SO_4 in the presence of traces of Cr^{+3} is lower when saturation is approached from the dilute side and higher when approached from supersaturation, and neither is the correct solubility for the pure substance. There is a tendency for higher charged cations to have the most effect: $\text{Cr}^{+3} > \text{Fe}^{+3} > \text{Al}^{+3} > \text{Ni}^{+2} > \text{Na}^+$. The presence of small amounts of colloidal substances and certain surfactants can have significant effects on nucleation of crystals. There also appears to be a threshold concentration of impurity above which the inhibiting effects may actually diminish. Adsorption of impurities onto growing crystal faces may also impede growth.

In the crystallization of burkeite ($\text{Na}_2\text{CO}_3 \cdot 2\text{Na}_2\text{SO}_4$) from solutions of Na_2CO_3 and Na_2SO_4 , the addition of Nd^{+3} was found to completely inhibit the nucleation of burkeite in the bulk solution (Shi 2003). Contrary to all previous tests by these authors without added metals, only Na_2SO_4 was crystallized when Nd^{+3} was added; no other metal added had this effect. Addition of EDTA also changed the nucleation behavior of burkeite, reducing the size and number of large crystals formed.

The width of the metastable region of potassium sulfate was measured in the presence of various concentrations of chromate, copper(II) and aluminum ions (Karel 1993). The dependence of the metastable region width on the impurity concentration is generally nonlinear and in some cases even changes its nature; while in low concentrations some impurities make the metastable region narrower, they make it broader if present in higher concentrations. The effect of the impurities increases in order $\text{K}_2\text{Cr}_2\text{O}_7 > \text{CuSO}_4 > \text{Al}_2(\text{SO}_4)_3$.

The effects of impurities on the crystallization of NaCl was studied (Al-Jibbouri 2001). The presence of MgCl_2 affected the solubility of NaCl , PbCl_2 reduced the growth rate of crystals, and $\text{K}_4\text{Fe}(\text{CN})_6 \cdot 3\text{H}_2\text{O}$ affected both. CuSO_4 had no effect on the crystallization process.

The effect of pH on crystallization and on the metastable zone width for the K_2SO_4 - H_2SO_4 - H_2O and K_2SO_4 - KOH - H_2O systems has been studied and modeled (Nývlt 1998). Tabulated solubility data was correlated using the relative activity expansion techniques (See Nývlt 2000). A plausible explanation tells that the presence of free acids or bases modifies the nature and the concentration of ions in solution. The H_3O^+ or OH^- ions can be adsorbed at the crystal surface and affect the active growth sites. The effect of pH on crystal growth in terms of structure of solution has been explained in terms of the hydration of ions. Most cations and OH^- ions are hydrated; the H^+ ion has the largest hydration enthalpy so that its presence in solution has a stronger tendency for interaction

with water molecules than, e.g., the K^+ ion, so that a competition of ions to acquire water molecules takes place. The K^+ ions have a smaller chance to be fully hydrated and therefore they tend to drift towards the crystal surface rather than to remain in the solution. On the other hand, the OH^- ion as a structure former has a stabilizing effect on the solution so that the K^+ ions try to remain in solution; nevertheless, at high OH^- concentrations, the tendency of hydration of the OH^- ions prevails and the K^+ ions are pushed towards the crystal surface again.

6.1.5 Alternative Procedure for Correlating Solubility Data

Solubility data for various systems were correlated using the method of the relative activity expansion (Nývlt 1977; Nývlt 1994; Nývlt 2000) (note: first reference was unavailable, but has been ordered; only abstract review for the others). These references and discussion below are provided to show how future solubility data generated could be correlated. This method is outlined below (Nývlt 1998):

The following applies to the systems $K_2SO_4 - H_2SO_4 - H_2O$ (AR, or acid region) and $K_2SO_4 - KOH - H_2O$ (BR, or base region).

$$\frac{1}{\alpha + \beta} \log [X_1^\alpha (X_1 + FB)^\beta] = \varphi_1, \quad (1)$$

where α is the number of non-common ions in a molecule of component 1, β is the number of common ions in a molecule of component 1, X_1 is the relative molality of component 1 related to its solubility in water, F is the number of common ions in a molecule of component 2 divided by the number of those ions in a molecule of component 1 and

$$B = m_2/m_1^0, \quad (2)$$

where m_2 is the molality of component 2 and m_1^0 is the molal solubility of component 1 in pure water. So, for the **AR**, $\alpha = 2$, $\beta = 1$ and $F = 1$, whereas for **BR** $\alpha = 1$, $\beta = 2$ and $F = 0.5$. The logarithm of the relative activity coefficient of substance 1 (related to the saturated solution of substance 1 in pure water) φ_1 can be written in a series of expansion form

$$\varphi_1 = Q_{12}m_2 + Q_{122}m_2^2 + Q_{1222}m_2^3 + \dots, \quad (3)$$

where Q are interaction constants which are characteristic for individual systems. They depend only slightly on temperature so that they allow reliable interpolation and, to some extent, extrapolation.

6.1.6 Enhanced and Alternative Crystallization Methods

Eutectic freeze crystallization of KNO_3 from aqueous solutions of KNO_3-HNO_3 has been described (Vaessen 2003). This process is a novel technique that results in an almost pure salt and liquid phase. The ice product produced contained 0.15 wt% salt, while the KNO_3 crystals were of high purity. Three washing cycles produced ice with only 15 ppm K^+ . Applicable phase diagrams are given in the reference.

Evaporative crystallization, with the goal of producing anhydrous sodium carbonate rather than the monohydrate, with addition of a second solvent is described in several

articles. Oosterhof describes these solvents as “antisolvents”. When antisolvents are applied to crystallize sodium carbonate from aqueous solutions, the transition temperature at which the hydrates are in equilibrium is decreased. Two models proposed can predict the influence of the amount and type of antisolvent on the transition temperature. Only binary data of the water-sodium carbonate system and measured vapor pressures over ternary soda-saturated mixtures of water and antisolvent are needed. To validate the two models, continuous crystallization experiments were carried out at various temperatures using ethylene glycol and diethylene glycol as antisolvent, in varying concentrations. Both models predict the influence of the antisolvent on the transition temperature with good accuracy (Oosterhof 2001a). Use of a mixture of water and the high-boiling second solvent lowers the transition point at which anhydrous Na_2CO_3 and $\text{Na}_2\text{CO}_3 \cdot \text{H}_2\text{O}$ are in equilibrium to below the atmospheric boiling point (Oosterhof 2001b). Extractive crystallization using addition of poly(ethylene glycol) has been used to crystallize Na_2CO_3 in the anhydrous form (Taboada 2004). The system was also found to form two aqueous phases: one free of sodium carbonate and the second free of poly (ethylene glycol).

Recovery by extractive crystallization using polar organic solvents has been described (Lynn 1996). Recovery of sodium sulfate from SO_2 scrubbing liquor by evaporative crystallization is very energy-intensive; extractive crystallization provides an attractive alternative when technically feasible. Liquid/liquid equilibrium data were determined for two-phase mixtures containing aqueous solutions of sodium carbonate, sulfate, or sulfite and a polar organic solvent: acetone, 2-propanol, and tert-butyl alcohol. No selectivity for dissolution by these solvents was found for one salt relative to the other. The data show that any one of these solvents can be used to extract water from a concentrated solution of either sodium sulfite or sodium sulfate in a countercurrent extractor at 35°C , causing the anhydrous salt to crystallize. The wet solvent can be dried for recycle in a similar countercurrent operation at 35°C , using a saturated solution of Na_2CO_3 as the drying agent. The process energy is about 10% of that required for single-stage evaporative crystallization of the same liquor.

6.1.7 Experimental and Analytical Methods

Differential scanning calorimetry (DSC) measurements have been found to correlate well with crystallization experiments to measure metastable crystallization zones (phase diagram determination) for the sodium carbonate – sodium sulfate system (Shi 2001). Differential thermal analysis (DTA) is also used to generate data for phase diagrams of aqueous systems.

The progress of crystallization experiments is typically monitored by light transmission methods, particle size measurements, solution conductivity, etc. DSC and DTA are also used, as previously described. An advanced method for monitoring crystallization processes using in-situ monitoring by synchrotron x-ray diffraction has been described (Davey 2002; Blagden 2003). Small-angle x-ray scattering, wide-angle diffraction and energy-dispersive x-ray diffraction methods are presented. These methods allow for monitoring crystallization at a molecular level.

Analysis of batch crystallization experiment data is usually mathematically more complicated than analysis of data from the often-used Mixed Suspension-Mixed Product Removal (a continuous) crystallizer. An improved method has been described whereby knowledge of the supersaturation course during a run and measurement of the final product crystal size distribution yield the growth rate of crystals and the nucleation rate in a wide range of supersaturation from only a single batch experiment. The evaluation method is refined by the interpolation of experimental data for short intervals of time. The method is illustrated using potassium sulfate crystallization as an example (Nývlt 1993).

6.1.8 Commercial Crystallization Equipment Supplier

HPD (formerly a division of US Filter, now a division of Veolia Water Systems; www.hpd.usfilter.com) is a commercial manufacturer of evaporation and crystallization systems for the salt, pulp and paper, fertilizer, chlor-alkali, and metals industries. HPD personnel are experienced in process analysis, piloting (50,000 ft² research center), process design and development, project management and execution. They supply crystallization processing equipment for the following industries: calcium chloride, sodium carbonate, sodium bicarbonate, sodium chloride, ammonium nitrate, ammonium phosphate, calcium nitrate, potassium chloride, potassium nitrate, potassium sulfate, sodium nitrate, sodium sulfate, alumina, aluminum hydroxide, lithium chloride, magnesium sulfate.

6.2 *Separation Processes*

6.2.1 *Separation Method Review – Previous Literature Reviews*

Poirier (Poirier 2000) has conducted a useful review of these technologies for application to the SRS program, and McCabe (McCabe 1995) has conducted a similar review of separation technologies for the Tanks Focus Area. Significantly, both of these reports are focused on the separation of sludge or sludge-like solids from HLW or LAW waste streams and do not specifically address the separation of precipitated salts from solution. Moreover, all of the reports from the DOE complex that were reviewed had a similar orientation. Section 1.1 gives a list of recent DOE reports on waste separations.

The following discussion is taken from Poirier (Poirier 2000). Poirier identified the following potential alternatives to the planned 0.5 μm Mott crossflow filter for removing insoluble solids from SRS high level waste:

- Other crossflow filters
 - Smaller pore size Mott filters
 - Graver filter
 - Centrifugal filter
 - Vibratory Shear Enhanced Processing (VSEP) Filter
 - Vacco filter
- Dead-end filtration
- Centrifugal methods

6.2.2 *Conventional Crossflow Filtration*

The Tanks Focus Area investigation (McCabe 1995) of solid-liquid separation technologies found that although many solid-liquid separation techniques are available (i.e., centrifuges, settling, dead-end filters, depth filters, etc.), crossflow filtration has a number of advantages over these technologies for use in solid-liquid separations of DOE wastes:

- Crossflow filters have minimal maintenance requirements compared with centrifuges.
- Crossflow filters generally do not require additives that increase waste volume and change process chemistry. Dead-end filters and depth filters generally require additives.
- Crossflow filters can rapidly concentrate slurries to [relatively] high insoluble solids levels.
- Crossflow filters can be employed for continuous washing of slurries.

- ▶ Crossflow filtration space requirements are typically less than other solid-liquid separation technologies.

Smaller nominal pore size filters (0.1 μm vs. 0.5 μm) are expected to be affected less by trapping of small particles in the pores, but also increase the membrane resistance to permeate flow. In most of the tests conducted by SRNL, the membrane resistance has been found to be small compared to the resistance due to the filter cake that forms on the membrane. The WTP program is using a nominal 0.1 μm filter (from GKN, an alternative vendor), and this pore size Mott filter has been recommended for the SRS salt processing program (Poirier 2002). Tests of the Graver filter with smaller pore size found no advantages. The Mott crossflow filter achieved filtration fluxes of 0.02-0.08 gpm/ft^2 in tests on simulated sludge and MST, which is significantly lower than the target flux of 0.25 gpm/ft^2 (Herman 2003). Tests of the Mott 0.1 μm filter on actual and simulated Hanford tank wastes gave average filter fluxes of less than 0.02 gpm/ft^2 (Duignan 2003; Poirier 2003; Zamecnik 2003a; Zamecnik 2003b; Duignan 2004). The particle size of these sludges ranged mostly from submicron to 10's of microns. However, during processing, particles larger than a few microns are typically size-reduced so that few particles larger than 5 μm remain. The particle size in the crystallization of NaNO_3 was found to be 50-190 μm , so the filtration flux from crossflow filtration should be significantly higher.

All of these filters used sintered metal membranes. Ceramic membrane crossflow filters are also available from numerous manufacturers. In radioactive service, these have generally been utilized with only low radioactivity streams. For highly radioactive streams, the sintered metal filters have been preferred.

Crossflow filtration was investigated at SRNL to separate solid precipitates from Hanford waste (Walker 1997). This work was done in support of a proposed process to use NaOH at high temperatures to remove aluminum from sludge. Upon cooling, the dissolved phosphates form $\text{Na}_7(\text{PO}_4)_2\text{F}\cdot 9\text{H}_2\text{O}$ as a precipitate. The results using a Mott 0.5 μm filter were a maximum filtration flux of 0.1 gpm/ft^2 . Problems with post-filtration precipitation occurred.

6.2.3 Centrifugal Filtration (Rotary Microfilter)

The centrifugal system combines centrifugation with membrane filtration. Solids are removed from the liquid at the membrane surface, and the centrifugal force acts to keep the surface clean, minimizing the formation of a polarization layer. The centrifugal force is used to slough off any buildup on the surface, rather than to separate the solids from the liquid. Centrifugal filter systems are commercially available (from SpinTek, ASPECT USA, Pall, and Canzler) and have been used in radioactive service both at Los Alamos National Laboratory (LANL) for Low-Level Waste and in Russia for High-Level Waste. The technology has been tested with actual SRS High-Level Waste at the SRNL Shielded Cells.

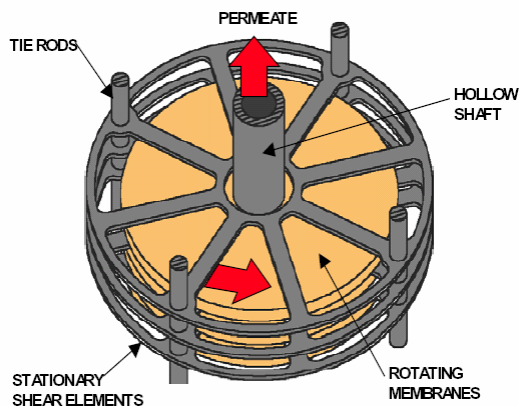


Figure 15 – SpinTek Filter

SRNL researchers tested a Spintek rotary microfilter as an alternative to the crossflow filters in the current baseline of the Salt Waste Processing Project and the Actinide Removal Project (ARP). The data show significant improvement in filter flux with the rotary microfilter over the crossflow filter (Herman 2003; Poirier 2004). Fluxes from 0.1 to 0.35 gpm/ft² were measured. These tests concentrated sludge and MST slurries to 11-13 wt% solids. The positive impacts of the rotary microfilter on the SRS HLW system were identified as:

- No new chemicals (such as flocculants) are added.
- Less frequent chemical cleaning (less oxalic acid) is required.
- Higher filtrate throughput than conventional crossflow.
- The Actinide Removal Process went to 12 wt % rather than 5 wt %.

The disadvantage of the rotary microfilter is the possibility of increased maintenance due to the rotating parts. Russia has deployed rotary filters in High Level Radioactive Waste treatment applications. Their units have operated for over four years and are still in service. Based on the Russian experience and design improvements identified, a “rad hardened” unit is believed to be operable for five years. The 3D flow regime of a crossflow filter with horizontal rotating discs was examined and modeled (Rainer 2002).

6.2.4 Novel Crossflow Filters

The Vibratory Shear Enhanced Processing (VSEP) filter, manufactured by New Logic, is similar to a plate and frame or disk stack filter. The filter pack consists of parallel disks. The feed moves slowly between the disks, and a pressure differential forces fluid through the filters. The filter elements vibrate vigorously to create shear of up to 200 G. A VSEP filter vibrating can produce a shear rate of 150,000 s⁻¹, which is about four times the shear rate attainable with conventional crossflow filters. The VSEP filter is commercially

available, but has not been demonstrated in radioactive service. The manufacturer recently sold a unit for use in low level radioactive service.

The VACCO filter is another crossflow filter. It is composed of a series of stacked disks that contain micro-channels or pores. As the fluid flows through the disks, a differential pressure drives liquid and soluble solids through the pores. It has a more structured packing than the Mott or Graver filters, but the smallest pore size available is 3 μ m. It was tested by SRNL with 3 wt% ORNL Radiochemical Engineering Development Center simulant and fouled very rapidly. The filter flux was about an order of magnitude less than the filter flux with a 0.5 μ m Mott crossflow filter using the same simulant.

6.2.5 Washing in Crossflow Filtration

Washing of solids in crossflow filter is easily conducted in a semi-batch mode where the wash liquid is continuously added to the recirculated slurry and the diluted permeate is removed. Washing is stopped when the aqueous phase of the slurry reaches a specified purity. Although easily conducted, washing in crossflow filtration is not very efficient. Continuous washing at best approaches CSTR behavior, and discrete step washing is even less efficient.

6.2.6 Intensified Filtration

Process intensification is the increasing of processing rate by application of alternative or higher “fields” such as electrical fields, ultrasonics, carrier mediation (surfactants), flow field changes, or high/ultra-high body forces or pressures (Process_Intensification 2004). The rotary filtration and VSEP filters described above are examples of intensified processes. Richard. J. Wakeman’s research group at Loughborough University performs research on filtration aided by such intensifying fields. A listing of articles by this group is given in references.

In the microfiltration of clays, titania, and similar minerals, these researchers have studied the effects of externally applied DC electric fields (see), ultrasound, and both electric fields and ultrasound. Both of these techniques work by reducing the thickness of the filter cake on the membrane by causing particle migration away from the membrane. A good review of DC electric methods has been published (Huotari 1999). Generally, these methods have been applied to particle suspensions in low ionic strength media, so their application to salt removal may be severely limited. A major drawback to these electric methods is that they generate H₂ and O₂ by electrolysis at the electrodes (this actually enhances the cake removal, but creates the undesirable H₂ and O₂). Also, there are few examples of applications of these techniques in industry. For dead-end filtration, electrically enhanced washing of ionic species from filter cakes has been reported (Tarleton 2003).

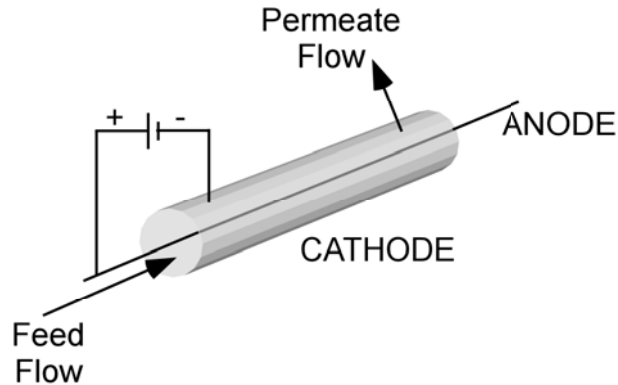


Figure 16 – Enhancement of Flux by Electric Fields

However, AEA Technologies Advanced Process Systems advertises commercial systems for “electro-kinetic dewatering”, or electrically aided crossflow filtration, and a patented process called “Direct Membrane Cleaning” that uses electrolytic generation of gas bubbles at the surface to break off material from the membrane surface.

Enhancement of crossflow filtration flux by introduction of two-phase flow has been described. In the filtration of titania suspensions (1, 5 v/v%), increases in flux of 50-80% were achieved (Pospisil 2004). The gas flow rates were 40-80% of the fluid flow rates. In a review of techniques to improve filtration (Wakeman 2002), 60-270% increases in filtration flux were reported. These authors conclude that the improvement in flux using a rotating membrane exceeds the improvement that can be gained by gas introduction. This review also discussed electrical and ultrasonic enhancement, flow field manipulation, and rotating membranes. Flow field manipulation by insertion of screw thread vortex generators was reviewed. Flux increases of 50-300% have been reported, but this technology is not commercially practiced.

6.2.7 Crossflow Filtration Modeling

There are numerous reviews and treatments of modeling of crossflow filtration in the literature. A recent review is given by Ripperger (Ripperger 2002). An interesting recent paper describes the effects of ionic strength and pH on the microfiltration of china clays (Smidova 2004). The authors show, that for low ionic strength acidic systems, filtration flux was maximized at the pH at the isoelectric point, where the zeta-potential, or net surface charge on the solid, is zero. At the isoelectric point, the filter cake has a more porous structure because the solids have more of a tendency to aggregate. Higher ionic strengths resulted in lower fluxes.

6.2.8 Dead-End Filters

This type of filter includes the familiar filter press used in many industries, tubular filters, rotary drum and disk filters, and centrifugal discharge filters. All of these filters build up a cake on the filtration medium that is then removed by some mechanical means. This mechanical removal can be by scrapers, centrifugal force, air bursts, vibration, etc. The filter press is not amenable to radioactive processing as this equipment requires

significant operator attention and generally is not designed to be enclosed. The tubular drum, disk, and centrifugal discharge filters can be enclosed. The filter media for most of these types of filters is usually some type of fabric, but other materials are available.

SRNL tested a Pall porous metal filter as a replacement for the ceramic crossflow filters at the SRS Effluent Treatment Facility (Poirier 2000). The filter fouled very rapidly and the time between backwashes was typically 5-6 minutes and about 50% of the filtrate was needed to backwash the filter. The filter had a pore size of 5 μm and was fouled by small, colloidal particles. Filter aids were not tested. Dead-end filtration was found to work best with low concentrations of large particles (McCabe 1995).

6.2.9 Tubular Filters

The most common tubular filters have filtration media (such as a fabric bag) either inside or outside of perforated vertical tubes. Tubes of sintered metal similar to crossflow filters are also available. The filter cake builds up on the filter and is removed by shocking with built-up air pressure in the vessel head to remove wet solids (back flushing) or by flexing the filtration tubes to remove “dry” solids (Fundabac candle-type filter). If frequent back flushing is required, these filters are not very efficient. Solids are removed from the bottom drain, while the filtered liquid is removed from the top outlet. Fabric filter media tends to need replacement often. For processes involving toxic or flammable materials, a closed filter system can be maintained by sloping the bottom of the horizontal cylinder to the drain nozzle for wet discharge or by using a screw conveyor in the bottom of the shell for dry discharge. Tubular filters are usually not used with high solids content feeds. Note that this type of equipment is similar to the baghouse used for gas cleaning.

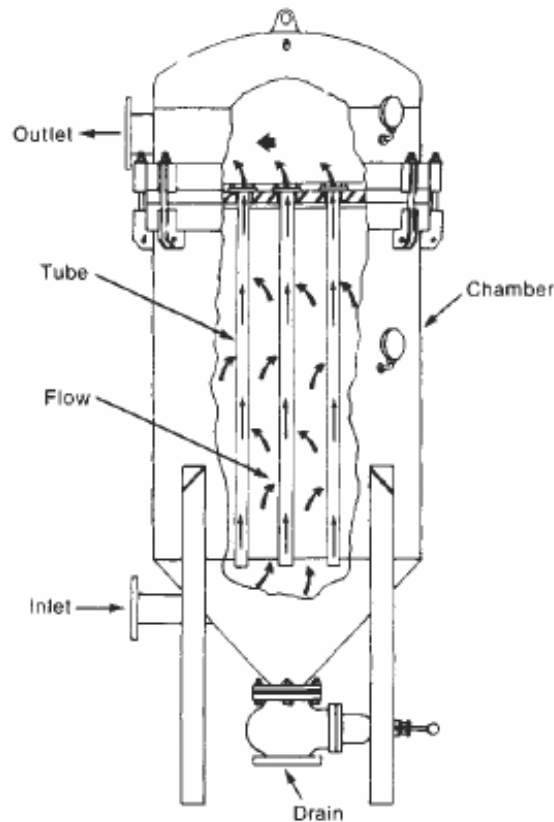


Figure 17 – Top Outlet Tubular Filter

6.2.10 Centrifugal-Discharge Filter

The centrifugal discharge filter is similar in many respects to the rotary microfilter. Horizontal top-surface filter plates may be mounted on a hollow motor-connected shaft that serves both as a filtrate-discharge manifold and as a drive shaft to permit centrifugal removal of the cake. An example is the Funda filter (Steri Technologies, www.steri.com). See .

The filtering surface may be a textile fabric, wire screen, sintered metal, or other material. The Funda filter is driven from the top, leaving the bottom unobstructed for inlet and drainage lines; a somewhat similar machine that employs a bottom drive, is the German-made Schenk filter. During filtration, the filtrate passes through the plates and out the hollow shaft, and cake is formed on the top surfaces of the plates. The cake may then be washed by introduction of wash liquid into the vessel. The cake is discharged, wet or dry, by rotation of the shaft at sufficiently high speed to sling away the solids. This mechanism would probably be ineffective with sticky micron sized particles such as waste sludges. It would most likely be effective with large crystals. An operating advantage of the centrifugal-discharge filter is its ability to discharge cake without being opened. Disadvantages are complexity and maintenance (stuffing boxes, high-speed drive) and cost. The Funda filter is made in sizes up to 537 ft². The largest Schenk filter provides 1075 ft² of area. The Funda filter from Steri is used for reactor pool water filtration at nuclear power plants in Mississippi and New Jersey (Zamecnik 2004).

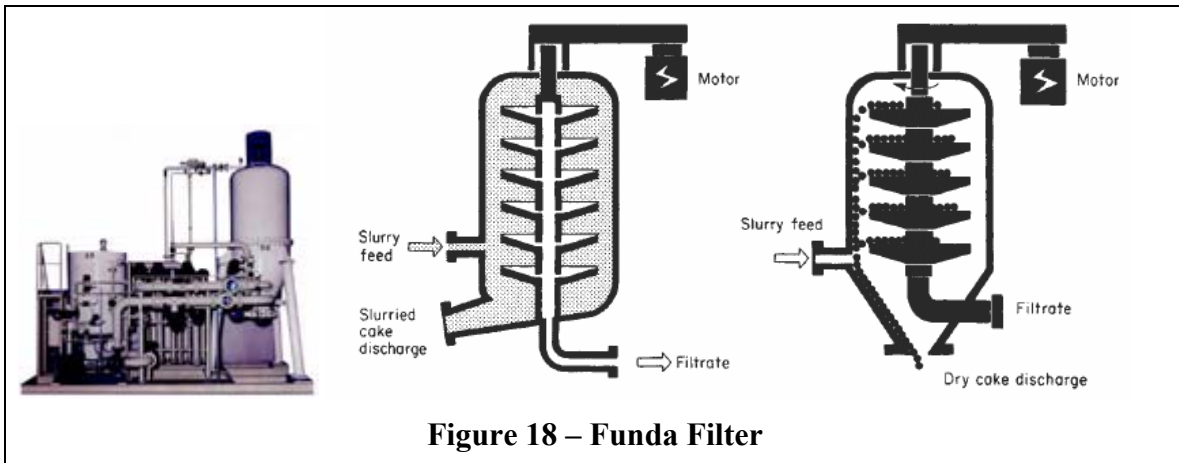


Figure 18 – Funda Filter

6.2.11 Rotary Drum Filters

The rotary drum filter is the most widely used of the semi-continuous filters. There are many design variations, including operation as either a pressure filter or a vacuum filter. The major difference between designs is in the technique for cake discharge. All the alternatives are characterized by a horizontal-axis drum covered on the cylindrical portion by filter media over a grid support structure to allow drainage to manifolds. The filter media may be fabric or multilayer metal. No reference to the availability of sintered metal was found. Filter areas range from 4 to 2000 ft².

Most drum filters are multi-compartment, wherein filtration, washing, and drying can be performed in a single unit. All multi-compartment drum filters utilize a rotary-valve arrangement to facilitate removal of filtrate and wash liquid and to allow introduction of air or gas for cake drying or blowback if needed. Blowback is a pulse of gas that may be used to dislodge solids from the filter. Generally, some type of scraper or wire is used to remove a layer of solids from the drum and discharge the cake. Most drum filters are fed by operating the drum with about 35 percent of its circumference submerged in a slurry trough. Some units contain an oscillating rake agitator or propellers or paddles in the trough to aid solids suspension. Drum filters operate at a rotation speed in the range of 0.1 to 60 rpm. Variable-speed drives are usually provided to allow adjustment for changing cake-formation and drainage rates. Disk stack filters that operate in a similar manner are also used.

Multi-compartment drum filters are space-efficient since filtration, washing, and drying can all be performed in a single unit. The rotary filter shown in was designed to filter, wash, and dry a crystallized solid (crystallized from a volatile solvent) (Perlmutter 2001). The washing specification was no more than 0.04% of the original solvent remaining in the solids. This washing was accomplished with two stages. Washing in a dead end filter can be significantly more efficient than crossflow filtration since the penetration of the wash liquid through the cake can approach plug flow. The initial filtrate and wash filtrates are collected separately. The manufacturer will custom design the filtration

system to achieve the needed separation and product purity. The typical dryness of NaNO_3 filtered on a drum filter is 3-4% moisture (Dickenson 1997).



Figure 19 – Rotary Filter with Enclosed and Pressure Control Head (BHS Filtration, (Perlmutter 2001)]

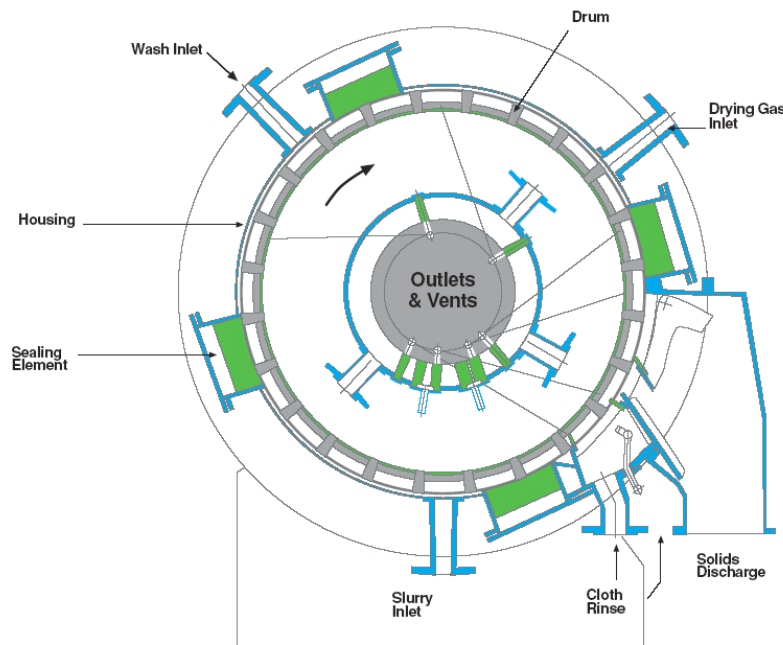
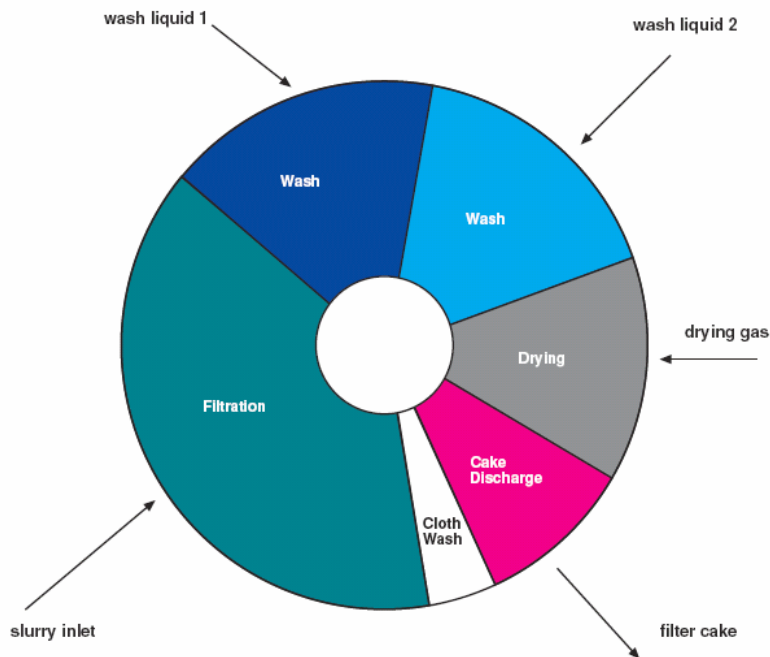


Figure 20 – Compartments in Rotary Filter [BHS Filtration, (Perlmutter 2001)]



**Figure 21 – Compartment Layout in Rotary Filter
[BHS filtration, Perlmutter 2001]**

6.2.12 Centrifugal Methods (Perry 1997)

The separation of crystallized sodium nitrate recovered from Chilean ore is achieved by continuous centrifugation (Kroschwitz 1998).

6.2.13 Sedimenting and Filtering Centrifuges

Under centrifugal force, the solid phase assumed to be denser than the liquid phase settles out to the bowl wall—sedimentation. Concurrently, the lighter, more buoyant liquid phase is displaced toward the smaller diameter—flotation. In a sedimenting centrifuge, the separation can be in the form of *clarification*, wherein solids are separated from the liquid phase in which *clarity of the liquid phase is of prime concern*. Polymers (flocculants) are used to agglomerate fine solids to facilitate clarification. Separation can also be in the form of *thickening*, where solids settle under centrifugal force to form a stream with concentrated solids. In *dewatering* or *deliquoring*, the *objective is to produce dry cake with high solids consistency* by centrifugation.

In a filtering centrifuge, separating solids from liquid does not require a density difference between the two phases. Should a density difference exist between the two phases, sedimentation is usually at a much more rapid rate compared to filtration. In both cases, the solid and liquid phases move toward the bowl under centrifugal force. The solids are retained by the filter medium, while the liquid flows through the cake solids and the filter.

When a spherical particle of diameter d settles in a viscous liquid under earth gravity g , the terminal velocity V_s is determined by the weight of the particle-balancing buoyancy and the viscous drag on the particle in accordance to Stokes' law. In a rotating flow,

Stokes' law is modified by the "centrifugal gravity" $G = \Omega^2 r$, thus $V_s = \frac{\Omega^2 r}{18\mu} (\rho_s - \rho_L) d^2$.

In order to have good separation or high settling velocity, a combination of the following conditions is generally sufficient:

- High centrifuge speed
- Large particle size
- Large density difference between solid and liquid
- Large radius
- Small viscosity

Among the five parameters, the settling velocity is very sensitive to change in speed and particle size. It varies as the square of both parameters. Sedimentation of particles is more favorable in a less viscous liquid.

Both sedimentation and filtering centrifuges come in a variety of configurations. Some centrifuges use both separation mechanisms. The major types of continuous centrifuges are:

- Disk-type, or disk stack bowl centrifuge
- Peeler centrifuges
- Pusher centrifuges
- Decanter centrifuges

6.2.14 Disk Stack Centrifuge

A disc stack centrifuge () separates solids and one or two liquid phases from each other in one single continuous process, using extremely high centrifugal forces. When the denser solids are subjected to such forces, they are forced outwards against the rotating bowl wall, while the less dense liquid phases form concentric inner layers (Alfa-Laval 2004b). Due to the close spacing of the disks, disk stacks are most suitable for clarification of liquids with small amounts of suspended solids.

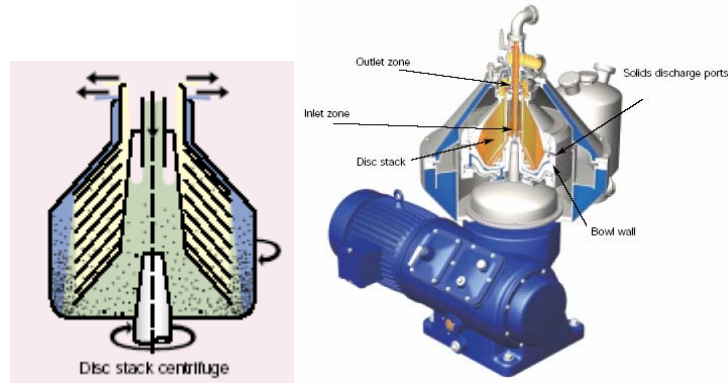


Figure 22 – Disk Stack centrifuge Configuration (Alfa-Lavel)

6.2.15 Peeler Centrifuges

Peeler centrifuges () are so-named because the accumulated filter cake is peeled off by a hydraulically activated peeling device. Peeler centrifuges are also called “horizontal (or vertical) axis basket centrifuges”. Most are oriented horizontally, but vertical arrangements are available. The separation may be accomplished by both centrifugal force and filtration. The wall of the centrifuge may be a basket, which can be made of a variety of materials, or the centrifuge can operate as a decanting centrifuge. This centrifuge operates in a cycle – filling, centrifuging, washing, and peeling, so it is a repeating batch process. This batch cycle can be adjusted, and batches can be added and processed automatically. Peeler centrifuges are commonly used for bulk chemicals (including crystallized salts), fine chemicals, pharmaceuticals, food products, etc. (Dickenson 1997).

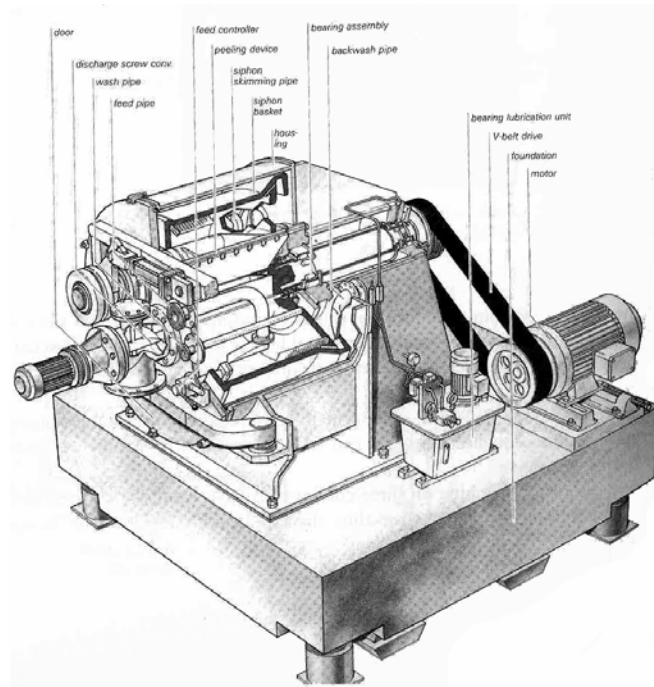


Figure 23 – Peeler Centrifuge

6.2.16 Pusher Centrifuges

Pusher centrifuges use continuous filtration to separate suspended, fast-draining crystalline and granular solids from liquids. As shown in , this centrifuge uses one or more filter baskets that are cleaned periodically by the pusher plate. The baskets may be made of a variety of materials. The solids on the basket may be washed during filtration, but this washing process is not as efficient as washing in a rotary drum filter. These centrifuges' typical use is in the plastics, chemicals, and minerals industries where high throughputs are required.

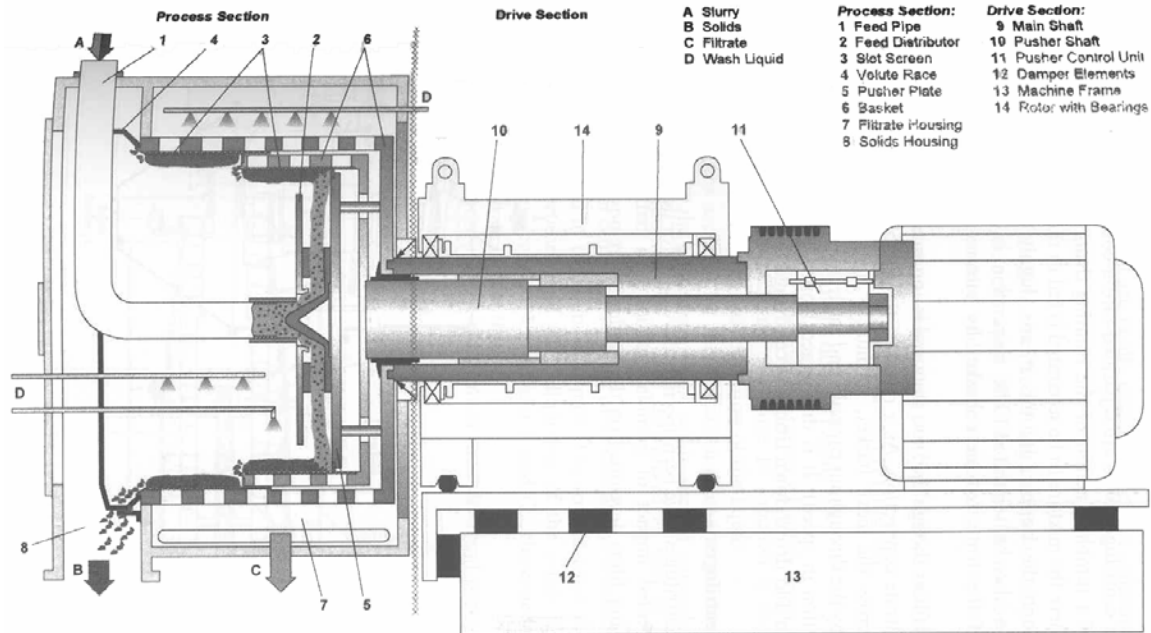


Figure 24 – Pusher Centrifuge (Dickenson 1997)

6.2.17 Decanter Centrifuges

The most common type of centrifuge used in industry is the decanter centrifuge (). The decanter centrifuge (also known as the solid-bowl or scroll centrifuge) consists of a solid bowl with a screw or scroll conveyor between the solid- and liquid-bowl heads, or hubs. Both the bowl and the conveyor rotate at a high speed, yet there is a difference in speed between the two, which is responsible for conveying the sediment along the machine from the cylinder to the conical discharge end. The bowl may be conical in shape or, in most instances; it has combined conical and cylindrical sections.

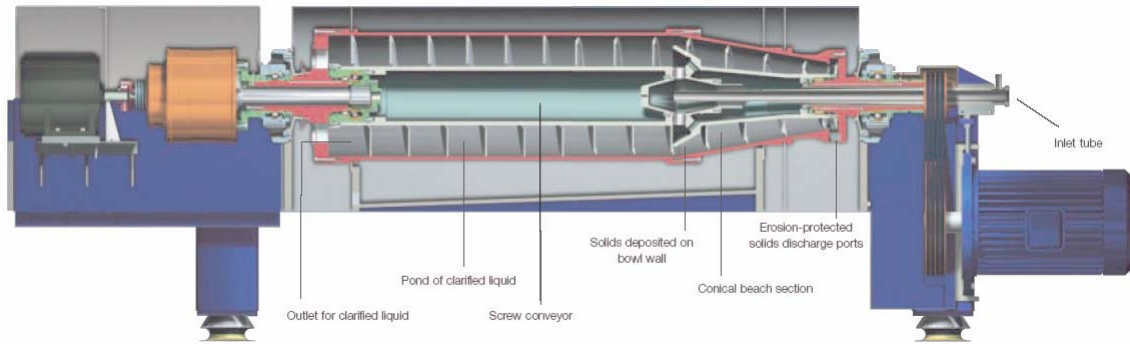


Figure 25 – Decanter Centrifuge (Alfa-Laval 2004a)

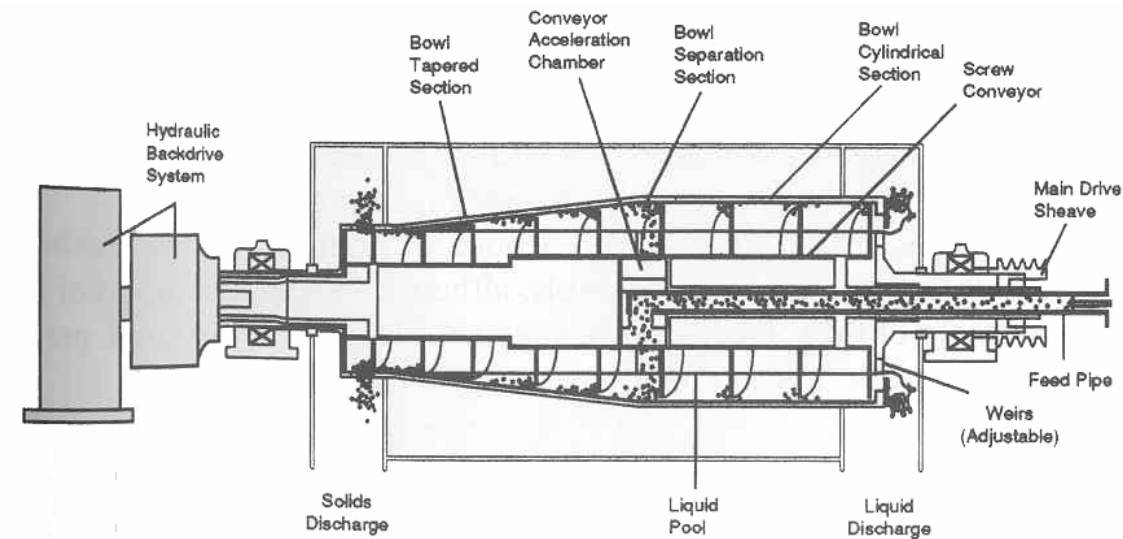


Figure 26 – Decanter Centrifuge

Slurry is introduced into the feed accelerator through a stationary pipe located near the axis of the machine. The feed slurry is accelerated through contact with the rotating surfaces to angular speed before discharging to the separation pool through a series of ports in the conveyor hub. In the separation pool, under centrifugal gravity, the solids settle toward the bowl wall, while the clarified liquid moves radially toward the pool surface. Subsequently, the liquid flows along the helical channel (or channels, if the screw conveyor has multiple leads) formed by adjacent blades of the conveyor to the liquid bowl head, from which it discharges over the weirs. The annular pool can be changed by adjusting the radial position of the weir openings, which take the form of circular holes or crescent-shaped slots.

The cake solids adjacent to the bowl wall are transported by the differential speed from the cylinder up the cone, also known as the beach. The half cone angle ranges between 5° and 20° . The cake is submerged in the pool when it is in the cylinder and at the

beginning of the beach. In this region, liquid buoyancy helps to reduce the effective weight of the cake under centrifugal gravity, resulting in lower conveyance torque. Farther up the beach, the cake emerges above the pool and moves along the “dry beach,” where buoyancy force is absent, resulting in more difficult conveyance and higher torque. But it is also in this section that the cake is dewatered, with expressed liquid returned back to the pool.

The centrifugal force helps to dewater, yet at the same time hinders the transport of the cake in the dry beach. Therefore, a balance in cake conveyance and cake dewatering is the key in setting the pool and the G-force for a given application. Also, clarification is important in dictating this decision. The cylindrical section provides clarification under high centrifugal gravity. In some cases, the pool should be shallow to maximize the G-force for separation. In other cases, when the cake layer is too thick inside the cylinder, the settled solids—especially the finer particles at the cake surface—entrain into the fast-moving liquid stream above, which eventually ends up in the centrate (clarified liquid).

Washing in a continuous decanter is *fairly* effective on solid particles larger than 80 μm , provided the particles are reasonably uniform in size with porous structure. Otherwise, the wash flows across the cake surface with little penetration because the pores at the cake surface are plugged by fines. Washing efficiency, the proportion of soluble impurities displaced from the solids, is in the range of 50 to 80 percent, depending on cake porosity, permeability, and mass-transfer rate. A wash-to-solids weight ratio of up to 0.25 is required. This washing efficiency is significantly less than that of the rotary drum filter. For the separation of crystallized salts from solution, decanter centrifuges are most often chosen by commercial industry (Dickenson 1997).

The screen bowl centrifuge () consists of a solid-bowl decanter to which, at the smaller conical end, a cylindrical screen has been added. The scroll spans the entire bowl, conforming to the profile of the bowl. It combines a sedimenting centrifuge together with a filtering centrifuge. Therefore, the solids which are processed are typically larger than 23 to 44 μm . As in a decanter, an accelerated feed is introduced to the separation pool. The denser solids settle toward the bowl wall and the effluent escapes through the ports at the large end of the machine. The sediment is scrolled toward the beach, typically with a steeper angle compared to the decanter centrifuge. As the solids are conveyed to the screen section, the liquid in the sediment cake further drains through the screen, resulting in drier cake. Washing of the sediment in the first half of the screen section is very effective in removing impurities, with the second half of the screen section reserved for dewatering of mother liquor and wash liquid.

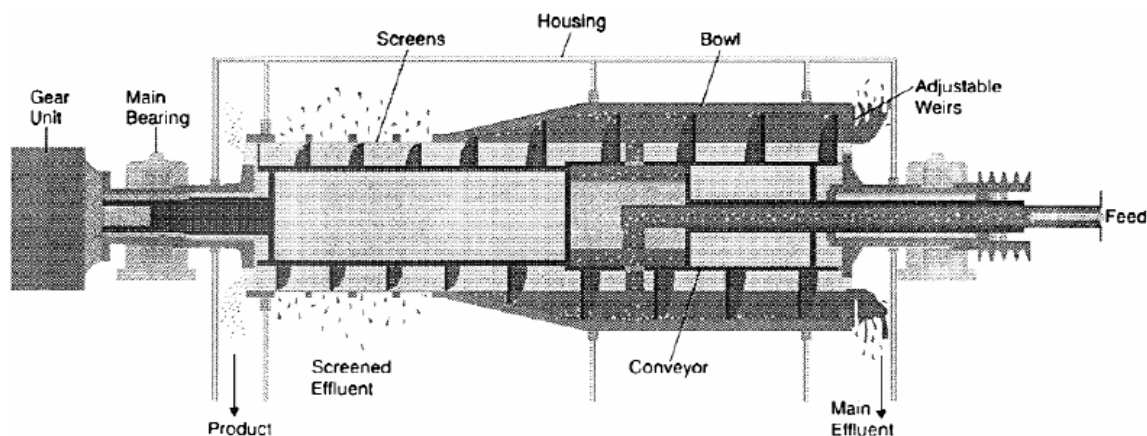


Figure 27 – Screen Bowl Centrifuge

6.2.18 SRNL Centrifuge Tests

SRNL Tested a decanter centrifuge for the removal of sludge and MST solids from simulated SRS dissolved salt (Poirier 2001). Solids loadings ranged from 0.29-6.0 wt%, and Cytec HX-400 flocculent was used for some tests. The centrifuge used was an Alfa-Laval Sharples P600. The primary goal of these tests was removal of solids to levels lower than 5-10 NTU (a turbidity unit). The actual results ranged from about 30-450 NTU, so the test showed that using a decanter centrifuge alone would not be sufficient. No data on the concentrated solids concentration was given. These authors included a list of Alfa-Laval centrifuges in nuclear service in Europe and Japan. They also note that centrifuges have been used successfully in the SRS canyons since 1953.

6.3 References for Crystallization/Separation

- Alfa-Laval (2004a). Decanter centrifuge technology, Alfa-Laval www.alfalaval.com.
- Alfa-Laval (2004b). Disc stack centrifuge technology, Alfa-Laval www.alfalaval.com.
- Al-Jibbouri, S., Ulrich, J. (2001). *The influence of Impurities on Crystallization Kinetics of Sodium Chloride*. Cryst. Res. Technol. **36**(12): 1365-1375.
- Blagden, N., Davey, R., Song, M., Quayle, M., Clark, S., Taylor, D., Nield, A. (2003). *A Novel Batch Cooling Crystallizer for in Situ Monitoring of Solution Crystallization Using Energy Dispersive X-ray Diffraction*. Cryst. Growth Des. **3**(2): 197-201.
- Cardew, P. T., Davey, R. J. (1985). *The kinetics of solvent-mediated phase transformations*. Proc. Royal Society **A398**: 415-428.
- Cesar, M. A. B., Ng, K. M. (1999). *Improving Product Recovery in Fractional Crystallization Processes: Retrofit of an Adipic Acid Plant*. Ind. Eng. Chem. Res. **38**: 823-832.
- Chang, W. C., Ng, K. M. (1998). *Synthesis of Processing System Around a Crystallizer*. AIChE J. **44**(10): 2240-2251.
- Cisternas, L. A., Swaney, R. E. (1998). *Separation System Synthesis for Fractional Crystallization from Solution Using a Network Flow Model*. Ind. Eng. Chem. Res. **37**: 2761-2769.

- Davey, R. J., Liu, W., Quayle, M. J., Tiddy, G. J. T. (2002). *In Situ Monitoring of Crystallization Processes Using Synchrotron X-ray Diffraction: The Search for Structural Precursors*. Cryst. Growth Des. **2**(4): 269-272.
- Dickenson, T. C. (1997). Filters and Filtration Handbook, Elsevier Advanced Technology.
- Duignan, M. R., *Final Report: Pilot-Scale Cross-Flow Ultrafiltration Test Using a Hanford Site Tank 241-AN-102 Waste Simulant*, **USDOE Report WSRC-TR-2003-00204, Rev. 0**, Savannah River National Laboratory (2003).
- Duignan, M. R., Zamecnik, J. R., Williams, M. R., *Interim Report: RPP-WTP Semi-Integrated Pilot Plant - Campaign I*, **WSRC-TR-2004-00201, Rev. 0**, Savannah River National Laboratory (2004).
- Herman, D. T., Poirier, M. R., Hobbs, D. T., Fink, S. D., *Testing of the SpinTek Rotary Microfilter Using Actual Waste*, **WSRC-TR-2003-00030, Rev. 0**, (2003).
- Herting, D. L., *Clean Salt Process Final Report*, **WHC-EP-0915**, Westinghouse Hanford Company (1996).
- Huotari, H. M., Tragardh, G., Huisman, I. H. (1999). *Crossflow Membrane Filtration Enhanced by an External DC Electric Field: A Review*. Trans. IChemE **77A**(July 1999): 461-468.
- Karel, M., Nyvlt, J. (1993). *Effect of Impurities on the Width of the Metastable Region of Potassium Sulfate*. Coll. Czech. Chem. Comm **58**(9): 1997-2002.
- Kroschwitz, J. I., Ed. (1998). Sodium Nitrate, Kirk-Othmer Encyclopedia of Chemical Technology, 4th Ed.
- Lynn, S., Schiozer, A. L., Jaecksch, W. L., Cos, R., Prausnitz, J. M. (1996). *Recovery of Anhydrous Na₂SO₄ from SO₂-Scrubbing Liquor by Extractive Crystallization: Liquid-Liquid Equilibria for Aqueous Solutions of Sodium Carbonate, Sulfate, and/or Sulfite Plus Acetone, 2-Propanol, or tert-Butyl Alcohol*. Ind. Eng. Chem. Res. **35**: 4236-4245.
- McCabe, D. J., *Evaluation and Ranking of the Tank Focus Area Solid Liquid Separation Needs*, **WSRC-TR-95-0337, Rev. 0**, Savannah River National Laboratory (1995).
- Mullin, J. W. (2001). Crystallization. 4th Ed., Butterworth Heinemann.
- Myerson, A. S. (2002). Handbook of Industrial Crystallization. 2nd Ed., Butterworth Heinemann.
- Nordhoff, S., Ulrich, J. (1999). *Solvent-Induced Phase Transformations of Hydrates*. J. Thermal Anal. Cal. **57**: 181-192.
- Nývlt, J. (1977). Solid-Liquid Phase Equilibria, Amsterdam, Elsevier.
- Nývlt, J. (1995). *The Ostwald Rule of Stages*. Cryst. Res. Technol. **30**(4): 443-449.
- Nývlt, J. (1997). *On the Kinetics of Solid-Liquid-Solid Phase Transformation*. Cryst. Res. Technol. **32**(5): 695-700.
- Nývlt, J. (2000). *Hydration Analysis and the Expansion of Relative Activity Coefficients*. Coll. Czech. Chem. Comm **65**(12): 1833-1838.
- Nývlt, J., Eysseltova, J. (1994). *Physical Interpretation of Solubility Interaction Constants From the Series Expansion of the Relative Activity Coefficients*. Coll. Czech. Chem. Comm **59**(9): 1911-1921.
- Nývlt, J., Hostomská, V. (1998). *Influence of the pH-Value on the Metastable Zone Width of Potassium Sulphate*. Cryst. Res. Technol. **33**(5): 767-775.

- Nývlt, J., Karel, M. (1993). *Improved Measurement of the Kinetics of Crystallization in a Batch Experiment*. Coll. Czech. Chem. Comm **58**(8): 1839-1847.
- Oosterhof, H., Witkamp, G. J., van Rosmalen, G. M. (2001a). *Antisolvent Crystallization of Anhydrous Sodium Carbonate at Atmospheric Conditions*. AIChE J. **47**(3): 602-608.
- Oosterhof, H., Witkamp, G. J., van Rosmalen, G. M. (2001b). *Evaporative Crystallization of Anhydrous Sodium Carbonate at Atmospheric Conditions*. AIChE J. **47**(10): 2220-2225.
- Parthasarathy, G., Dunn, R. F., El-Halwagi, M. M. (2001a). *Development of Heat-Integrated Evaporation and Crystallization Networks for Ternary Wastewater Systems. 1. Design of the Separation System*. Ind. Eng. Chem. Res. **40**: 2827-2841.
- Parthasarathy, G., Dunn, R. F., El-Halwagi, M. M. (2001b). *Development of Heat-Integrated Evaporation and Crystallization Networks for Ternary Wastewater Systems. 2. Interception Task Identification for the Separation and Allocation Network*. Ind. Eng. Chem. Res. **40**: 2842-2856.
- Perlmutter, B. A. (2001). *Improving Process Operations with a Rotary Pressure Filter*. Chemical Processing (see www.bhs-filtration.com) **January**.
- Perry (1997). *Liquid-Solid Operations and Equipment*. Perry's Chemical Engineers' Handbook. R. H. G. Perry, D.W., McGraw-Hill.
- Person, J. C., *Literature Survey for Fractional Crystallization*, **RPP-21695, Rev. 0 (EDT-820947)**, CH2M Hill Hanford Group (2004).
- Poirier, M. R., *Evaluation of Solid-Liquid Separation Technologies to Remove Sludge and Monosodium Titanate from SRS High Level Waste*, **WSRC-TR-2000-00288**, Savannah River National Laboratory (2000).
- Poirier, M. R., Burket, P. R., Siler, J. L., Zamecnik, J. R., *Filtration, Washing, and Leaching of a Hanford AY-102/C-106 Sample*, **WSRC-TR-2003-00240, Rev. 0**, Savannah River National Laboratory (2003).
- Poirier, M. R., Fink, S. D., *Recommendation for Using Smaller (0.1 μ) Pore-Size Media for Filtration in Salt Waste Processing Project*, **WSRC-TR-2002-00341, Rev. 0**, Savannah River National Laboratory (2002).
- Poirier, M. R., Herman, D. T., Martin, K. B., Siler, J. L., Fink, S. D., *Impact of a Rotary Microfilter on the Savannah River Site High Level Waste System*, **WSRC-RP-2004-00234, Rev. 0**, Savannah River National Laboratory (2004).
- Poirier, M. R., Norato, M. A., Fink, S. D., *Evaluating Centrifuges for Solid-Liquid Separation in the SRS Salt Processing Program*, **WSRC-TR-2001-00555**, Savannah River National Laboratory (2001).
- Pospisil, P., Wakeman, R. J., Hodgson, I. O. A., Mikulášek, P. (2004). *Shear Stress-based Modeling of Steady State Permeate Flux in Microfiltration Enhanced by Two-Phase Flows*. Chem. Eng. J. **97**: 257-263.
- Process_Intensification (2004). What is Process Intensification?, Process Intensification and Miniaturisation Research Group, www.ncl.ac.uk/pim/intensi.htm.
- Rainer, M., Hoflinger, W., Koch, W., Pongratz, E., Oechsle, D. (2002). *3D-flow simulation and optimization of a cross flow filtration with rotating discs*. Sep. Purif. Tech. **26**: 121-131.

- Ripperger, S., Altmann, J. (2002). *Crossflow microfiltration - state of the art*. Sep. Pur. Tech **26**: 19-31.
- Samant, K. D., Ng, K., M. (2001). *Representation of High-Dimensional Solid-Liquid Phase Diagrams of Ionic Systems*. AIChE J. **47**(4): 861-879.
- Shi, B., Frederick, Jr., J., Rousseau, R. W. (2003). *Effects of Calcium and Other Ionic Impurities on the Primary Nucleation of Burkeite*. Ind. Eng. Chem. Res. **42**: 2861-2869.
- Shi, B., Rousseau, R. W. (2001). *Crystal Properties and Nucleation Kinetics from Aqueous Solutions of Na₂CO₃ and Na₂SO₄*. Ind. Eng. Chem. Res. **40**: 1541-1547.
- Smidova, D., Mikulášek, P., Wakeman, R. J., Velikovska, P. (2004). *Influence of ionic strength and pH of dispersed systems on microfiltration*. Desalination **163**: 323-332.
- Taboada, M. E., Graber, T. A., Cisternas, L. A. (2004). *Sodium Carbonate Extractive Crystallization with Poly(ethylene glycol) Equilibrium Data and Conceptual Process Design*. Ind. Eng. Chem. Res. **43**: 835-838.
- Tarleton, E. S., Wakeman, R. J., Liang, Y. (2003). *Electrically Enhanced Washing of Ionic Species from Fine Particle Filter Cakes*. Trans. IChemE **81A**: 201-210.
- Vaessen, R., Seckler, M., Witkamp, G. J. (2003). *Eutectic Freeze Crystallization with an Aqueous KNO₃-HNO₃ Solution in a 100-L Cooled-Disk Column Crystallizer*. Ind. Eng. Chem. Res. **42**: 4874-4880.
- Wakeman, R. J., Williams, C. J. (2002). *Additional techniques to improve filtration*. Sep. Pur. Tech **26**: 3-18.
- Walker, B., McCabe, D., *Hanford Phosphate Precipitation Filtration Process Evaluation*, **WSRC-TR-97-00352**, Savannah River National Laboratory (1997).
- Wibowo, C., Chang, W. C., Ng, K. M. (2001). *Design of Integrated Crystallization Systems*. AIChE J. **47**(11): 2474-2492.
- Wibowo, C., Ng, K. M. (2000). *Unified Approach for Synthesizing Crystallization-Based Separation Processes*. AIChE J. **46**(7): 1400-1421.
- Wibowo, C., Ng, K. M. (2002). *Visualization of High-Dimensional Phase Diagrams of Molecular and Ionic Species*. AIChE J. **48**(5): 991-1000.
- Zamecnik, J. (2004). Personal Communication: Conversation with C. Nigg of Steri Technologies.
- Zamecnik, J. R., Baich, M. R., Hansen, E. K., Poirier, M. R., *AN-102 Simulant Sr/TRU Precipitation and Ultrafiltration*, **USDOE Report WSRC-TR-2003-00056, Rev. 0**, Savannah River National Laboratory (2003a).
- Zamecnik, J. R., Burket, P. R., Eibling, R. E., Poirier, M. R., Hansen, E. K., *Tank 241-AY-102 Simulant Development, Ultrafiltration, and Washing*, **WSRC-TR-2003-00547, Rev. 0**, Savannah River National Laboratory (2003b)

6.3.1 Bibliography of Selected DOE Crossflow Filtration References

WSRC-TR-2001-00175

Improving the Filtration of Sludge/Monosodium Titanate Slurries by the Addition of Flocculants

Poirier, M.R.

2001

WSRC-MS-99-00467

Pilot-Scale Cross-Flow Filtration Test for Radioactive Waste Simulants with High Solids

Duignan, M.R.

2001

WSRC-TR-2001-00214, Rev. 1

Filtration Systems, Inc. Report for SRS SpinTek Rotary Microfilter Testing

Poirier, M.R.

2001

DOE/MC/31388-13-Pt.4

Task 9 - Centrifugal membrane filtration. Semi-annual report, April 1--September 30, 1997

Stepan, D.J.; et al.

1997

WSRC-TR-2001-00214

Filtration Systems, Inc. Report for SRS SpinTek Rotary Microfilter Testing

Poirier, M.R.

2001

EMSP-55146-97

Adsorption/membrane filtration as a contaminant concentration and separation process for mixed wastes and tank wastes. Progress report, 1996--1997

Benjamin, M.M.; et al.

1997

WSRC-TR-2001-00212

Cross-Flow Filtration Demonstration for Slurries Containing High Level Waste Sludge and Monosodium Titanate

Poirier, M.R.

2001

WSRC-TR-2002-00194

Comparison of Cross Flow Filtration Performance for Manganese Oxide/Sludge Mixtures and Monosodium Titanate/Sludge Mixtures

Poirier, M.R.

2002

WSRC-TR-2003-00295, Rev 0 SRT-RPP-2003-00137
Filtration of a Hanford AN-104 Sample
Poirier, Michael R
2004

WSRC-MS-2004-00211, Rev. 0
Mixing Effects on the Precipitation and Cross Flows Filtration of a Hanford Simulated
Precipitated Radioactive Waste
Duignan, Mark
2004

DOE/MC/31388—5500
Task 9 - centrifugal membrane filtration. Semi-annual report April 1--September 30,
1996
Stepan, D.J.; et al.
1997

DOE/ER/62313;
Project Number 55146 Adsorption/Membrane Filtration as a Contaminant Concentration
and Separation Process for Mixed Wastes and Tank Wastes - Final Report
Benjamin, M.M.
1999

EMSP-55146-98
Adsorption/membrane filtration as a contaminant concentration and separation process
for mixed wastes and tank wastes. 1998 annual progress report
Benjamin, M.M.; et al.
1998

RPP-13437, Rev.0 Technical basis document for ventilation system filtration failures
leading to unfiltered release
Himes, D.A.
2003

WSRC-TR-2002-00134, Rev. 0 Filtration of Actual Savannah River Waste Treated with
Permanganate or Monosodium Titanate
Poirier, M.R.
2002

WSRC-TR-2001-00195
Cross-Flow Filtration of Simulated High-Level Waste Sludge (Tank 8F)
Poirier, M.R.
2001

PNNL—11652

Bench-scale crossflow filtration of Hanford tank C-106, C-107, B-110, and U-110 sludge slurries

Geeting, J.G.H.; et al.
1997

WSRC-TR-95-0483

Filtration of Tank 48H Contents with a Cells Unit Filter

Nash, C.A.
2002

WSRC-TR-2002-00341

Recommendation for Using Smaller (0.1 micro sign) Pore-Size Media for Filtration in Salt Waste Processing Project

Poirier, M.R.
2003

WSRC-MS-2001-00134

Crossflow Filtration and Rheology of a Strontium Carbonate/Manganese Oxide Slurry

Nash, C.A.
2001

WSRC-MS-2004-00208

Filtration of a Hanford AN-104 Sample

Poirier, Michael
2004

WSRC-TR-2000-00341

Entrained Solids, Strontium-Transuranic Precipitation, and Crossflow Filtration of AN102 Small C

Nash, C.A.
2000

WSRC-RP-2000-00685, Rev. 0

Monosodium Titanate Sludge Filtration

Dworjanyn, L.O.
2000

DE--FC21-94MC31388-30

Centrifugal Membrane Filtration

Daniel J. Stepan; et al.
1999

DE-FC21-94MC31388-17
EM Task 9 - Centrifugal Membrane Filtration
Stevens, B.G.; et al.
1998

ORNL/CP--94960;
CONF-9710103-- Magnetic-seeding filtration
Ying, T.Y.; et al.
1997

CONF-9609234--2 Magnetic flocculation and filtration
Yiacoumi, Sotira; et al.
1996

WSRC-TR--97-00353
Hanford underground storage tank waste filtration process evaluation
Walker, B.W.; et al.
1997

BNF-003-98-0226
Final Report: Pilot-Scale X-Flow Filtration Test - Env C Plus Entrained Solids Plus
Sr/TRU
Duignan, M.R.
2000

WSRC-TR-96-0232
Hanford and Oak Ridge underground storage tank waste filtration process evaluation
McCabe, D.J.
1996

WSRC-TR-97-00354
Oak Ridge National Laboratory Melton Valley Storage Tanks Waste filtration process
evaluation
Walker, B.W.; et al.
1997

WSRC-TR-97-00354, Rev. 1 Oak Ridge National Laboratory Melton Valley Storage
Tanks Waste Filtration Process Evaluation
Walker, B.W.
1998

WSRC-TR-97-00352 Hanford phosphate precipitation filtration process evaluation
Walker, B.W.; et al.
1997

WSRC-MS-98-00039

CONF-980543-- Cross-Flow Filtration of Department of Energy Hanford Waste Streams Using Sintered Metal Mott and Graver Filters at the Savannah River Technology Center
Walker, B.W.; et al.

1998

BNF-003-98-0221 Final Report: Pilot-scale Cross-flow Filtration Test - Envelope A+
Entrained Solids

Duignan, M.R.

2000

WSRC-TR-2001-00213

Evaluation of Flocculation and Filtration Procedures Applied to WSRC Sludge: A Report
from B. Yarar, Colorado School of Mines

Poirier, M.R.

2001

PNNL—11032

Results of HWVP transuranic process waste treatment laboratory and pilot-scale filtration
tests using specially ground zeolite

Eakin, D.E.

1996

PNNL—11376

Bench-scale cross flow filtration of Tank S-107 sludge slurries and Tank C-107
supernatant

Geeting, J.G.H.; et al.

1996

WSRC-TR-2000-00506

Strontium-Transuranic Precipitation and Crossflow Filtration of 241-AN-102 Large C
Nash, C.A.

2001

WSRC-MS-2001-00071

Transuranic/Strontium Precipitation and Filtration of Hanford Complexant Waste
Nash, C.A.

2001

WSRC-TR-2002-00530, Rev. 0 SRT-RPP-2002-00263, Rev. 0

Filtration of a Hanford AW-101 Waste Sample

Poirier, M. R.

2004

WSRC-MS--96-0524;
CONF-970321--1 Cross flow filtration of aqueous radioactive tank wastes
McCabe, D.J.; et al.
1997

ORNL/TM-2000/27
Development and Deployment of a Full-Scale Cross-Flow Filtration System for
Treatment of Liquid Low-Level Waste at Oak Ridge National Laboratory
Kent, T.E.
2000

DOE/MC/31388—5775
Task 9- Centrifugal Membrane Filtration. Semiannual report, November 1, 1996--March
31, 1997
Stephan, Daniel J.; et al.
1997

WSRC-TR-98-00364 Salt disposition alternatives filtration at SRTC
Walker, B. W.; et al.
2000

WSRC-MS-2003-00756, Rev. 0
Filtration of a Hanford Site Tank 241-AN-102 Waste Sample with Alternate Sr/TRU
Precipitation Conditions at Bench and Pilot Scales
Zamecnik, J. R.
2004

6.3.2 Bibliography of Selected Publications

6.3.2.1 Publications of K. M. Ng:

- Dye, S. R., and Ng, K. M., "Bypassing Eutectics with Extractive Crystallization: Design Alternatives and Tradeoffs," *AIChE J.*, 41, 1456-1470 (1995).
- Dye, S. R., and Ng, K. M., "Fractional Crystallization: Design Alternatives and Tradeoffs," *AIChE J.*, 41, 2427-2438 (1995).
- Berry, D. A., and Ng, K. M., "Separation of Quaternary Conjugate Salt Systems by Fractional Crystallization," *AIChE J.*, 42, 2162-2174 (1996).
- Berry, D. A., Dye, S. R., and Ng, K. M., "Synthesis of Drowning-Out Crystallization-Based Separations," *AIChE J.*, 43, 91-103 (1997). [This article was featured in *Chem. Eng. Progress.*]
- Berry, D. A., and Ng, K. M., "Synthesis of Reactive Crystallization Processes," *AIChE J.*, 43, 1737-1750 (1997).
- Berry, D. A., and Ng, K. M., "Synthesis of Crystallization-Distillation Hybrid Separation Processes," *AIChE J.*, 43, 1751-1762 (1997).
- O'Young, L., Natori, Y., Pressly, T. G., and Ng, K. M., "A Physical Limitation Based Framework for Separations Synthesis," *Comp. Chem. Eng.*, 21, S223-230 (1997).
- Chang, W. C., and Ng, K. M., "Synthesis of the Processing System Around a Crystallizer," *AIChE J.*, 44, 2240-2251 (1998).
- Pressly, T. G., and Ng, K. M., "A Break-Even Analysis of Distillation-Membrane Hybrids," *AIChE J.*, 44, 93-105 (1998).
- Cesar, M. A. B., and Ng, K. M., "Improving Product Recovery in Fractional Crystallization Processes: Retrofit of an Adipic Acid Plant," *Ind. Eng. Chem. Res.*, 38, 823-832 (1999).
- Kelkar, V. V., and Ng, K. M., "Design of Reactive Crystallization Systems Incorporating Kinetics and Mass Transfer Effects," *AIChE J.*, 45, 69-81 (1999).
- Pressly, T. G., and Ng, K. M., "A Process Boundary Approach for Separations Synthesis," *AIChE J.*, 45, 1939-1952 (1999).
- Samant, K. D., Berry, D. A., and Ng, K. M., "Framework for Representation of High-Dimensional, Molecular Solid-Liquid Phase Diagrams," *AIChE J.*, 46, 2435-2455 (2000).
- Wibowo, C., and Ng, K. M., "Unified Approach for Synthesizing Crystallization-Based Separation Processes," *AIChE J.*, 46, 1400-1421 (2000).
- Samant, K. D., and Ng, K. M., "Representation of High-Dimensional Solid-Liquid Phase Diagrams for Ionic Systems," *AIChE J.*, 47, 861-879 (2001).
- Schroer, J. W., Wibowo, C., and Ng, K. M., "Synthesis of Chiral Crystallization Processes," *AIChE J.*, 47, 369-387 (2001).
- Wibowo, C., Chang, W. C., and Ng, K. M., "Design of Integrated Crystallization Systems," *AIChE J.*, 47, 2474-2492 (2001).
- Wibowo, C., and Ng, K. M., "Visualization of High-Dimensional Phase Diagrams of Molecular and Ionic Mixtures," accepted for publication in *AIChE J.* (2001).
- Wibowo, C., Samant, K. D., and Ng, K. M., "Visualization of High-Dimensional Solid-Liquid Phase Diagrams Involving Compounds and Polymorphs," to appear in *AIChE J.* (2001).

Wibowo, C., and Ng, K. M. "Visualization of High Dimensional Systems via Geometric Modeling with Homogeneous Coordinates," accepted for publication in *Ind. Eng. Chem. Res.* (2002).

6.3.2.2 Selected Publications of R. J. Wakeman

Books - Authored

Wakeman, R.J. and Tarleton, E.S., *Filtration Equipment Selection Modeling and Process Simulation*, Elsevier Advanced Technology, Oxford, 1999, xxvi + 446 pages, ISBN 1 85617 345 3.

Edited Works: Contributions

Wakeman, R.J., "Decanters", in *International Encyclopedia of Heat and Mass Transfer*, Hewitt, G.F., Shires, G.L. & Polezhaev, Y.V. (Eds), CRC Press, Boca Raton, 1997, p 293, ISBN 0 8493 9356 6.

Wakeman, R.J., "Centrifuges", in *International Encyclopedia of Heat and Mass Transfer*, Hewitt, G.F., Shires, G.L. & Polezhaev, Y.V. (Eds), CRC Press, Boca Raton, 1997, pp 144-146, ISBN 0 8493 9356 6.

Wakeman, R.J., "Classifiers", in *International Encyclopedia of Heat and Mass Transfer*, Hewitt, G.F., Shires, G.L. & Polezhaev, Y.V. (Eds), CRC Press, Boca Raton, 1997, pp 164-165, ISBN 0 8493 9356 6.

Wakeman, R.J., "Liquid-Solid Separation", in *International Encyclopedia of Heat and Mass Transfer*, Hewitt, G.F., Shires, G.L. & Polezhaev, Y.V. (Eds), CRC Press, Boca Raton, 1997, pp 682-685, ISBN 0 8493 9356 6.

Wakeman, R.J., "Sedimentation", in *International Encyclopedia of Heat and Mass Transfer*, Hewitt, G.F., Shires, G.L. & Polezhaev, Y.V. (Eds), CRC Press, Boca Raton, 1997, pp 992-994, ISBN 0 8493 9356 6.

Tarleton, E.S. and Wakeman, R.J., "Ultrasonically Assisted Separation Processes", in *Ultrasound in Food Processing*, Povey, M.J.W. & Mason, T. (eds), Chapman and Hall, London, 1997, pp 193-218.

Wakeman, R.J., "Extraction, Liquid-Solid", in *Encyclopedia of Separation Technology*, Ruthven, Douglas M. (Ed), Wiley-Interscience, New York, 1997, pp 814-828, ISBN 0 471 16124 1.

Wakeman, R.J., "Extraction: Liquid-Solid", in *Kirk-Othner Concise Encyclopedia of Chemical Technology 4th Edition*, Kroschwitz, J.I. (Ed), Wiley-Interscience, New York, 1999, pp 797-799, ISBN 0 471 29698 8.

Wakeman, R.J., "Filtration - Electrifying and vibrating the technology", in *Frontiers in Particle Science and Technology*, D.T. Goddard, S. Lawson and R.A. Williams, University of Leeds, 2002, 74-85, ISBN 0 85316 231 X.

Journal Papers - Academic Journals

- Akay, G. and Wakeman, R.J., "Crossflow Microfiltration Behaviour of a Double Chain Surfactant Dispersion in Water - I: The Effect of Process and Membrane Characteristics on Permeate Flux and Surfactant Rejection", *Chemical Engineering Science*, 49(2), 1994, pp 271-283.
- Wakeman, R.J., "Visualisation of Cake Formation in Crossflow Microfiltration", *Transactions of The Institution of Chemical Engineers, Part A*, 72, 1994, pp 530-540, ISSN 0263 8762.
- Tarleton, E.S. and Wakeman, R.J., "Understanding Flux Decline in Crossflow Microfiltration: Part III - Effects of Membrane Morphology", *Transactions of Institution of Chemical Engineers*, 72(A), 1994, pp 521-529, ISSN 0263 8762.
- Akay, G. and Wakeman, R.J., "Mechanisms of Permeate Flux Decay, Solute Rejection and Concentration Polarisation in Crossflow Filtration of a Double Chain Ionic Surfactant Dispersion", *Journal of Membrane Science*, 88, 1994, pp 177-195.
- Tarleton, E.S. and Wakeman, R.J., "Understanding Flux Decline in Crossflow Microfiltration: Part II - Effects of Process Parameters", *Transactions of the Institution of Chemical Engineers*, 72(A), May 1994, pp 431-440, ISSN 0263 8762.
- Koenders, M.A. and Wakeman, R.J., "Radial Flow Dependence in Filtration Experiments", *Chemical Engineering Science*, 50(23), 1995, pp 3777-3782, ISSN 0009 2509.
- Wakeman, R.J. and Sabri, M.N., "Utilizing Pulsed Electric Fields in Crossflow Microfiltration of Titania Suspensions", *Transactions of The Institution of Chemical Engineers, Part A*, 73, 1995, pp 455-463.
- Koenders, M.A. and Wakeman, R.J., "The Initial Stages of Compact Formation from Suspensions by Filtration", *Chemical Engineering Science*, 51(16), 1996, pp 3897-3908, ISSN 0009 2509.
- Akay, G. and Wakeman, R.J., "Electric Field Intensification of Surfactant Mediated Separation Processes", *Transactions of Institution of Chemical Engineers, Part A*, 74(A5), 1996, pp 517-525, ISSN 0263 8762.
- Koenders, M.A. "Curt" and Wakeman, R.J., "Initial Deposition of Interacting Particles by Filtration of Dilute Suspensions", *AIChE Journal*, 43(4), 1997, pp 946-958, ISSN 0001 1541.
- Mikulasek, P., Wakeman, R.J. and Marchant, J.Q., "The Influence of pH and Temperature on the Rheology and Stability of Aqueous Titanium Dioxide Dispersions", *The Chemical Engineering Journal*, 67, 1997, pp 97-102, ISSN 1385 8947.
- Mikulasek, P., Wakeman, R.J. and Marchant, J.Q., "Crossflow Microfiltration of Shear-thinning Aqueous Titanium Dioxide Dispersions", *The Journal of Chemical Engineering*, 69, 1998, pp 53-61, ISSN 1385 8947.
- Mikulasek, P., Wakeman, R.J. and Marchant, J.W., "The Rheological Behaviour and Crossflow Microfiltration of Concentrated, Non-Newtonian Dispersions", *Chemical and Biochemical Engineering*, 13(2), 1999, pp 73-90, ISSN 0352 9568.

- Wakeman, R.J. and Kotzian, R., "Cu²⁺ and Cd²⁺ Removal from Aqueous Solutions using Lecithin Enhanced Ultrafiltration", *Transactions of the Filtration Society*, 1(1), 2000, pp 8-13, ISSN 1471 3640.
- Smythe, M.C. and Wakeman, R.J., "The Use Of Acoustic Fields As A Filtration And Dewatering Aid", *Ultrasonics*, 38, 2000, pp 657-661, ISSN 0041-624X.
- Wakeman, R.J. and Smythe, M.C., "Clarifying Filtration of Fine Particle Suspensions Aided by Electrical and Acoustic Fields", *Transactions of the Institution of Chemical Engineers, Part A*, 78, 2000, pp 125-135, ISSN 0263 8762.
- Wakeman, R.J. and Bailey, A.J.L., "Sonothickening: Continuous In-line Concentration/Clarification Of Fine Particle Suspensions By Power Ultrasound", *Transactions Of The Institution Of Chemical Engineers*, 78A4, 2000, pp 651-661, ISSN 0263-8762.
- Wakeman, R.J., Wu, P. and Koenders, M.A., "Simulation of the motion of particles settling towards a vibrating filter medium", *Transactions of the Filtration Society*, 21, 2001, 13-19, ISSN 1471-3640.
- Wakeman, R.J. and Williams, C.J., "Additional techniques to improve microfiltration", *Separation and Purification Technology*, 26, 2002, 3-18.
- Wakeman, R.J. and Butt, G., "An investigation of high gradient dielectrophoretic filtration", *Transactions of Institution of Chemical Engineers, Part A*, 81, 2003, 924-935, ISSN 0263-8762.
- Tarleton, E.S., Wakeman, R.J. and Liang, Y., "Electrically enhanced washing of ionic species from fine particle filter cakes", *Transactions IChemE*, 81(A), 2003, 201-210.
- Smidova, D., Mikulasek, P., Wakeman, R.J. and Velikovska, P., "Influence of ionic strength and pH of dispersed systems on microfiltration", *Desalination*, 163, 2004, 323-332, ISSN 0011-9164.
- Smidova, D., Mikulasek, P., Wakeman, R.J. and Velikovska, P., "Charge effects of dispersed systems and membrane surface on cross-flow microfiltration", *Filtration*, 4, 2004, 204-209, ISSN 1479-0602.
- Pospisil, P., Wakeman, R.J., Hodgson, I.O.A. and Mikulasek, P., "Shear stress-based modelling of steady state permeate flux in microfiltration enhanced by two-phase flows", *Chemical Engineering Journal*, 97, 2004, 257-263, ISSN 1385-8947.
- Journal Papers - Professional Journals*
- Wakeman, R.J., "Modelling Slurry Dewatering and Cake Growth in Filtering Centrifuges", *Filtration and Separation*, 31(1), 1994, pp 75-81.
- Akay, G. and Wakeman, R.J., "Permeate Flux Decay During Crossflow Microfiltration of a Cationic Surfactant Dispersion", *Filtration and Separation*, 31(7), 1994, pp 727-731.
- Wakeman, R.J., "Selection of Equipment for Solid/Liquid Separation Processes", *Filtration and Separation*, 32(4), 1995, pp 337-341.
- Wakeman, R.J., "Fouling in Crossflow Ultra- and Micro-filtration", *Membrane Technology*, 70, 1996, pp 5-8, ISSN 0958 2118.

- Wakeman, R.J., "Post-Filtration Processes and Their Impact on Drying", *Chemical Processing Technology International*, 11(SpecialACHEMA), 1997, pp 117-125, ISBN 1 85938 091 3.
- Wakeman, R.J. and Akay, G., "Membrane-Solute and Liquid-Particle Interaction Effects in Filtration", *Filtration & Separation*, 34(5), 1997, pp 511-519, ISSN 0015 1882.
- Williams, C.J. and Wakeman, R.J., "Membrane Fouling and Alternative Techniques for Its Alleviation", *Membrane Technology*, 124, 2000, pp 4-10, ISSN 0958 2118.
- Wakeman, R.J., "Pretreatment Methods For Membrane Filtration", *The Journal of The Filtration Society*, 24, 2002, 17-22, ISSN 1471-8047.

Official Reports

- Wakeman, R.J., *Dynamic Filters - Separation Processes Service State-of-the-Art Report*, 1995, pp iv+66, AEA Publications, Harwell.
- Wakeman, R.J., *Membrane Fouling and Techniques for its Prevention*, 1996, pp v+133, AEA Publications, Harwell.

Review Articles in Academic Publications - Books

- Wakeman, R.J., "Extraction: Liquid/Solid", *Kirk-Othmer Encyclopedia of Chemical Technology, Volume 10, 4th Edition*, Howe-Grant, M. & Kroschwitz, J.I. (eds), Wiley Interscience, New York, 1994, pp 181-195.

7.0 Appendix C - OLI Modeling for AP104

7.1 ESP Modeling

The purpose of this work was two-fold; (1) to assess how well the Environmental Simulation Program (ESP) can predict the volume fraction of bulk solids that were formed during a recent boildown of the composite AP-104 supernate sample¹¹, and (2) to determine if any work can be done on the ESP database to improve its predictive capability. The boildown was conducted under varying vacuum to nominally 50% WVR, at which point the pot was completely filled with settled solids. The semi-batch operation of AP-104 boildown was modeled using the ESP version 6.7, while the chemistry of AP-104 supernate was modeled using the ESP software default PUBLIC database along with two private databases.

The WTPBASE database has been optimized extensively for the Hanford waste chemistry, whereas the NAFPO4 database contains only one species, $Na_7F(PO_4)_2 \cdot 19H_2O$, and was put together from the available literature data for that double salt with no subsequent validation. As noted by the PNNL personnel¹³, some of the solids in the databases lacked the reference volume data, and the missing reference molar volumes of $Na_2C_2O_4$ and $Na_7F(PO_4)_2 \cdot 19H_2O$ were added to the PUBLIC and NAFPO4 databases, respectively, during this work:

- The molar volume of 0.05903 L was calculated for $Na_2C_2O_4$ from its reported density of 2.27 g/ml¹⁴.
- The molar volume of 0.216 L was estimated for $Na_7F(PO_4)_2 \cdot 19H_2O$ by the linear interpolation of the plot of reference molar volumes of $Na_xH_yPO_4 \cdot zH_2O$ found in the PUBLIC database vs. molar ratio of hydrated H₂O to sodium, z/x.

7.2 Feed Composition

The composition of AP-104 supernate was developed from the Best Basis Inventory (BBI) published on April 8, 2004. The results of charge balance are shown in Table 10, and the molar feed rates used in the actual ESP model runs are shown in Table 11 for the total feed rate of 1.0 liter/hr. Some of the highlights of charge balance include:

- Based on the BBI history of Tank 241-AP-104, the makeup of total organic carbon (TOC) was assumed to be identical to that of the SY-101 convective layer sample, excluding the normal paraffin hydrocarbons (NPH)¹⁵.

¹³ Private Communication with L. A. Mahoney, Pacific Northwest National Laboratory, Richland, WA August 31, 2004.

¹⁴ *Lange's Handbook of Chemistry*, 11th Ed., J. A. Dean, Ed., p 4-121, McGraw Hill, New York (1973).

- The resulting concentrations of acetate and formate in the AP-104 supernate were 1.9 and 6.4 times the BBI concentration of oxalate, respectively.
- The concentration of carbonate ion, CO_3^{-2} , was varied to balance the charges. The final concentration of 0.472 M shown in Table 1 reflects an increase of 64% from the BBI data reported as total inorganic carbon (TIC).
- Without assuming any complexation, the ESP model predicted that the feed would be saturated with oxalate at 30 °C at its BBI concentration. This result is consistent with the BBI statement that the TOC has little complexing strength.
- The aluminate, $NaAl(OH)_4$, was added as bayerite and NaOH in order to keep all the BBI of aluminum in solution. All other forms of aluminum precipitates including gibbsite were excluded from the model¹³.
- The BBI concentration of free hydroxide was assumed to include that required to dissolve 100% bayerite.
- The predicted density of 1.251 g/ml for the AP-104 supernate was 2% lower than 1.277 g/ml, which was estimated from the BBI volume and mass data. The difference increases to 9% when only the fractional densities are considered.

¹⁵ Campbell, J. A., "Flammable Gas Safety Program - Organic Analysis and Analytical Methods Development: FY1995 Progress Report," PNL-10776, Pacific Northwest National Laboratory, Richland, Washington, September 1, 1995

Table 10 – Charge Balance Results of BBI AP-104 Supernate Data.

	FW	Conc (mg/l)	Conc (M)	Equiv (M)
Anions				
NO2	46	6.3713E+04	1.3851E+00	1.3851E+00
NO3	62	1.0036E+05	1.6187E+00	1.6187E+00
OH	17	9.0591E+03	5.3289E-01	5.3289E-01
SO4	98.058	3.6168E+03	3.6884E-02	7.3768E-02
C2O4	88.02	9.0778E+02	1.0313E-02	2.0627E-02
Al(OH)4	94.98154	5.8853E+04	6.1963E-01	6.1963E-01
F	19	2.2443E+02	1.1812E-02	1.1812E-02
Cl	35.453	5.1737E+03	1.4593E-01	1.4593E-01
CO3	60.009	2.8336E+04	4.7220E-01	9.4439E-01
PO4	94.9714	4.5509E+03	4.7919E-02	1.4376E-01
AsO4	138.9216	3.2244E+00	2.3210E-05	6.9630E-05
B4O7	155.24	1.7628E+02	1.1356E-03	2.2711E-03
CrO4	115.996	1.1168E+03	9.6276E-03	1.9255E-02
HgO(OH)	233.59	1.4058E-03	6.0182E-09	6.0182E-09
MoO4	159.94	1.0462E+02	6.5410E-04	1.3082E-03
RuO4	165.07	3.5207E+01	2.1329E-04	4.2657E-04
Se	78.96	6.8263E+00	8.6453E-05	1.7291E-04
SiO3	76.0855	9.7981E+01	1.2878E-03	2.5755E-03
CH3COO	59.0446	1.1236E+03	1.9030E-02	1.9030E-02
H2EDTA (-2)	290.247	3.4504E+03	1.1888E-02	2.3776E-02
COOH	45.0177	2.9614E+03	6.5782E-02	6.5782E-02
OCH2COOH	75.042	8.4625E+02	1.1277E-02	1.1277E-02
citrate (-1)	191.0962	4.7889E+02	2.5060E-03	2.5060E-03
IDA (-2)	131.084	1.6014E+03	1.2217E-02	2.4433E-02
NTA (-1)	190.116	4.9132E+02	2.5843E-03	2.5843E-03
Total Anions			5.0196E+00	5.6720E+00
Cations				
Na	22.99	1.2790E+05	5.5635E+00	5.5635E+00
Ag	107.868	6.9701E-01	6.4617E-06	6.4617E-06
Ba	137.33	6.0359E-02	4.3952E-07	8.7904E-07
Ca	40.08	4.8623E+01	1.2131E-03	2.4263E-03
Cd	112.41	1.5210E+00	1.3530E-05	2.7061E-05
Ce	140.12	5.8922E-02	4.2051E-07	1.2615E-06
Cu	63.546	3.8802E+00	6.1062E-05	1.2212E-04
Fe	55.847	5.0299E+00	9.0066E-05	2.7020E-04
K	39.0983	2.0958E+03	5.3604E-02	5.3604E-02
La	138.906	9.9880E-02	7.1905E-07	2.1571E-06
Mg	24.305	2.7784E+00	1.1432E-04	2.2863E-04
Mn	54.938	1.0084E+00	1.8355E-05	3.6710E-05
Nd	144.24	2.5389E+00	1.7602E-05	5.2806E-05
NH4	18	8.9524E+02	4.9736E-02	4.9736E-02
Ni	58.71	4.5749E+01	7.7923E-04	1.5585E-03
Pb	207.2	1.3916E+01	6.7163E-05	1.3433E-04
Sr	87.62	2.6826E-01	3.0617E-06	6.1233E-06
U	238.029	1.1808E+01	4.9609E-05	2.9765E-04
Zn	65.38	5.3413E-01	8.1697E-06	1.6339E-05
Zr	91.22	5.8922E-01	6.4593E-06	2.5837E-05
Total Cations			5.6693E+00	5.6720E+00

Table 11 – Composition of AP-104 Supernate for ESP Model

Species	MW	Conc (M)	g/liter	instant. feed rate (mole/hr)	TOC (g/liter)
NaNO2	69	1.3851E+00	9.5569E+01	1.3851E+00	0
NaNO3	85	1.6187E+00	1.3759E+02	1.6187E+00	0
NaOH	40.07	4.2453E-01	1.7011E+01	4.2453E-01	0
Na2SO4	142.04	3.6884E-02	5.2390E+00	3.6884E-02	0
Na2C2O4	134	1.0313E-02	1.3820E+00	1.0313E-02	0.2475
NaAl(OH)4	117.97154	6.1963E-01	7.3099E+01	6.1963E-01	0
NaF	41.99	1.1812E-02	4.9599E-01	1.1812E-02	0
NaCl	58.443	1.4593E-01	8.5286E+00	1.4593E-01	0
Na2CO3	106	4.7220E-01	5.0053E+01	4.7220E-01	0
Na3PO4	163.944	4.7919E-02	7.8560E+00	4.7919E-02	0
Na3AsO4	207.8916	2.3210E-05	4.8251E-03	2.3210E-05	0
Na2B4O7	201.22	1.1356E-03	2.2850E-01	1.1356E-03	0
Na2CrO4	161.976	9.6276E-03	1.5594E+00	9.6276E-03	0
Na(HgO(OH))	256.58	6.0182E-09	1.5441E-06	6.0182E-09	0
Na2MoO4	205.92	6.5410E-04	1.3469E-01	6.5410E-04	0
Na2RuO4	211.05	2.1329E-04	4.5014E-02	2.1329E-04	0
Na2Se	101.95	8.6453E-05	8.8139E-03	8.6453E-05	0
Na2SiO3	122.07	1.2878E-03	1.5720E-01	1.2878E-03	0
NaCH3COO	82.0346	1.9030E-02	1.5611E+00	1.9030E-02	0.4567
Na2H2EDTA	336.227	1.1888E-02	3.9970E+00	1.1888E-02	1.4265
Na3HEDTA	344.206	0.0000E+00	0.0000E+00	0.0000E+00	0
NaCOOH	68.0077	6.5782E-02	4.4737E+00	6.5782E-02	0.7894
NaOCH2COOH	98.032	1.1277E-02	1.1055E+00	1.1277E-02	0.2706
NaH2Citrate	214.086	2.5060E-03	5.3650E-01	2.5060E-03	0.1804
Na2IDA	177.064	1.2217E-02	2.1631E+00	1.2217E-02	0.5864
NaH2NTA	213.106	2.5843E-03	5.5073E-01	2.5843E-03	0.1861
AgOH	124.868	6.4617E-06	8.0685E-04	6.4617E-06	0
Ba(OH)2	171.33	4.3952E-07	7.5303E-05	4.3952E-07	0
Ca(OH)2	74.08	1.2131E-03	8.9870E-02	1.2131E-03	0
Cd(OH)2	146.41	1.3530E-05	1.9810E-03	1.3530E-05	0
Ce(OH)3	191.12	4.2051E-07	8.0368E-05	4.2051E-07	0
Cu(OH)2	97.546	6.1062E-05	5.9563E-03	6.1062E-05	0
Fe(OH)3	106.847	9.0066E-05	9.6233E-03	9.0066E-05	0
KOH	56.0983	5.3604E-02	3.0071E+00	5.3604E-02	0
La(OH)3	189.906	7.1905E-07	1.3655E-04	7.1905E-07	0
Mg(OH)2	58.305	1.1432E-04	6.6652E-03	1.1432E-04	0
Mn(OH)2	88.938	1.8355E-05	1.6325E-03	1.8355E-05	0
Nd(OH)3	195.24	1.7602E-05	3.4366E-03	1.7602E-05	0
NH4OH	35	4.9736E-02	1.7408E+00	4.9736E-02	0
Ni(OH)2	92.71	7.7923E-04	7.2242E-02	7.7923E-04	0
Pb(OH)2	241.2	6.7163E-05	1.6200E-02	6.7163E-05	0
Sr(OH)2	121.62	3.0617E-06	3.7236E-04	3.0617E-06	0
UO2(OH)2	304.029	4.9609E-05	1.5083E-02	4.9609E-05	0
Zn(OH)2	99.38	8.1697E-06	8.1190E-04	8.1697E-06	0
Zr(OH)4	159.22	6.4593E-06	1.0285E-03	6.4593E-06	0
H2O	18.02	4.7608E+01	8.5790E+02	4.7608E+01	0
Total			1.2762E+03	5.2626E+01	4.1437

The concentrations of halides and phosphate in the resulting AP-104 supernate are compared in Table 12 with those in four pretreated LAW feeds used in the previous SRNL studies¹⁶. Noting that of those SRNL feeds the formation of $Na_7F(PO_4)_2 \cdot 19H_2O$ crystals was observed only in the concentrated AZ-101 simulant, the same double salt is certainly expected to form also during the AP-104 boildown due to its high phosphate level. A Hanford study showed that although the crystals of $Na_7F(PO_4)_2 \cdot 19H_2O$ formed readily for a wide range of F/PO₄ ratios, its formation was not observed at a ratio of 10¹⁷. It also seems that the chloride level has no impact on the double salt formation.

Table 12 – Comparison of Halides and Phosphate Levels in Pretreated LAW Feeds and AP-104 Supernate (Normalized to 5.0 M Na)

Sample	AN-103 (Active)	AN-105 (Simulant)	AN-107 (Simulant)	AZ-101 (Simulant)	AP-104 (Active)
Cl (mg/liter)	2,597	4,263	1,073	210	4,650
F (mg/liter)	100	89	78	1,914	201
PO ₄ (mg/liter)	540	268	651	1,586	4,090
F/PO ₄ (mole/mole)	0.9	1.7	0.6	6.0	0.05

7.3 Overview of Model

A schematic of the AP-104 evaporation model is shown in Figure 28. The model was built as a series of evaporation stages each consisting of four ESP blocks; two MIX blocks representing the evaporator pot and the storage tank for the concentrate and two SEPARATE blocks used to separate the overhead vapor from the liquid and to condense steam and other condensable gases in the overhead. The model effectively simulates a semi-batch evaporator by passing the concentrate from one stage to the next with no fresh feed coming into or the bottoms being withdrawn from the system.

¹⁶ Calloway, T. B., Monson, P. M., and Choi, A. S., “Evaporation of Hanford Envelope B Simulant (AZ-101) Preliminary Report, **BNF-003-98-0166**, Westinghouse Savannah River Co., Aiken, South Carolina, January 2000.

¹⁷ Herting, D. L., “Clean Salt Process Final Report,” WHC-EP-0915, Westinghouse Hanford Co., Richland, Washington, September 1996.

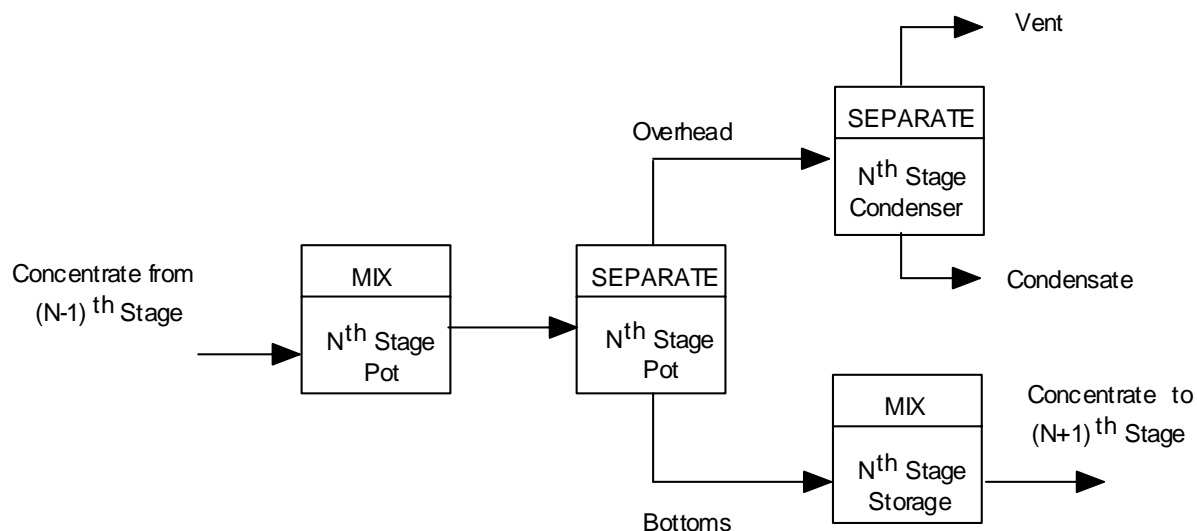


Figure 28 – Schematic of AP-104 Semi-Batch Evaporation Model

The validity of approximating the semi-batch evaporator as a series of continuous still pots, as shown in Figure 28, was confirmed by running the model to simulate the batch distillation experiment performed earlier at 1 atm.¹⁸ In Figure 29, the calculated acidity of the condensate is compared with the data taken during the batch distillation of 4 M nitric acid to complete dryness in 10 equal volume increments. It can be seen that the model predicted the data well except at the 70% volume reduction mark, while the degree of discrepancy seen at the 100% volume reduction mark or at the point of complete dryness, was expected.

¹⁸ Ryan, P., "The Concentration of Technetium-99 by Acid Distillation," DPST-83-386, E. I. du Pont de Nemours & Co., Aiken, South Carolina, March 23, 1983

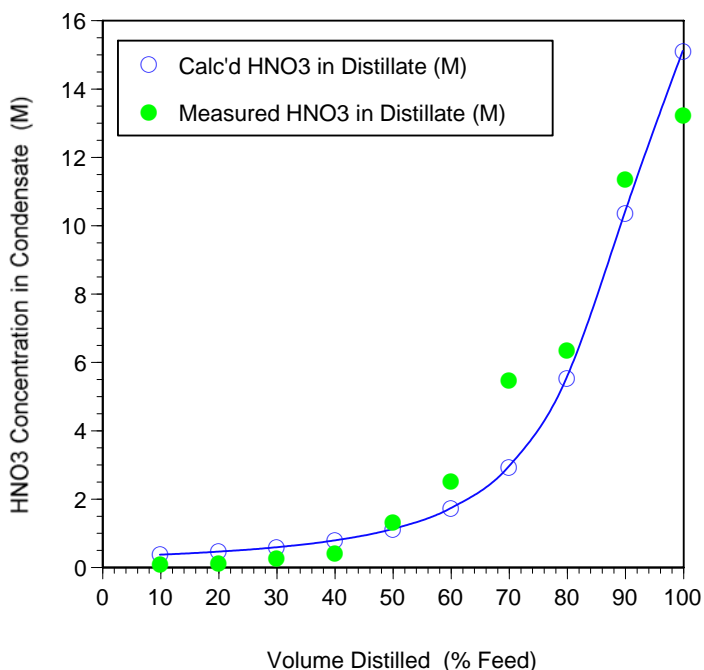


Figure 29 – Calculated vs. Measured HNO₃ Concentrations in Condensate During Batch Distillation of 4M Nitric Acid – Data by P. Ryan¹⁸

Since the evaporator has no design air purges, the flow rates of noncondensable gases in the overhead and the vent are likely to be determined by the air leakage into the system. For the simplicity of calculations, however, no air inleakage was allowed in this work, since it will have no impact on the pot liquid compositions to be calculated at various WVR's. The air inleakage will have a profound effect on the air emission of volatile organics and metals in those systems operating under vacuum. The following operating conditions were assumed in the model:

- The operating pressure in the pot is constant at 60 torr.
- The operating temperature in the primary condenser is constant at 40 °C.
- The AP-104 supernate is fed to the 1st stage at 30 °C, while the concentrate from every stage thereafter is cooled to 18 °C.

7.4 Model Output Files - Bulk Liquid Compositions at Various WVR

STREAM: AP-104 Supernate (0% WVR)

TO : Still_1

Phases----->	Aqueous	Solid	Vapor	Organic
Temperature, C	30.	30.	30.	30.
Pressure, atm	1.	1.	1.	1.
pH	13.8306			
Total mol/hr	57.08277	0.0	0.0	0.0
-----	mol/hr-----	mol/hr-----	mol/hr-----	mol/hr--
H2O	46.9301	0.0	0.0	0.0
ACETACID	3.49140E-12	0.0	0.0	0.0
CO2	4.16953E-14	0.0	0.0	0.0
H2F2	0.0	0.0	0.0	0.0
ACET2	0.0	0.0	0.0	0.0
HCL	8.10479E-22	0.0	0.0	0.0
HCOOH	1.08488E-12	0.0	0.0	0.0
HF	2.56883E-14	0.0	0.0	0.0
HNO2	7.01020E-12	0.0	0.0	0.0
HNO3	6.11910E-20	0.0	0.0	0.0
NH3	0.049149	0.0	0.0	0.0
CAHCTRT	8.69270E-21	0.0	0.0	0.0
CAHPO4	3.24080E-14	0.0	0.0	0.0
CASO4	9.29959E-12	0.0	0.0	0.0
ALF3	4.36512E-25	0.0	0.0	0.0
GLYCOLACID	2.74908E-13	0.0	0.0	0.0
ALOH3	1.03485E-08	0.0	0.0	0.0
H3PO4	1.18418E-25	0.0	0.0	0.0
CAACET2	2.21367E-12	0.0	0.0	0.0
CAC2O4	1.42137E-10	0.0	0.0	0.0
CACL2	2.76661E-29	0.0	0.0	0.0
CACO3	4.37103E-09	0.0	0.0	0.0
CACOOH2	3.02115E-11	0.0	0.0	0.0
KACET	5.37597E-05	0.0	0.0	0.0
KCL	1.56946E-05	0.0	0.0	0.0
KCOOH	3.16566E-04	0.0	0.0	0.0
KGLYCOLAT	3.96643E-05	0.0	0.0	0.0
KHSO4	4.27085E-19	0.0	0.0	0.0
NAACET	0.00946337	0.0	0.0	0.0
NACOOH	0.0407308	0.0	0.0	0.0
NAF	0.00449637	0.0	0.0	0.0
NAGLYCOLAT	0.00510437	0.0	0.0	0.0
NAHCO3	4.41581E-06	0.0	0.0	0.0
NANO3	0.0935101	0.0	0.0	0.0
CAGLYCOL2	1.77985E-12	0.0	0.0	0.0
NH4ACET	1.43700E-08	0.0	0.0	0.0
NH4NO3	4.00657E-06	0.0	0.0	0.0
NIACET2	1.98646E-23	0.0	0.0	0.0
NIC2O4	1.44896E-17	0.0	0.0	0.0
NICOOH2	1.06248E-21	0.0	0.0	0.0
NIGLYCOL2	1.30876E-22	0.0	0.0	0.0
NIOH2	7.00567E-13	0.0	0.0	0.0
NISO4	3.49335E-22	0.0	0.0	0.0

OHION	0.418957	0.0	0.0	0.0
ALACETION	0.0	0.0	0.0	0.0
ALEDTAION	4.36476E-22	0.0	0.0	0.0
ALF2ION	3.29720E-26	0.0	0.0	0.0
ALF4ION	2.49225E-24	0.0	0.0	0.0
ALF5ION	3.36372E-24	0.0	0.0	0.0
ALF6ION	3.51221E-24	0.0	0.0	0.0
ALOH2ION	7.72410E-17	0.0	0.0	0.0
ALOH4ION	0.612438	0.0	0.0	0.0
ALOHION	5.14685E-25	0.0	0.0	0.0
CAACETION	7.14791E-11	0.0	0.0	0.0
CACLION	1.70022E-14	0.0	0.0	0.0
CACOOHION	6.67427E-10	0.0	0.0	0.0
CACTRTION	6.50847E-11	0.0	0.0	0.0
CAEDTAION	0.00119617	0.0	0.0	0.0
CAFION	4.20895E-13	0.0	0.0	0.0
CAGLYCOLION	1.39356E-10	0.0	0.0	0.0
CAH2CTRTION	0.0	0.0	0.0	0.0
CAH2PO4ION	5.22379E-22	0.0	0.0	0.0
CAHC2O4ION	4.93121E-21	0.0	0.0	0.0
CAHCO3ION	4.79433E-14	0.0	0.0	0.0
CAHEDTAION	6.01008E-15	0.0	0.0	0.0
CAION	5.51024E-09	0.0	0.0	0.0
CANO3ION	1.25171E-09	0.0	0.0	0.0
CANTA2ION	2.55099E-06	0.0	0.0	0.0
CANTAION	1.01285E-07	0.0	0.0	0.0
CAOHION	7.83108E-09	0.0	0.0	0.0
CAPO4ION	7.91371E-08	0.0	0.0	0.0
CITRATION	1.03123E-04	0.0	0.0	0.0
CLION	0.144221	0.0	0.0	0.0
CO3ION	0.300862	0.0	0.0	0.0
COOHION	0.0239691	0.0	0.0	0.0
CR2O7ION	1.49436E-18	0.0	0.0	0.0
CRO4ION	0.00951823	0.0	0.0	0.0
EDTAION	0.00176606	0.0	0.0	0.0
FION	0.00634739	0.0	0.0	0.0
GLYCOLATION	0.00600395	0.0	0.0	0.0
H2CITRATION	3.46432E-23	0.0	0.0	0.0
H2EDTAION	3.34251E-16	0.0	0.0	0.0
H2NTAION	6.42609E-21	0.0	0.0	0.0
H2PO4ION	2.26641E-13	0.0	0.0	0.0
HCITRATION	1.31046E-12	0.0	0.0	0.0
HCO3ION	7.77384E-06	0.0	0.0	0.0
HCRO4ION	2.68429E-11	0.0	0.0	0.0
HEDTAION	1.16923E-08	0.0	0.0	0.0
HF2ION	1.18085E-16	0.0	0.0	0.0
HION	1.06817E-14	0.0	0.0	0.0
HNTAION	1.58110E-08	0.0	0.0	0.0
HOXALATION	8.20929E-14	0.0	0.0	0.0
HP2O7ION	1.48111E-19	0.0	0.0	0.0
HPO4ION	2.81073E-05	0.0	0.0	0.0
HSO4ION	1.78452E-15	0.0	0.0	0.0
K1EDTAION	1.02430E-04	0.0	0.0	0.0
KCTRTION	1.35214E-05	0.0	0.0	0.0
KGLYCOL2ION	5.47122E-07	0.0	0.0	0.0
KION	0.0519544	0.0	0.0	0.0

KSO4ION	4.85281E-04	0.0	0.0	0.0
NA2FION	8.29169E-04	0.0	0.0	0.0
NACO3ION	0.165844	0.0	0.0	0.0
NACTRTION	0.00239388	0.0	0.0	0.0
NAEDTAION	0.00791737	0.0	0.0	0.0
NAION	5.15287	0.0	0.0	0.0
NANTAION	0.0144231	0.0	0.0	0.0
NASO4ION	0.0312319	0.0	0.0	0.0
NH2CO2ION	6.79068E-07	0.0	0.0	0.0
NH4ION	5.05440E-06	0.0	0.0	0.0
NH4SO4ION	2.65946E-08	0.0	0.0	0.0
NIACETION	1.37074E-21	0.0	0.0	0.0
NIC2O42ION	6.22666E-19	0.0	0.0	0.0
NICLION	9.78300E-23	0.0	0.0	0.0
NICOOHION	1.11953E-20	0.0	0.0	0.0
NICTRTION	2.64969E-20	0.0	0.0	0.0
NIEDTAION	6.68019E-07	0.0	0.0	0.0
NIGLYCOLION	3.40788E-21	0.0	0.0	0.0
NIHEDTAION	3.49708E-18	0.0	0.0	0.0
NIION	9.27166E-20	0.0	0.0	0.0
NINH32ION	5.47583E-17	0.0	0.0	0.0
NINH33ION	2.71327E-16	0.0	0.0	0.0
NINH34ION	3.84743E-16	0.0	0.0	0.0
NINH35ION	2.02747E-16	0.0	0.0	0.0
NINH36ION	1.97664E-17	0.0	0.0	0.0
NINH3ION	3.33148E-18	0.0	0.0	0.0
NINO3ION	8.25763E-21	0.0	0.0	0.0
NINTA2ION	6.50528E-10	0.0	0.0	0.0
NINTAION	8.96582E-14	0.0	0.0	0.0
NIOH3ION	2.43989E-09	0.0	0.0	0.0
NIOHEDTAION	7.69287E-04	0.0	0.0	0.0
NIOHION	4.66611E-17	0.0	0.0	0.0
NO2ION	1.36902	0.0	0.0	0.0
NO3ION	1.55475	0.0	0.0	0.0
NTAION	1.99906E-04	0.0	0.0	0.0
ACETATEION	0.00929198	0.0	0.0	0.0
OXALATION	0.0101903	0.0	0.0	0.0
P2O7ION	2.16781E-12	0.0	0.0	0.0
PO4ION	0.0473356	0.0	0.0	0.0
SO4ION	0.00473476	0.0	0.0	0.0
=====				
Total g/hr	1260.93	0.0	0.0	0.0
Volume, L/hr	1.0081	0.0	0.0	0.0
Enthalpy, cal/hr	-4.00765E+06	0.0	0.0	0.0
Density, g/L	1250.79			
Vapor fraction	0.0	0.0	0.0	0.0
Solid fraction	0.0	0.0	0.0	0.0
Organic fraction	0.0	0.0	0.0	0.0
Osmotic Pres, atm	240.583			
Redox Pot, volts	0.0			
E-Con, 1/ohm-cm	0.232419			
E-Con, cm2/ohm-mol	41.7143			
Abs Visc, cP	2.76973			
Rel Visc	3.47051			
Ionic Strength	6.77614			

STREAM: Concentrate_1 (6% WVR)
 TO : Still_2
 FROM : Concentrate_1 Storage

Phases----->	Aqueous	Solid	Vapor	Organic
Temperature, C	18.	18.	18.	18.
Pressure, atm	1.	1.	1.	1.
pH	14.3782			
Total mol/hr	54.29929	0.0063518	0.0	0.0
-----	mol/hr-----	mol/hr-----	mol/hr-----	mol/hr--
H2O	44.2307	0.0	0.0	0.0
ACETACID	9.14775E-13	0.0	0.0	0.0
CO2	4.45145E-15	0.0	0.0	0.0
ACET2	0.0	0.0	0.0	0.0
HCL	1.07049E-22	0.0	0.0	0.0
HCOOH	2.78210E-13	0.0	0.0	0.0
HF	4.47489E-15	0.0	0.0	0.0
HNO2	2.50700E-12	0.0	0.0	0.0
NH3	0.0105891	0.0	0.0	0.0
CAHCTRT	1.65289E-21	0.0	0.0	0.0
CAHPO4	5.98998E-15	0.0	0.0	0.0
CASO4	5.67257E-12	0.0	0.0	0.0
GLYCOLACID	7.69223E-14	0.0	0.0	0.0
ALOH3	4.86542E-09	0.0	0.0	0.0
CAACET2	2.05256E-12	0.0	0.0	0.0
CAC2O4	3.47065E-11	0.0	0.0	0.0
CACL2	0.0	0.0	0.0	0.0
CACO3	2.44400E-09	0.0	0.0	0.0
CACOOH2	2.78083E-11	0.0	0.0	0.0
KACET	4.96074E-05	0.0	0.0	0.0
KCL	1.24256E-05	0.0	0.0	0.0
KCOOH	2.95393E-04	0.0	0.0	0.0
KGLYCOLAT	3.77669E-05	0.0	0.0	0.0
KHSO4	5.99183E-20	0.0	0.0	0.0
NAACET	0.00995165	0.0	0.0	0.0
NACOOH	0.0427548	0.0	0.0	0.0
NAF	0.00366197	0.0	0.0	0.0
NAGLYCOLAT	0.00546767	0.0	0.0	0.0
NAHCO3	2.29503E-06	0.0	0.0	0.0
NANO3	0.0686898	0.0	0.0	0.0
CAGLYCOL2	1.74885E-12	0.0	0.0	0.0
NH4ACET	2.04253E-09	0.0	0.0	0.0
NH4NO3	4.37518E-07	0.0	0.0	0.0
NIACET2	1.66997E-23	0.0	0.0	0.0
NIC2O4	4.45989E-18	0.0	0.0	0.0
NICOOH2	9.24539E-22	0.0	0.0	0.0
NIGLYCOL2	1.25330E-22	0.0	0.0	0.0
NIHCTRT	0.0	0.0	0.0	0.0
NIOH2	1.08218E-12	0.0	0.0	0.0
NISO4	1.23199E-22	0.0	0.0	0.0
OHION	0.418918	0.0	0.0	0.0
ALEDTAION	1.61217E-23	0.0	0.0	0.0
ALF2ION	2.19687E-27	0.0	0.0	0.0
ALF4ION	9.40845E-26	0.0	0.0	0.0
ALF5ION	9.44291E-26	0.0	0.0	0.0
ALF6ION	7.74471E-26	0.0	0.0	0.0

ALFION	9.98693E-30	0.0	0.0	0.0
ALOH2ION	2.28524E-17	0.0	0.0	0.0
ALOH4ION	0.612438	0.0	0.0	0.0
ALOHCLION	4.12367E-26	0.0	0.0	0.0
ALOHION	8.68465E-26	0.0	0.0	0.0
CAACETION	5.59698E-11	0.0	0.0	0.0
CACLION	6.03276E-15	0.0	0.0	0.0
CACOOHION	5.45447E-10	0.0	0.0	0.0
CACTRTION	6.04014E-11	0.0	0.0	0.0
CAEDTAION	0.0011964	0.0	0.0	0.0
CAFION	1.11319E-13	0.0	0.0	0.0
CAGLYCOLION	1.18661E-10	0.0	0.0	0.0
CAH2CTRITION	0.0	0.0	0.0	0.0
CAH2PO4ION	3.82385E-23	0.0	0.0	0.0
CAHC2O4ION	7.91801E-22	0.0	0.0	0.0
CAHCO3ION	1.57716E-14	0.0	0.0	0.0
CAHEDTAION	1.69371E-15	0.0	0.0	0.0
CAION	3.98306E-09	0.0	0.0	0.0
CANO3ION	9.47573E-10	0.0	0.0	0.0
CANTA2ION	2.40034E-06	0.0	0.0	0.0
CANTAION	7.57411E-08	0.0	0.0	0.0
CAOHION	6.88144E-09	0.0	0.0	0.0
CAPO4ION	2.83431E-08	0.0	0.0	0.0
CITRATION	8.82217E-05	0.0	0.0	0.0
CLION	0.144224	0.0	0.0	0.0
CO3ION	0.267825	0.0	0.0	0.0
COOHION	0.0219664	0.0	0.0	0.0
CR2O7ION	1.40987E-19	0.0	0.0	0.0
CRO4ION	0.00951823	0.0	0.0	0.0
EDTAION	0.00168966	0.0	0.0	0.0
FION	0.0045104	0.0	0.0	0.0
GLYCOLATION	0.00564238	0.0	0.0	0.0
H2EDTAION	4.55168E-17	0.0	0.0	0.0
H2NNTAION	5.58858E-22	0.0	0.0	0.0
H2P2O7ION	9.20094E-30	0.0	0.0	0.0
H2PO4ION	1.36960E-14	0.0	0.0	0.0
H3EDTAION	6.59088E-30	0.0	0.0	0.0
HCITRATION	3.34753E-13	0.0	0.0	0.0
HCO3ION	2.53656E-06	0.0	0.0	0.0
HCRO4ION	6.43981E-12	0.0	0.0	0.0
HEDTAION	3.99734E-09	0.0	0.0	0.0
HF2ION	1.63809E-17	0.0	0.0	0.0
HION	2.62493E-15	0.0	0.0	0.0
HNTAION	5.43196E-09	0.0	0.0	0.0
HOXALATION	1.56482E-14	0.0	0.0	0.0
HP2O7ION	1.41802E-21	0.0	0.0	0.0
HPO4ION	5.98297E-06	0.0	0.0	0.0
HSO4ION	2.84655E-16	0.0	0.0	0.0
K1EDTAION	8.31363E-05	0.0	0.0	0.0
KCTRITION	1.20520E-05	0.0	0.0	0.0
KGLYCOL2ION	6.28494E-07	0.0	0.0	0.0
KION	0.0520932	0.0	0.0	0.0
KSO4ION	3.97669E-04	0.0	0.0	0.0
NA2FION	6.23618E-04	0.0	0.0	0.0
NACO3ION	0.19889	0.0	0.0	0.0
NACTRTION	0.00241025	0.0	0.0	0.0

NAEDTAION	0.00801285	0.0	0.0	0.0
NAION	5.11935	0.0	0.0	0.0
NANTAION	0.0144612	0.0	0.0	0.0
NASO4ION	0.0276629	0.0	0.0	0.0
NH2CO2ION	6.91545E-08	0.0	0.0	0.0
NH4ION	7.56210E-07	0.0	0.0	0.0
NH4SO4ION	4.16466E-09	0.0	0.0	0.0
NIACET3ION	4.39746E-24	0.0	0.0	0.0
NIACETION	8.60958E-22	0.0	0.0	0.0
NIC2O42ION	1.98039E-19	0.0	0.0	0.0
NICLION	4.96476E-23	0.0	0.0	0.0
NICOOHION	7.20852E-21	0.0	0.0	0.0
NICTRTION	2.08436E-20	0.0	0.0	0.0
NIEDTAION	4.97301E-07	0.0	0.0	0.0
NIFION	2.78948E-23	0.0	0.0	0.0
NIGLYCOLION	2.32216E-21	0.0	0.0	0.0
NIHEDTAION	7.32697E-19	0.0	0.0	0.0
NIION	4.72742E-20	0.0	0.0	0.0
NINH32ION	2.39468E-18	0.0	0.0	0.0
NINH33ION	3.60881E-18	0.0	0.0	0.0
NINH34ION	1.55790E-18	0.0	0.0	0.0
NINH35ION	2.55810E-19	0.0	0.0	0.0
NINH36ION	7.78389E-21	0.0	0.0	0.0
NINH3ION	4.80177E-19	0.0	0.0	0.0
NINO3ION	5.14337E-21	0.0	0.0	0.0
NINTA2ION	4.07407E-10	0.0	0.0	0.0
NINTAION	4.71205E-14	0.0	0.0	0.0
NIOH3ION	8.56370E-09	0.0	0.0	0.0
NIOHEDTAION	7.69452E-04	0.0	0.0	0.0
NIOHION	3.43195E-17	0.0	0.0	0.0
NO2ION	1.36902	0.0	0.0	0.0
NO3ION	1.57958	0.0	0.0	0.0
NTAION	1.62169E-04	0.0	0.0	0.0
ACETATEION	0.00880787	0.0	0.0	0.0
OXALATION	0.00671549	0.0	0.0	0.0
P2O7ION	7.90198E-14	0.0	0.0	0.0
PO4ION	0.0416039	0.0	0.0	0.0
SO4ION	0.00839133	0.0	0.0	0.0
NA2C2O4	0.0	0.00347485	0.0	0.0
NAFPO4.19H2O	0.0	0.00287695	0.0	0.0
=====				
Total g/hr	1210.11	2.51448	0.0	0.0
Volume, L/hr	0.950029	8.26541E-04	0.0	0.0
Enthalpy, cal/hr	-3.82900E+06	-7953.84	0.0	0.0
Density, g/L	1273.77	3042.18		
Vapor fraction	0.0	0.0	0.0	0.0
Solid fraction	0.0	1.	0.0	0.0
Organic fraction	0.0	0.0	0.0	0.0
Osmotic Pres, atm	250.736			
Redox Pot, volts	0.0			
E-Con, 1/ohm-cm	0.17904			
E-Con, cm2/ohm-mol	18.2026			
Abs Visc, cP	3.93402			
Rel Visc	3.73616			
Ionic Strength	7.08425			

STREAM: Concentrate_2 (10% WVR)
 TO : Still_3
 FROM : Concentrate_2 Storage

Phases----->	Aqueous	Solid	Vapor	Organic
Temperature, C	18.	18.	18.	18.
Pressure, atm	1.	1.	1.	1.
pH	14.4339			
Total mol/hr	51.58749	0.00796084	0.0	0.0
-----	mol/hr-----	mol/hr-----	mol/hr-----	mol/hr--
H2O	41.5488	0.0	0.0	0.0
ACETACID	7.73892E-13	0.0	0.0	0.0
CO2	3.09760E-15	0.0	0.0	0.0
ACET2	0.0	0.0	0.0	0.0
HCL	9.38767E-23	0.0	0.0	0.0
HCOOH	2.34476E-13	0.0	0.0	0.0
HF	3.30634E-15	0.0	0.0	0.0
HNO2	2.11237E-12	0.0	0.0	0.0
NH3	0.00205872	0.0	0.0	0.0
CAHCTRT	1.22553E-21	0.0	0.0	0.0
CAHPO4	4.18431E-15	0.0	0.0	0.0
CASO4	5.44164E-12	0.0	0.0	0.0
ALF3	1.13968E-26	0.0	0.0	0.0
GLYCOLACID	6.54252E-14	0.0	0.0	0.0
ALOH3	4.24314E-09	0.0	0.0	0.0
CAACET2	2.04334E-12	0.0	0.0	0.0
CAC2O4	2.65749E-11	0.0	0.0	0.0
CACL2	0.0	0.0	0.0	0.0
CACO3	2.10154E-09	0.0	0.0	0.0
CACOOH2	2.74752E-11	0.0	0.0	0.0
KACET	5.01595E-05	0.0	0.0	0.0
KCL	1.30236E-05	0.0	0.0	0.0
KCOOH	2.97555E-04	0.0	0.0	0.0
KGLYCOLAT	3.83924E-05	0.0	0.0	0.0
KHSO4	5.49024E-20	0.0	0.0	0.0
NAACET	0.0102078	0.0	0.0	0.0
NACOOH	0.0436901	0.0	0.0	0.0
NAF	0.00342562	0.0	0.0	0.0
NAGLYCOLAT	0.00563855	0.0	0.0	0.0
NAHCO3	1.91222E-06	0.0	0.0	0.0
NANO3	0.0681458	0.0	0.0	0.0
CAGLYCOL2	1.75974E-12	0.0	0.0	0.0
NH4ACET	3.73315E-10	0.0	0.0	0.0
NH4NO3	7.84974E-08	0.0	0.0	0.0
NIACET2	1.43380E-23	0.0	0.0	0.0
NIC2O4	2.94523E-18	0.0	0.0	0.0
NICOOH2	7.87819E-22	0.0	0.0	0.0
NIGLYCOL2	1.08764E-22	0.0	0.0	0.0
NIHCTRT	0.0	0.0	0.0	0.0
NIOH2	1.02430E-12	0.0	0.0	0.0
NISO4	1.01927E-22	0.0	0.0	0.0
OXALAC	3.41570E-28	0.0	0.0	0.0
OHION	0.418915	0.0	0.0	0.0
ALEDTAION	1.11950E-23	0.0	0.0	0.0
ALF2ION	1.33987E-27	0.0	0.0	0.0
ALF4ION	5.50962E-26	0.0	0.0	0.0

ALF5ION	5.49722E-26	0.0	0.0	0.0
ALF6ION	4.54044E-26	0.0	0.0	0.0
ALOH2ION	1.81617E-17	0.0	0.0	0.0
ALOH4ION	0.612438	0.0	0.0	0.0
ALOHION	5.70135E-26	0.0	0.0	0.0
CAACETION	5.45500E-11	0.0	0.0	0.0
CACLION	1.38765E-14	0.0	0.0	0.0
CACOOHION	5.29606E-10	0.0	0.0	0.0
CACTRTION	5.35081E-11	0.0	0.0	0.0
CAEDTAION	0.00119657	0.0	0.0	0.0
CAFION	9.89528E-14	0.0	0.0	0.0
CAGLYCOLION	1.16274E-10	0.0	0.0	0.0
CAH2CTRITION	0.0	0.0	0.0	0.0
CAH2PO4ION	2.45870E-23	0.0	0.0	0.0
CAHC2O4ION	5.58219E-22	0.0	0.0	0.0
CAHCO3ION	1.30892E-14	0.0	0.0	0.0
CAHEDTAION	1.46141E-15	0.0	0.0	0.0
CAION	3.54201E-09	0.0	0.0	0.0
CANO3ION	8.92737E-10	0.0	0.0	0.0
CANTA2ION	2.25016E-06	0.0	0.0	0.0
CANTAION	6.68388E-08	0.0	0.0	0.0
CAOHION	6.83155E-09	0.0	0.0	0.0
CAPO4ION	2.36560E-08	0.0	0.0	0.0
CITRATION	7.49427E-05	0.0	0.0	0.0
CLION	0.144223	0.0	0.0	0.0
CO3ION	0.255678	0.0	0.0	0.0
COOHION	0.0210288	0.0	0.0	0.0
CR2O7ION	1.20765E-19	0.0	0.0	0.0
CRO4ION	0.00951823	0.0	0.0	0.0
EDTAION	0.00164299	0.0	0.0	0.0
FION	0.00407031	0.0	0.0	0.0
GLYCOLATION	0.0054707	0.0	0.0	0.0
H2CITRATION	1.61094E-24	0.0	0.0	0.0
H2EDTAION	3.67736E-17	0.0	0.0	0.0
H2NNTAION	3.76227E-22	0.0	0.0	0.0
H2P2O7ION	4.51950E-30	0.0	0.0	0.0
H2PO4ION	9.07586E-15	0.0	0.0	0.0
H3EDTAION	4.33621E-30	0.0	0.0	0.0
HCITRATION	2.77670E-13	0.0	0.0	0.0
HCO3ION	2.12368E-06	0.0	0.0	0.0
HCRO4ION	5.41966E-12	0.0	0.0	0.0
HEDTAION	3.30739E-09	0.0	0.0	0.0
HF2ION	1.23562E-17	0.0	0.0	0.0
HION	2.06600E-15	0.0	0.0	0.0
HNTAION	4.48783E-09	0.0	0.0	0.0
HOXALATION	1.09157E-14	0.0	0.0	0.0
HP2O7ION	7.13156E-22	0.0	0.0	0.0
HPO4ION	4.76569E-06	0.0	0.0	0.0
HSO4ION	2.48770E-16	0.0	0.0	0.0
K1EDTAION	9.31307E-05	0.0	0.0	0.0
KCTRITION	1.18219E-05	0.0	0.0	0.0
KGLYCOL2ION	7.21371E-07	0.0	0.0	0.0
KION	0.0520419	0.0	0.0	0.0
KSO4ION	4.35142E-04	0.0	0.0	0.0
NA2FION	6.53912E-04	0.0	0.0	0.0
NACO3ION	0.211037	0.0	0.0	0.0

NACTRTION	0.00242375	0.0	0.0	0.0
NAEDTAION	0.00804936	0.0	0.0	0.0
NAION	5.10094	0.0	0.0	0.0
NANTAION	0.0144862	0.0	0.0	0.0
NASO4ION	0.0267534	0.0	0.0	0.0
NH2CO2ION	1.18537E-08	0.0	0.0	0.0
NH4ION	1.36826E-07	0.0	0.0	0.0
NH4SO4ION	8.38239E-10	0.0	0.0	0.0
NIACET3ION	4.24225E-24	0.0	0.0	0.0
NIACETION	7.23700E-22	0.0	0.0	0.0
NIC2O42ION	1.23204E-19	0.0	0.0	0.0
NICLION	4.32007E-23	0.0	0.0	0.0
NICOOHION	6.03644E-21	0.0	0.0	0.0
NICTRTION	1.59250E-20	0.0	0.0	0.0
NIEDTAION	4.28958E-07	0.0	0.0	0.0
NIFION	2.13855E-23	0.0	0.0	0.0
NIGLYCOLION	1.96246E-21	0.0	0.0	0.0
NIHEDTAION	5.45245E-19	0.0	0.0	0.0
NIION	3.81444E-20	0.0	0.0	0.0
NINH32ION	8.83394E-20	0.0	0.0	0.0
NINH33ION	2.87616E-20	0.0	0.0	0.0
NINH34ION	2.68244E-21	0.0	0.0	0.0
NINH35ION	9.51589E-23	0.0	0.0	0.0
NINH36ION	6.25560E-25	0.0	0.0	0.0
NINH3ION	8.19913E-20	0.0	0.0	0.0
NINO3ION	4.17903E-21	0.0	0.0	0.0
NINTA2ION	3.29385E-10	0.0	0.0	0.0
NINTAION	3.58626E-14	0.0	0.0	0.0
NIOH3ION	9.56267E-09	0.0	0.0	0.0
NIOHEDTAION	7.69520E-04	0.0	0.0	0.0
NIOHION	2.97657E-17	0.0	0.0	0.0
NO2ION	1.36902	0.0	0.0	0.0
NO3ION	1.58012	0.0	0.0	0.0
NTAION	1.37415E-04	0.0	0.0	0.0
ACETATEION	0.00855114	0.0	0.0	0.0
OXALATION	0.00575259	0.0	0.0	0.0
P2O7ION	4.67433E-14	0.0	0.0	0.0
PO4ION	0.0403128	0.0	0.0	0.0
SO4ION	0.00926336	0.0	0.0	0.0
NA2C2O4	0.0	0.00443775	0.0	0.0
NAFPO4.19H2O	0.0	0.00352309	0.0	0.0
=====				
Total g/hr	1161.28	3.10367	0.0	0.0
Volume, L/hr	0.9027	0.00102295	0.0	0.0
Enthalpy, cal/hr	-3.64420E+06	-9797.96	0.0	0.0
Density, g/L	1286.46	3034.05		
Vapor fraction	0.0	0.0	0.0	0.0
Solid fraction	0.0	1.	0.0	0.0
Organic fraction	0.0	0.0	0.0	0.0
Osmotic Pres, atm	268.011			
Redox Pot, volts	0.0			
E-Con, 1/ohm-cm	0.181873			
E-Con, cm2/ohm-mol	17.5855			
Abs Visc, cP	4.20548			
Rel Visc	3.99398			
Ionic Strength	7.49511			

STREAM: Concentrate_3 (15% WVR)
 TO : Still_4
 FROM : Concentrate_3 Storage

Phases----->	Aqueous	Solid	Vapor	Organic
Temperature, C	18.	18.	18.	18.
Pressure, atm	1.	1.	1.	1.
pH	14.4964			
Total mol/hr	48.87574	0.00939883	0.0	0.0
-----	mol/hr-----	mol/hr-----	mol/hr-----	mol/hr--
H2O	38.8588	0.0	0.0	0.0
ACETACID	6.41662E-13	0.0	0.0	0.0
CO2	2.07162E-15	0.0	0.0	0.0
ACET2	0.0	0.0	0.0	0.0
HCL	8.09760E-23	0.0	0.0	0.0
HCOOH	1.93630E-13	0.0	0.0	0.0
HF	2.38731E-15	0.0	0.0	0.0
HNO2	1.74141E-12	0.0	0.0	0.0
HNO3	4.43817E-21	0.0	0.0	0.0
NH3	3.57149E-04	0.0	0.0	0.0
CAHCTRT	8.70309E-22	0.0	0.0	0.0
CAHPO4	2.80154E-15	0.0	0.0	0.0
CASO4	5.14063E-12	0.0	0.0	0.0
ALF3	6.32653E-27	0.0	0.0	0.0
GLYCOLACID	5.45565E-14	0.0	0.0	0.0
ALOH3	3.63652E-09	0.0	0.0	0.0
H3PO4	5.66393E-28	0.0	0.0	0.0
CAACET2	2.01142E-12	0.0	0.0	0.0
CAC2O4	1.96565E-11	0.0	0.0	0.0
CACL2	0.0	0.0	0.0	0.0
CACO3	1.76494E-09	0.0	0.0	0.0
CACOOH2	2.68287E-11	0.0	0.0	0.0
KACET	5.06928E-05	0.0	0.0	0.0
KCL	1.36929E-05	0.0	0.0	0.0
KCOOH	2.99509E-04	0.0	0.0	0.0
KGLYCOLAT	3.90224E-05	0.0	0.0	0.0
KHSO4	4.96079E-20	0.0	0.0	0.0
NAACET	0.0104805	0.0	0.0	0.0
NACOOH	0.0446766	0.0	0.0	0.0
NAF	0.00321825	0.0	0.0	0.0
NAGLYCOLAT	0.00582225	0.0	0.0	0.0
NAHCO3	1.56049E-06	0.0	0.0	0.0
NANO3	0.0673615	0.0	0.0	0.0
CAGLYCOL2	1.75212E-12	0.0	0.0	0.0
NH4ACET	6.03308E-11	0.0	0.0	0.0
NH4NO3	1.24162E-08	0.0	0.0	0.0
NIACET2	1.19827E-23	0.0	0.0	0.0
NIC2O4	1.84951E-18	0.0	0.0	0.0
NICOOH2	6.53117E-22	0.0	0.0	0.0
NIGLYCOL2	9.19400E-23	0.0	0.0	0.0
NIHCTRT	0.0	0.0	0.0	0.0
NIOH2	9.57418E-13	0.0	0.0	0.0
NISO4	8.17490E-23	0.0	0.0	0.0
OXALAC	1.98253E-28	0.0	0.0	0.0
OHION	0.418913	0.0	0.0	0.0
ALEDTAION	7.50342E-24	0.0	0.0	0.0

ALF2ION	7.90513E-28	0.0	0.0	0.0
ALF4ION	3.18598E-26	0.0	0.0	0.0
ALF5ION	3.19488E-26	0.0	0.0	0.0
ALF6ION	2.68905E-26	0.0	0.0	0.0
ALFION	3.61759E-30	0.0	0.0	0.0
ALOH2ION	1.40415E-17	0.0	0.0	0.0
ALOH4ION	0.612438	0.0	0.0	0.0
ALOHION	3.54998E-26	0.0	0.0	0.0
CAACETION	5.25698E-11	0.0	0.0	0.0
CACLION	3.79271E-14	0.0	0.0	0.0
CACOOHION	5.08327E-10	0.0	0.0	0.0
CACTRTION	4.64336E-11	0.0	0.0	0.0
CAEDTAION	0.00119676	0.0	0.0	0.0
CAFION	8.72635E-14	0.0	0.0	0.0
CAGLYCOLION	1.12696E-10	0.0	0.0	0.0
CAH2CTRITION	0.0	0.0	0.0	0.0
CAH2PO4ION	1.50072E-23	0.0	0.0	0.0
CAHC2O4ION	3.76593E-22	0.0	0.0	0.0
CAHCO3ION	1.05820E-14	0.0	0.0	0.0
CAHEDTAION	1.23973E-15	0.0	0.0	0.0
CAION	3.07165E-09	0.0	0.0	0.0
CANO3ION	8.27545E-10	0.0	0.0	0.0
CANTA2ION	2.07318E-06	0.0	0.0	0.0
CANTAION	5.77880E-08	0.0	0.0	0.0
CAOHION	6.72710E-09	0.0	0.0	0.0
CAPO4ION	1.93542E-08	0.0	0.0	0.0
CITRATION	6.21980E-05	0.0	0.0	0.0
CLION	0.144223	0.0	0.0	0.0
CO3ION	0.243271	0.0	0.0	0.0
COOHION	0.0200404	0.0	0.0	0.0
CR2O7ION	1.01545E-19	0.0	0.0	0.0
CRO4ION	0.00951823	0.0	0.0	0.0
EDTAION	0.00157976	0.0	0.0	0.0
FION	0.00368398	0.0	0.0	0.0
GLYCOLATION	0.00528613	0.0	0.0	0.0
H2EDTAION	2.91896E-17	0.0	0.0	0.0
H2NTAION	2.42180E-22	0.0	0.0	0.0
H2P2O7ION	2.07324E-30	0.0	0.0	0.0
H2PO4ION	5.78624E-15	0.0	0.0	0.0
H3EDTAION	2.73717E-30	0.0	0.0	0.0
HCITRATION	2.25466E-13	0.0	0.0	0.0
HCO3ION	1.74882E-06	0.0	0.0	0.0
HCRO4ION	4.47423E-12	0.0	0.0	0.0
HEDTAION	2.68333E-09	0.0	0.0	0.0
HF2ION	9.26004E-18	0.0	0.0	0.0
HION	1.58378E-15	0.0	0.0	0.0
HNTAION	3.63022E-09	0.0	0.0	0.0
HOXALATION	7.34154E-15	0.0	0.0	0.0
HP2O7ION	3.34288E-22	0.0	0.0	0.0
HPO4ION	3.72457E-06	0.0	0.0	0.0
HSO4ION	2.13690E-16	0.0	0.0	0.0
K1EDTAION	1.06336E-04	0.0	0.0	0.0
KCTRITION	1.15702E-05	0.0	0.0	0.0
KGLYCOL2ION	8.39007E-07	0.0	0.0	0.0
KION	0.05198	0.0	0.0	0.0
KSO4ION	4.80188E-04	0.0	0.0	0.0

NA2FION	6.97035E-04	0.0	0.0	0.0
NACO3ION	0.223445	0.0	0.0	0.0
NACTRTION	0.00243675	0.0	0.0	0.0
NAEDTAION	0.00809919	0.0	0.0	0.0
NAION	5.08349	0.0	0.0	0.0
NANTAION	0.0145102	0.0	0.0	0.0
NASO4ION	0.0255498	0.0	0.0	0.0
NH2CO2ION	1.79130E-09	0.0	0.0	0.0
NH4ION	2.19066E-08	0.0	0.0	0.0
NH4SO4ION	1.52761E-10	0.0	0.0	0.0
NIACET3ION	4.03616E-24	0.0	0.0	0.0
NIACETION	5.92113E-22	0.0	0.0	0.0
NIC2O42ION	7.26936E-20	0.0	0.0	0.0
NICLION	3.67148E-23	0.0	0.0	0.0
NICOOHION	4.91899E-21	0.0	0.0	0.0
NICTRTION	1.17327E-20	0.0	0.0	0.0
NIEDTAION	3.64241E-07	0.0	0.0	0.0
NIFION	1.60114E-23	0.0	0.0	0.0
NIGLYCOLION	1.61484E-21	0.0	0.0	0.0
NIHEDTAION	3.92691E-19	0.0	0.0	0.0
NIION	2.98060E-20	0.0	0.0	0.0
NINH32ION	2.56410E-21	0.0	0.0	0.0
NINH33ION	1.62716E-22	0.0	0.0	0.0
NINH34ION	2.95792E-24	0.0	0.0	0.0
NINH3ION	1.22099E-20	0.0	0.0	0.0
NINO3ION	3.28869E-21	0.0	0.0	0.0
NINTA2ION	2.57652E-10	0.0	0.0	0.0
NINTAION	2.63243E-14	0.0	0.0	0.0
NIOH3ION	1.07613E-08	0.0	0.0	0.0
NIOHEDTAION	7.69583E-04	0.0	0.0	0.0
NIOHION	2.52508E-17	0.0	0.0	0.0
NO2ION	1.36902	0.0	0.0	0.0
NO3ION	1.58091	0.0	0.0	0.0
NTAION	1.13802E-04	0.0	0.0	0.0
ACETATEION	0.00827796	0.0	0.0	0.0
OXALATION	0.00486517	0.0	0.0	0.0
P2O7ION	2.59933E-14	0.0	0.0	0.0
PO4ION	0.0392127	0.0	0.0	0.0
SO4ION	0.010422	0.0	0.0	0.0
NA2C2O4	0.0	0.00532517	0.0	0.0
NAFPO4.19H2O	0.0	0.00407366	0.0	0.0
=====				
Total g/hr	1112.47	3.61468	0.0	0.0
Volume, L/hr	0.85553	0.00119426	0.0	0.0
Enthalpy, cal/hr	-3.45913E+06	-11390.5	0.0	0.0
Density, g/L	1300.33	3026.72		
Vapor fraction	0.0	0.0	0.0	0.0
Solid fraction	0.0	1.	0.0	0.0
Organic fraction	0.0	0.0	0.0	0.0
Osmotic Pres, atm	288.206			
Redox Pot, volts	0.0			
E-Con, 1/ohm-cm	0.184467			
E-Con, cm2/ohm-mol	16.9073			
Abs Visc, cP	4.53373			
Rel Visc	4.30572			
Ionic Strength	7.96656			

STREAM: Concentrate_4 (20% WVR)
 TO : Still_5
 FROM : Concentrate_4 Storage

Phases----->	Aqueous	Solid	Vapor	Organic
Temperature, C	18.	18.	18.	18.
Pressure, atm	1.	1.	1.	1.
pH	14.5695			
Total mol/hr	46.17315	0.0106437	0.0	0.0
-----	mol/hr-----	mol/hr-----	mol/hr-----	mol/hr--
H2O	36.1737	0.0	0.0	0.0
ACETACID	5.16422E-13	0.0	0.0	0.0
CO2	1.31352E-15	0.0	0.0	0.0
ACET2	0.0	0.0	0.0	0.0
HCL	6.80472E-23	0.0	0.0	0.0
HCOOH	1.55184E-13	0.0	0.0	0.0
HF	1.67187E-15	0.0	0.0	0.0
HNO2	1.38970E-12	0.0	0.0	0.0
HNO3	3.46321E-21	0.0	0.0	0.0
NH3	5.44833E-05	0.0	0.0	0.0
CAHCTRT	5.83169E-22	0.0	0.0	0.0
CAHPO4	1.77184E-15	0.0	0.0	0.0
CASO4	4.72649E-12	0.0	0.0	0.0
ALF3	3.33868E-27	0.0	0.0	0.0
GLYCOLACID	4.41741E-14	0.0	0.0	0.0
ALOH3	3.03144E-09	0.0	0.0	0.0
H3PO4	2.72170E-28	0.0	0.0	0.0
CAACET2	1.95171E-12	0.0	0.0	0.0
CAC2O4	1.39501E-11	0.0	0.0	0.0
CACL2	0.0	0.0	0.0	0.0
CACO3	1.44761E-09	0.0	0.0	0.0
CACOOH2	2.58144E-11	0.0	0.0	0.0
KACET	5.12037E-05	0.0	0.0	0.0
KCL	1.44413E-05	0.0	0.0	0.0
KCOOH	3.01258E-04	0.0	0.0	0.0
KGLYCOLAT	3.96544E-05	0.0	0.0	0.0
KHSO4	4.34935E-20	0.0	0.0	0.0
NAACET	0.0107669	0.0	0.0	0.0
NACOOH	0.0457051	0.0	0.0	0.0
NAF	0.00304543	0.0	0.0	0.0
NAGLYCOLAT	0.00601761	0.0	0.0	0.0
NAHCO3	1.24133E-06	0.0	0.0	0.0
NANO3	0.0662502	0.0	0.0	0.0
CAGLYCOL2	1.72076E-12	0.0	0.0	0.0
NH4ACET	8.43053E-12	0.0	0.0	0.0
NH4NO3	1.69129E-09	0.0	0.0	0.0
NIACET2	9.63341E-24	0.0	0.0	0.0
NIC2O4	1.08753E-18	0.0	0.0	0.0
NICOOH2	5.20672E-22	0.0	0.0	0.0
NIGLYCOL2	7.48126E-23	0.0	0.0	0.0
NIHCTRT	0.0	0.0	0.0	0.0
NIOH2	8.85794E-13	0.0	0.0	0.0
NISO4	6.22755E-23	0.0	0.0	0.0
OXALAC	1.06902E-28	0.0	0.0	0.0
OHION	0.418912	0.0	0.0	0.0
ALEDTAION	4.71168E-24	0.0	0.0	0.0

ALF2ION	4.40311E-28	0.0	0.0	0.0
ALF4ION	1.79205E-26	0.0	0.0	0.0
ALF5ION	1.83478E-26	0.0	0.0	0.0
ALF6ION	1.60025E-26	0.0	0.0	0.0
ALOH2ION	1.03813E-17	0.0	0.0	0.0
ALOH4ION	0.612438	0.0	0.0	0.0
ALOHION	2.03986E-26	0.0	0.0	0.0
CAACETION	4.99652E-11	0.0	0.0	0.0
CACLION	1.28883E-13	0.0	0.0	0.0
CACOOHION	4.81117E-10	0.0	0.0	0.0
CACTRTION	3.93028E-11	0.0	0.0	0.0
CAEDTAION	0.00119697	0.0	0.0	0.0
CAFION	7.64030E-14	0.0	0.0	0.0
CAGLYCOLION	1.07763E-10	0.0	0.0	0.0
CAH2CTRITION	0.0	0.0	0.0	0.0
CAH2PO4ION	8.51024E-24	0.0	0.0	0.0
CAHC2O4ION	2.39819E-22	0.0	0.0	0.0
CAHCO3ION	8.28874E-15	0.0	0.0	0.0
CAHEDTAION	1.02473E-15	0.0	0.0	0.0
CAION	2.58290E-09	0.0	0.0	0.0
CANO3ION	7.51805E-10	0.0	0.0	0.0
CANTA2ION	1.87042E-06	0.0	0.0	0.0
CANTAION	4.87441E-08	0.0	0.0	0.0
CAOHION	6.59668E-09	0.0	0.0	0.0
CAPO4ION	1.54622E-08	0.0	0.0	0.0
CITRATION	5.02098E-05	0.0	0.0	0.0
CLION	0.144222	0.0	0.0	0.0
CO3ION	0.231857	0.0	0.0	0.0
COOHION	0.0190101	0.0	0.0	0.0
CR2O7ION	8.25432E-20	0.0	0.0	0.0
CRO4ION	0.00951823	0.0	0.0	0.0
EDTAION	0.00149632	0.0	0.0	0.0
FION	0.00335708	0.0	0.0	0.0
GLYCOLATION	0.00508983	0.0	0.0	0.0
H2CITRATION	6.29781E-25	0.0	0.0	0.0
H2EDTAION	2.24462E-17	0.0	0.0	0.0
H2NTAION	1.46206E-22	0.0	0.0	0.0
H2P2O7ION	0.0	0.0	0.0	0.0
H2PO4ION	3.48634E-15	0.0	0.0	0.0
HCITRATION	1.77542E-13	0.0	0.0	0.0
HCO3ION	1.41256E-06	0.0	0.0	0.0
HCRO4ION	3.59031E-12	0.0	0.0	0.0
HEDTAION	2.11534E-09	0.0	0.0	0.0
HF2ION	6.88813E-18	0.0	0.0	0.0
HION	1.17079E-15	0.0	0.0	0.0
HNTAION	2.84835E-09	0.0	0.0	0.0
HOXALATION	4.70757E-15	0.0	0.0	0.0
HP2O7ION	1.41732E-22	0.0	0.0	0.0
HPO4ION	2.83077E-06	0.0	0.0	0.0
HSO4ION	1.77519E-16	0.0	0.0	0.0
K1EDTAION	1.24330E-04	0.0	0.0	0.0
KCTRITION	1.13013E-05	0.0	0.0	0.0
KGLYCOL2ION	9.91908E-07	0.0	0.0	0.0
KION	0.0519072	0.0	0.0	0.0
KSO4ION	5.31474E-04	0.0	0.0	0.0
NA2FION	7.59434E-04	0.0	0.0	0.0

NACO3ION	0.23486	0.0	0.0	0.0
NACTRTION	0.00244901	0.0	0.0	0.0
NAEDTAION	0.00816442	0.0	0.0	0.0
NAION	5.0685	0.0	0.0	0.0
NANTAION	0.0145327	0.0	0.0	0.0
NASO4ION	0.0239949	0.0	0.0	0.0
NH2CO2ION	2.34642E-10	0.0	0.0	0.0
NH4ION	3.03697E-09	0.0	0.0	0.0
NH4SO4ION	2.47055E-11	0.0	0.0	0.0
NIACET3ION	3.75467E-24	0.0	0.0	0.0
NIACETION	4.66281E-22	0.0	0.0	0.0
NIC2O42ION	4.00976E-20	0.0	0.0	0.0
NICLION	3.01359E-23	0.0	0.0	0.0
NICOOHION	3.85741E-21	0.0	0.0	0.0
NICTRTION	8.22812E-21	0.0	0.0	0.0
NIEDTAION	3.01842E-07	0.0	0.0	0.0
NIFION	1.16150E-23	0.0	0.0	0.0
NIGLYCOLION	1.27939E-21	0.0	0.0	0.0
NIHEDTAION	2.68935E-19	0.0	0.0	0.0
NIION	2.22921E-20	0.0	0.0	0.0
NINH32ION	5.63774E-23	0.0	0.0	0.0
NINH33ION	6.21181E-25	0.0	0.0	0.0
NINH34ION	1.96061E-27	0.0	0.0	0.0
NINH35ION	2.35377E-30	0.0	0.0	0.0
NINH3ION	1.54619E-21	0.0	0.0	0.0
NINO3ION	2.47524E-21	0.0	0.0	0.0
NINTA2ION	1.92595E-10	0.0	0.0	0.0
NINTAION	1.83972E-14	0.0	0.0	0.0
NIOH3ION	1.23588E-08	0.0	0.0	0.0
NIOHEDTAION	7.69644E-04	0.0	0.0	0.0
NIOHION	2.08575E-17	0.0	0.0	0.0
NO2ION	1.36902	0.0	0.0	0.0
NO3ION	1.58202	0.0	0.0	0.0
NTAION	9.17107E-05	0.0	0.0	0.0
ACETATEION	0.00799099	0.0	0.0	0.0
OXALATION	0.00405759	0.0	0.0	0.0
P2O7ION	1.32577E-14	0.0	0.0	0.0
PO4ION	0.038339	0.0	0.0	0.0
SO4ION	0.0119256	0.0	0.0	0.0
NA2C2O4	0.0	0.006132733	0.0	0.0
NAFPO4.19H2O	0.0	0.004510967	0.0	0.0
=====				
Total g/hr	1063.82	4.03434	0.0	0.0
Volume, L/hr	0.808649	0.00133639	0.0	0.0
Enthalpy, cal/hr	-3.27457E+06	-12687.9	0.0	0.0
Density, g/L	1315.56	3018.84		
Vapor fraction	0.0	0.0	0.0	0.0
Solid fraction	0.0	1.	0.0	0.0
Organic fraction	0.0	0.0	0.0	0.0
Osmotic Pres, atm	311.89			
Redox Pot, volts	0.0			
E-Con, 1/ohm-cm	0.187239			
E-Con, cm2/ohm-mol	16.2216			
Abs Visc, cP	4.93151			
Rel Visc	4.68349			
Ionic Strength	8.51393			

STREAM: Concentrate_5 (24% WVR)
 TO : Still_6
 FROM : Concentrate_5 Storage

Phases----->	Aqueous	Solid	Vapor	Organic
Temperature, C	18.	18.	18.	18.
Pressure, atm	1.	1.	1.	1.
pH	14.6614			
Total mol/hr	43.47896	0.0116518	0.0	0.0
-----	mol/hr-----	mol/hr-----	mol/hr-----	mol/hr--
H2O	33.4908	0.0	0.0	0.0
ACETACID	3.95278E-13	0.0	0.0	0.0
CO2	7.67394E-16	0.0	0.0	0.0
HCL	5.45764E-23	0.0	0.0	0.0
HCOOH	1.18283E-13	0.0	0.0	0.0
HF	1.11841E-15	0.0	0.0	0.0
HNO2	1.04974E-12	0.0	0.0	0.0
HNO3	2.55379E-21	0.0	0.0	0.0
NH3	7.11970E-06	0.0	0.0	0.0
CAHCTRT	3.58013E-22	0.0	0.0	0.0
CAHPO4	1.02895E-15	0.0	0.0	0.0
CASO4	4.13895E-12	0.0	0.0	0.0
ALF3	1.60010E-27	0.0	0.0	0.0
GLYCOLACID	3.40286E-14	0.0	0.0	0.0
ALOH3	2.40527E-09	0.0	0.0	0.0
H3PO4	1.12591E-28	0.0	0.0	0.0
CAACET2	1.85875E-12	0.0	0.0	0.0
CAC2O4	9.38520E-12	0.0	0.0	0.0
CACL2	0.0	0.0	0.0	0.0
CACO3	1.16276E-09	0.0	0.0	0.0
CACOOH2	2.43794E-11	0.0	0.0	0.0
KACET	5.17058E-05	0.0	0.0	0.0
KCL	1.52806E-05	0.0	0.0	0.0
KCOOH	3.02938E-04	0.0	0.0	0.0
KGLYCOLAT	4.03003E-05	0.0	0.0	0.0
KHSO4	3.57938E-20	0.0	0.0	0.0
NAACET	0.0110626	0.0	0.0	0.0
NACOOH	0.0467637	0.0	0.0	0.0
NAF	0.00292207	0.0	0.0	0.0
NAGLYCOLAT	0.00622256	0.0	0.0	0.0
NAHCO3	9.53422E-07	0.0	0.0	0.0
NANO3	0.0646646	0.0	0.0	0.0
CAGLYCOL2	1.65991E-12	0.0	0.0	0.0
NH4ACET	9.76458E-13	0.0	0.0	0.0
NH4NO3	1.89756E-10	0.0	0.0	0.0
NIACET2	7.28164E-24	0.0	0.0	0.0
NIC2O4	5.80697E-19	0.0	0.0	0.0
NICOOH2	3.90273E-22	0.0	0.0	0.0
NIGLYCOL2	5.72770E-23	0.0	0.0	0.0
NIHCTRT	0.0	0.0	0.0	0.0
NIOH2	8.17139E-13	0.0	0.0	0.0
NISO4	4.32823E-23	0.0	0.0	0.0
OXALAC	5.12323E-29	0.0	0.0	0.0
OHION	0.41891	0.0	0.0	0.0
ALEDTAION	2.59522E-24	0.0	0.0	0.0
ALF2ION	2.19803E-28	0.0	0.0	0.0

ALF4ION	9.49378E-27	0.0	0.0	0.0
ALF5ION	1.01853E-26	0.0	0.0	0.0
ALF6ION	9.46022E-27	0.0	0.0	0.0
ALFION	0.0	0.0	0.0	0.0
ALOH2ION	7.07708E-18	0.0	0.0	0.0
ALOH4ION	0.612438	0.0	0.0	0.0
ALOHCLION	1.30495E-26	0.0	0.0	0.0
ALOHION	1.02177E-26	0.0	0.0	0.0
CAACETION	4.66828E-11	0.0	0.0	0.0
CACLION	5.86379E-13	0.0	0.0	0.0
CACOOHION	4.47634E-10	0.0	0.0	0.0
CACTRTION	3.22231E-11	0.0	0.0	0.0
CAEDTAION	0.00119721	0.0	0.0	0.0
CAFION	6.66653E-14	0.0	0.0	0.0
CAGLYCOLION	1.01332E-10	0.0	0.0	0.0
CAH2PO4ION	4.29264E-24	0.0	0.0	0.0
CAHC2O4ION	1.40297E-22	0.0	0.0	0.0
CAHCO3ION	6.23028E-15	0.0	0.0	0.0
CAHEDTAION	8.09605E-16	0.0	0.0	0.0
CAION	2.08771E-09	0.0	0.0	0.0
CANO3ION	6.65357E-10	0.0	0.0	0.0
CANTA2ION	1.64340E-06	0.0	0.0	0.0
CANTAION	3.98362E-08	0.0	0.0	0.0
CAOHION	6.51260E-09	0.0	0.0	0.0
CAPO4ION	1.19918E-08	0.0	0.0	0.0
CITRATION	3.91278E-05	0.0	0.0	0.0
CLION	0.144221	0.0	0.0	0.0
CO3ION	0.223909	0.0	0.0	0.0
COOHION	0.0179499	0.0	0.0	0.0
CR2O7ION	6.27365E-20	0.0	0.0	0.0
CRO4ION	0.00951823	0.0	0.0	0.0
EDTAION	0.00138784	0.0	0.0	0.0
FION	0.00310554	0.0	0.0	0.0
GLYCOLATION	0.00488382	0.0	0.0	0.0
H2CITRATION	3.43057E-25	0.0	0.0	0.0
H2EDTAION	1.61903E-17	0.0	0.0	0.0
H2NTAION	7.94439E-23	0.0	0.0	0.0
H2P2O7ION	0.0	0.0	0.0	0.0
H2PO4ION	1.91100E-15	0.0	0.0	0.0
H3EDTAION	0.0	0.0	0.0	0.0
HCITRATION	1.32891E-13	0.0	0.0	0.0
HCO3ION	1.11251E-06	0.0	0.0	0.0
HCRO4ION	2.74582E-12	0.0	0.0	0.0
HEDTAION	1.58853E-09	0.0	0.0	0.0
HF2ION	5.07613E-18	0.0	0.0	0.0
HION	8.17135E-16	0.0	0.0	0.0
HNTAION	2.12493E-09	0.0	0.0	0.0
HOXALATION	2.81019E-15	0.0	0.0	0.0
HP2O7ION	5.11022E-23	0.0	0.0	0.0
HPO4ION	2.05345E-06	0.0	0.0	0.0
HSO4ION	1.37933E-16	0.0	0.0	0.0
K1EDTAION	1.50058E-04	0.0	0.0	0.0
KCTRTION	1.10252E-05	0.0	0.0	0.0
KGLYCOL2ION	1.20005E-06	0.0	0.0	0.0
KION	0.0518256	0.0	0.0	0.0
KSO4ION	5.83709E-04	0.0	0.0	0.0

NA2FION	8.55570E-04	0.0	0.0	0.0
NACO3ION	0.242808	0.0	0.0	0.0
NACTRTION	0.00246037	0.0	0.0	0.0
NAEDTAION	0.00824694	0.0	0.0	0.0
NAION	5.05891	0.0	0.0	0.0
NANTAION	0.0145535	0.0	0.0	0.0
NASO4ION	0.0220707	0.0	0.0	0.0
NH2CO2ION	2.58557E-11	0.0	0.0	0.0
NH4ION	3.49855E-10	0.0	0.0	0.0
NH4SO4ION	3.40757E-12	0.0	0.0	0.0
NIACET3ION	3.35940E-24	0.0	0.0	0.0
NIACETION	3.45763E-22	0.0	0.0	0.0
NIC2O42ION	2.00888E-20	0.0	0.0	0.0
NICLION	2.33698E-23	0.0	0.0	0.0
NICOOHION	2.84846E-21	0.0	0.0	0.0
NICTRTION	5.35410E-21	0.0	0.0	0.0
NIEDTAION	2.39612E-07	0.0	0.0	0.0
NIFION	8.04358E-24	0.0	0.0	0.0
NIGLYCOLION	9.54823E-22	0.0	0.0	0.0
NIHEDTAION	1.68637E-19	0.0	0.0	0.0
NIION	1.56030E-20	0.0	0.0	0.0
NINH32ION	8.77077E-25	0.0	0.0	0.0
NINH33ION	1.46235E-27	0.0	0.0	0.0
NINH34ION	0.0	0.0	0.0	0.0
NINH3ION	1.58963E-22	0.0	0.0	0.0
NINO3ION	1.73847E-21	0.0	0.0	0.0
NINTA2ION	1.34305E-10	0.0	0.0	0.0
NINTAION	1.19330E-14	0.0	0.0	0.0
NIOH3ION	1.49086E-08	0.0	0.0	0.0
NIOHEDTAION	7.69704E-04	0.0	0.0	0.0
NIOHION	1.66523E-17	0.0	0.0	0.0
NO2ION	1.36902	0.0	0.0	0.0
NO3ION	1.5836	0.0	0.0	0.0
NTAION	7.13857E-05	0.0	0.0	0.0
ACETATEION	0.00769479	0.0	0.0	0.0
OXALATION	0.00332833	0.0	0.0	0.0
P2O7ION	5.91273E-15	0.0	0.0	0.0
PO4ION	0.0377823	0.0	0.0	0.0
SO4ION	0.0137976	0.0	0.0	0.0
NA2C2O4	0.0	0.006862039	0.0	0.0
NAFPO4.19H2O	0.0	0.004789761	0.0	0.0
=====				
Total g/hr	1015.29	4.33058	0.0	0.0
Volume, L/hr	0.76205	0.00143965	0.0	0.0
Enthalpy, cal/hr	-3.09038E+06	-13582.8	0.0	0.0
Density, g/L	1332.31	3008.08		
Vapor fraction	0.0	0.0	0.0	0.0
Solid fraction	0.0	1.	0.0	0.0
Organic fraction	0.0	0.0	0.0	0.0
Osmotic Pres, atm	340.345			
Redox Pot, volts	0.0			
E-Con, 1/ohm-cm	0.189795			
E-Con, cm2/ohm-mol	15.4955			
Abs Visc, cP	5.41722			
Rel Visc	5.14477			
Ionic Strength	9.1654			

STREAM: Concentrate_6 (29% WVR)
 TO : Still_7
 FROM : Concentrate_6 Storage

Phases----->	Aqueous	Solid	Vapor	Organic
Temperature, C	18.	18.	18.	18.
Pressure, atm	1.	1.	1.	1.
pH	14.7873			
Total mol/hr	40.80112	0.0123295	0.0	0.0
-----	mol/hr-----	mol/hr-----	mol/hr-----	mol/hr---
H2O	30.8117	0.0	0.0	0.0
ACETACID	2.76998E-13	0.0	0.0	0.0
CO2	3.93247E-16	0.0	0.0	0.0
HCL	4.01723E-23	0.0	0.0	0.0
HCOOH	8.25822E-14	0.0	0.0	0.0
HF	6.95303E-16	0.0	0.0	0.0
HNO2	7.19512E-13	0.0	0.0	0.0
HNO3	1.70612E-21	0.0	0.0	0.0
NH3	7.69128E-07	0.0	0.0	0.0
CAHCTRT	1.91102E-22	0.0	0.0	0.0
CAHPO4	5.22014E-16	0.0	0.0	0.0
CASO4	3.31723E-12	0.0	0.0	0.0
ALF3	6.37256E-28	0.0	0.0	0.0
GLYCOLACID	2.40080E-14	0.0	0.0	0.0
ALOH3	1.74242E-09	0.0	0.0	0.0
H3PO4	3.58359E-29	0.0	0.0	0.0
CAACET2	1.72716E-12	0.0	0.0	0.0
CAC2O4	5.87472E-12	0.0	0.0	0.0
CACL2	0.0	0.0	0.0	0.0
CACO3	9.25360E-10	0.0	0.0	0.0
CACOOH2	2.24862E-11	0.0	0.0	0.0
KACET	5.22494E-05	0.0	0.0	0.0
KCL	1.62193E-05	0.0	0.0	0.0
KCOOH	3.04991E-04	0.0	0.0	0.0
KGLYCOLAT	4.10005E-05	0.0	0.0	0.0
KHSO4	2.59532E-20	0.0	0.0	0.0
NAACET	0.011354	0.0	0.0	0.0
NACOOH	0.047818	0.0	0.0	0.0
NAF	0.00287679	0.0	0.0	0.0
NAGLYCOLAT	0.00642984	0.0	0.0	0.0
NAHCO3	6.97195E-07	0.0	0.0	0.0
NANO3	0.0623487	0.0	0.0	0.0
CAGLYCOL2	1.56341E-12	0.0	0.0	0.0
NH4ACET	8.77517E-14	0.0	0.0	0.0
NH4NO3	1.63404E-11	0.0	0.0	0.0
NIACET2	4.96747E-24	0.0	0.0	0.0
NIC2O4	2.66863E-19	0.0	0.0	0.0
NICOOH2	2.64275E-22	0.0	0.0	0.0
NIGLYCOL2	3.96064E-23	0.0	0.0	0.0
NIOH2	7.64308E-13	0.0	0.0	0.0
NISO4	2.54678E-23	0.0	0.0	0.0
OXALAC	2.01195E-29	0.0	0.0	0.0
OHION	0.418909	0.0	0.0	0.0
ALEDTAION	1.10354E-24	0.0	0.0	0.0
ALF2ION	8.89926E-29	0.0	0.0	0.0

ALF4ION	4.44345E-27	0.0	0.0	0.0
ALF5ION	5.22323E-27	0.0	0.0	0.0
ALF6ION	5.41255E-27	0.0	0.0	0.0
ALFION	0.0	0.0	0.0	0.0
ALOH2ION	4.15234E-18	0.0	0.0	0.0
ALOH4ION	0.612438	0.0	0.0	0.0
ALOHCLION	7.17950E-27	0.0	0.0	0.0
ALOHION	4.01535E-27	0.0	0.0	0.0
CAACETION	4.27140E-11	0.0	0.0	0.0
CACLION	4.00685E-12	0.0	0.0	0.0
CACOOHION	4.08070E-10	0.0	0.0	0.0
CACTRTION	2.53313E-11	0.0	0.0	0.0
CAEDTAION	0.00119748	0.0	0.0	0.0
CAFION	5.85135E-14	0.0	0.0	0.0
CAGLYCOLION	9.33490E-11	0.0	0.0	0.0
CAH2PO4ION	1.78095E-24	0.0	0.0	0.0
CAHC2O4ION	7.19410E-23	0.0	0.0	0.0
CAHCO3ION	4.43967E-15	0.0	0.0	0.0
CAHEDTAION	5.89760E-16	0.0	0.0	0.0
CAION	1.60223E-09	0.0	0.0	0.0
CANO3ION	5.68596E-10	0.0	0.0	0.0
CANTA2ION	1.39558E-06	0.0	0.0	0.0
CANTAION	3.12262E-08	0.0	0.0	0.0
CAOHION	6.63161E-09	0.0	0.0	0.0
CAPO4ION	8.95972E-09	0.0	0.0	0.0
CITRATION	2.91110E-05	0.0	0.0	0.0
CLION	0.14422	0.0	0.0	0.0
CO3ION	0.224979	0.0	0.0	0.0
COOHION	0.0168935	0.0	0.0	0.0
CR2O7ION	4.18056E-20	0.0	0.0	0.0
CRO4ION	0.00951823	0.0	0.0	0.0
EDTAION	0.00124838	0.0	0.0	0.0
FION	0.00296323	0.0	0.0	0.0
GLYCOLATION	0.00467523	0.0	0.0	0.0
H2CITRATION	1.55881E-25	0.0	0.0	0.0
H2EDTAION	1.02876E-17	0.0	0.0	0.0
H2NTAION	3.60237E-23	0.0	0.0	0.0
H2P2O7ION	0.0	0.0	0.0	0.0
H2PO4ION	8.88394E-16	0.0	0.0	0.0
H3EDTAION	0.0	0.0	0.0	0.0
HCITRATION	9.11256E-14	0.0	0.0	0.0
HCO3ION	8.48366E-07	0.0	0.0	0.0
HCRO4ION	1.92961E-12	0.0	0.0	0.0
HEDTAION	1.09516E-09	0.0	0.0	0.0
HF2ION	3.69449E-18	0.0	0.0	0.0
HION	5.18263E-16	0.0	0.0	0.0
HNTAION	1.45274E-09	0.0	0.0	0.0
HOXALATION	1.49741E-15	0.0	0.0	0.0
HP2O7ION	1.40127E-23	0.0	0.0	0.0
HPO4ION	1.37389E-06	0.0	0.0	0.0
HSO4ION	9.41054E-17	0.0	0.0	0.0
K1EDTAION	1.89395E-04	0.0	0.0	0.0
KCTRTION	1.07676E-05	0.0	0.0	0.0
KGLYCOL2ION	1.50473E-06	0.0	0.0	0.0
KION	0.0517429	0.0	0.0	0.0
KSO4ION	6.22806E-04	0.0	0.0	0.0

NA2FION	0.00101738	0.0	0.0	0.0
NACO3ION	0.241739	0.0	0.0	0.0
NACTRTION	0.00247064	0.0	0.0	0.0
NAEDTAION	0.00834681	0.0	0.0	0.0
NAION	5.06099	0.0	0.0	0.0
NANTAION	0.0145723	0.0	0.0	0.0
NASO4ION	0.0199269	0.0	0.0	0.0
NH2CO2ION	2.30726E-12	0.0	0.0	0.0
NH4ION	3.14259E-11	0.0	0.0	0.0
NH4SO4ION	3.76554E-13	0.0	0.0	0.0
NIACET3ION	2.80774E-24	0.0	0.0	0.0
NIACETION	2.32268E-22	0.0	0.0	0.0
NIC2O42ION	8.70311E-21	0.0	0.0	0.0
NICLION	1.64528E-23	0.0	0.0	0.0
NICOOHION	1.90642E-21	0.0	0.0	0.0
NICTRTION	3.09010E-21	0.0	0.0	0.0
NIEDTAION	1.75954E-07	0.0	0.0	0.0
NIFION	5.18324E-24	0.0	0.0	0.0
NIGLYCOLION	6.45777E-22	0.0	0.0	0.0
NIHEDTAION	9.01882E-20	0.0	0.0	0.0
NIION	9.83494E-21	0.0	0.0	0.0
NINH32ION	8.74475E-27	0.0	0.0	0.0
NINH33ION	1.86978E-30	0.0	0.0	0.0
NINH3ION	1.23588E-23	0.0	0.0	0.0
NINO3ION	1.09060E-21	0.0	0.0	0.0
NINTA2ION	8.37338E-11	0.0	0.0	0.0
NINTAION	6.86733E-15	0.0	0.0	0.0
NIOH3ION	2.00047E-08	0.0	0.0	0.0
NIOHEDTAION	7.69762E-04	0.0	0.0	0.0
NIOHION	1.27150E-17	0.0	0.0	0.0
NO2ION	1.36902	0.0	0.0	0.0
NO3ION	1.58592	0.0	0.0	0.0
NTAION	5.30836E-05	0.0	0.0	0.0
ACETATEION	0.00740285	0.0	0.0	0.0
OXALATION	0.00267638	0.0	0.0	0.0
P2O7ION	2.11938E-15	0.0	0.0	0.0
PO4ION	0.0377314	0.0	0.0	0.0
SO4ION	0.0159022	0.0	0.0	0.0
NA2C2O4	0.0	0.007513972	0.0	0.0
NAFPO4.19H2O	0.0	0.004815528	0.0	0.0
=====				
Total g/hr	966.928	4.4363	0.0	0.0
Volume, L/hr	0.715895	0.0014837	0.0	0.0
Enthalpy, cal/hr	-2.90677E+06	-13850.5	0.0	0.0
Density, g/L	1350.66	2990.02		
Vapor fraction	0.0	0.0	0.0	0.0
Solid fraction	0.0	1.	0.0	0.0
Organic fraction	0.0	0.0	0.0	0.0
Osmotic Pres, atm	375.723			
Redox Pot, volts	0.0			
E-Con, 1/ohm-cm	0.191835			
E-Con, cm2/ohm-mol	14.7135			
Abs Visc, cP	6.00764			
Rel Visc	5.7055			
Ionic Strength	9.96963			

STREAM: Concentrate_7 (33% WVR)
 TO : Still_8
 FROM : Concentrate_7 Storage

Phases----->	Aqueous	Solid	Vapor	Organic
Temperature, C	18.	18.	18.	18.
Pressure, atm	1.	1.	1.	1.
pH	14.971			
Total mol/hr	38.16246	0.0124992	0.0	0.0
-----	mol/hr-----	mol/hr-----	mol/hr-----	mol/hr--
H2O	28.1434	0.0	0.0	0.0
ACETACID	1.67281E-13	0.0	0.0	0.0
CO2	1.65634E-16	0.0	0.0	0.0
HCL	2.54345E-23	0.0	0.0	0.0
HCOOH	4.97799E-14	0.0	0.0	0.0
HF	3.83836E-16	0.0	0.0	0.0
HNO2	4.16980E-13	0.0	0.0	0.0
HNO3	9.62836E-22	0.0	0.0	0.0
NH3	6.58573E-08	0.0	0.0	0.0
CAHCTRT	8.12980E-23	0.0	0.0	0.0
CAHPO4	2.12849E-16	0.0	0.0	0.0
CASO4	2.24738E-12	0.0	0.0	0.0
ALF3	1.82877E-28	0.0	0.0	0.0
GLYCOLACID	1.46025E-14	0.0	0.0	0.0
ALOH3	1.07270E-09	0.0	0.0	0.0
H3PO4	7.33368E-30	0.0	0.0	0.0
CAACET2	1.55195E-12	0.0	0.0	0.0
CAC2O4	3.30606E-12	0.0	0.0	0.0
CACL2	0.0	0.0	0.0	0.0
CACO3	7.50863E-10	0.0	0.0	0.0
CACOOH2	2.01307E-11	0.0	0.0	0.0
KACET	5.29899E-05	0.0	0.0	0.0
KCL	1.72453E-05	0.0	0.0	0.0
KCOOH	3.08743E-04	0.0	0.0	0.0
KGLYCOLAT	4.18796E-05	0.0	0.0	0.0
KHSO4	1.48199E-20	0.0	0.0	0.0
NAACET	0.0116022	0.0	0.0	0.0
NACOOH	0.0487733	0.0	0.0	0.0
NAF	0.00295034	0.0	0.0	0.0
NAGLYCOLAT	0.00661749	0.0	0.0	0.0
NAHCO3	4.80440E-07	0.0	0.0	0.0
NANO3	0.0587956	0.0	0.0	0.0
CAGLYCOL2	1.42502E-12	0.0	0.0	0.0
NH4ACET	5.61113E-15	0.0	0.0	0.0
NH4NO3	9.79933E-13	0.0	0.0	0.0
NIACET2	2.86921E-24	0.0	0.0	0.0
NIC2O4	9.65370E-20	0.0	0.0	0.0
NICOOH2	1.52083E-22	0.0	0.0	0.0
NIGLYCOL2	2.32057E-23	0.0	0.0	0.0
NIOH2	7.39650E-13	0.0	0.0	0.0
NISO4	1.10911E-23	0.0	0.0	0.0
OXALAC	5.68267E-30	0.0	0.0	0.0
OHION	0.418908	0.0	0.0	0.0
ALEDTAION	2.96396E-25	0.0	0.0	0.0
ALF2ION	2.50139E-29	0.0	0.0	0.0
ALF4ION	1.66508E-27	0.0	0.0	0.0

ALF5ION	2.31113E-27	0.0	0.0	0.0
ALF6ION	2.88829E-27	0.0	0.0	0.0
ALFION	0.0	0.0	0.0	0.0
ALOH2ION	1.88105E-18	0.0	0.0	0.0
ALOH4ION	0.612438	0.0	0.0	0.0
ALOHCLION	2.76990E-27	0.0	0.0	0.0
ALOHION	1.05245E-27	0.0	0.0	0.0
CAACETION	3.81467E-11	0.0	0.0	0.0
CACLION	5.01893E-11	0.0	0.0	0.0
CACOOHION	3.63767E-10	0.0	0.0	0.0
CACTRTION	1.87750E-11	0.0	0.0	0.0
CAEDTAION	0.00119775	0.0	0.0	0.0
CAFION	5.24467E-14	0.0	0.0	0.0
CAGLYCOLION	8.39677E-11	0.0	0.0	0.0
CAH2PO4ION	5.37547E-25	0.0	0.0	0.0
CAHC2O4ION	3.00506E-23	0.0	0.0	0.0
CAHCO3ION	2.99337E-15	0.0	0.0	0.0
CAHEDTAION	3.74425E-16	0.0	0.0	0.0
CAION	1.14576E-09	0.0	0.0	0.0
CANO3ION	4.62502E-10	0.0	0.0	0.0
CANTA2ION	1.13224E-06	0.0	0.0	0.0
CANTAION	2.30866E-08	0.0	0.0	0.0
CAOHION	7.23652E-09	0.0	0.0	0.0
CAPO4ION	6.36491E-09	0.0	0.0	0.0
CITRATION	2.02958E-05	0.0	0.0	0.0
CLION	0.144219	0.0	0.0	0.0
CO3ION	0.249291	0.0	0.0	0.0
COOHION	0.0159345	0.0	0.0	0.0
CR2O7ION	2.21032E-20	0.0	0.0	0.0
CRO4ION	0.00951823	0.0	0.0	0.0
EDTAION	0.00107034	0.0	0.0	0.0
FION	0.00299309	0.0	0.0	0.0
GLYCOLATION	0.00448569	0.0	0.0	0.0
H2CITRATION	5.25018E-26	0.0	0.0	0.0
H2EDTAION	5.22734E-18	0.0	0.0	0.0
H2NTAION	1.21139E-23	0.0	0.0	0.0
H2P2O7ION	0.0	0.0	0.0	0.0
H2PO4ION	3.14041E-16	0.0	0.0	0.0
H3EDTAION	0.0	0.0	0.0	0.0
HCITRATION	5.40557E-14	0.0	0.0	0.0
HCO3ION	6.30021E-07	0.0	0.0	0.0
HCRO4ION	1.17700E-12	0.0	0.0	0.0
HEDTAION	6.54024E-10	0.0	0.0	0.0
HF2ION	2.64735E-18	0.0	0.0	0.0
HION	2.81691E-16	0.0	0.0	0.0
HNTAION	8.59529E-10	0.0	0.0	0.0
HOXALATION	6.67161E-16	0.0	0.0	0.0
HP2O7ION	2.45065E-24	0.0	0.0	0.0
HPO4ION	8.03593E-07	0.0	0.0	0.0
HSO4ION	5.04757E-17	0.0	0.0	0.0
K1EDTAION	2.56224E-04	0.0	0.0	0.0
KCTRTION	1.05987E-05	0.0	0.0	0.0
KGLYCOL2ION	2.01221E-06	0.0	0.0	0.0
KION	0.0516731	0.0	0.0	0.0
KSO4ION	6.19041E-04	0.0	0.0	0.0
NA2FION	0.0013204	0.0	0.0	0.0

NACO3ION	0.217427	0.0	0.0	0.0
NACTRTION	0.00247962	0.0	0.0	0.0
NAEDTAION	0.00845776	0.0	0.0	0.0
NAION	5.09006	0.0	0.0	0.0
NANTAION	0.0145889	0.0	0.0	0.0
NASO4ION	0.0182094	0.0	0.0	0.0
NH2CO2ION	1.62459E-13	0.0	0.0	0.0
NH4ION	2.03049E-12	0.0	0.0	0.0
NH4SO4ION	3.09501E-14	0.0	0.0	0.0
NIACET3ION	2.10999E-24	0.0	0.0	0.0
NIACETION	1.33339E-22	0.0	0.0	0.0
NIC2O42ION	3.01823E-21	0.0	0.0	0.0
NICLION	9.87726E-24	0.0	0.0	0.0
NICOOHION	1.09241E-21	0.0	0.0	0.0
NICTRTION	1.47223E-21	0.0	0.0	0.0
NIEDTAION	1.13130E-07	0.0	0.0	0.0
NIFION	2.98638E-24	0.0	0.0	0.0
NIGLYCOLION	3.73393E-22	0.0	0.0	0.0
NIHEDTAION	3.68061E-20	0.0	0.0	0.0
NIION	5.28229E-21	0.0	0.0	0.0
NINH32ION	4.96032E-29	0.0	0.0	0.0
NINH3ION	6.62086E-25	0.0	0.0	0.0
NINO3ION	5.70179E-22	0.0	0.0	0.0
NINTA2ION	4.36683E-11	0.0	0.0	0.0
NINTAION	3.26369E-15	0.0	0.0	0.0
NIOH3ION	3.26026E-08	0.0	0.0	0.0
NIOHEDTAION	7.69813E-04	0.0	0.0	0.0
NIOHION	9.12846E-18	0.0	0.0	0.0
NO2ION	1.36902	0.0	0.0	0.0
NO3ION	1.58947	0.0	0.0	0.0
NTAION	3.70190E-05	0.0	0.0	0.0
ACETATEION	0.0071539	0.0	0.0	0.0
OXALATION	0.00210019	0.0	0.0	0.0
P2O7ION	5.33410E-16	0.0	0.0	0.0
PO4ION	0.0385448	0.0	0.0	0.0
SO4ION	0.0176235	0.0	0.0	0.0
NA2C2O4	0.0	0.008090124	0.0	0.0
NAFPO4.19H2O	0.0	0.004409076	0.0	0.0
=====				
Total g/hr	918.931	4.22407	0.0	0.0
Volume, L/hr	0.670664	0.00142993	0.0	0.0
Enthalpy, cal/hr	-2.72440E+06	-13064.6	0.0	0.0
Density, g/L	1370.18	2954.05		
Vapor fraction	0.0	0.0	0.0	0.0
Solid fraction	0.0	1.	0.0	0.0
Organic fraction	0.0	0.0	0.0	0.0
Osmotic Pres, atm	421.284			
Redox Pot, volts	0.0			
E-Con, 1/ohm-cm	0.192863			
E-Con, cm2/ohm-mol	13.8715			
Abs Visc, cP	6.68113			
Rel Visc	6.34511			
Ionic Strength	11.0265			

STREAM: Concentrate_8 (38% WVR)
 TO : Still_9
 FROM : Concentrate_8 Storage

Phases----->	Aqueous	Solid	Vapor	Organic
Temperature, C	18.	18.	18.	18.
Pressure, atm	1.	1.	1.	1.
pH	15.1955			
Total mol/hr	35.59365	0.0121235	0.0	0.0
-----	mol/hr-----	mol/hr-----	mol/hr-----	mol/hr--
H2O	25.4796	0.0	0.0	0.0
ACETACID	8.92026E-14	0.0	0.0	0.0
CO2	6.51554E-17	0.0	0.0	0.0
HCL	1.40033E-23	0.0	0.0	0.0
HCOOH	2.66524E-14	0.0	0.0	0.0
HF	1.87469E-16	0.0	0.0	0.0
HNO2	2.03789E-13	0.0	0.0	0.0
HNO3	4.59443E-22	0.0	0.0	0.0
NH3	4.37603E-09	0.0	0.0	0.0
CAHCTRT	2.66112E-23	0.0	0.0	0.0
CAHPO4	6.65806E-17	0.0	0.0	0.0
CASO4	1.08314E-12	0.0	0.0	0.0
ALF3	4.22347E-29	0.0	0.0	0.0
GLYCOLACID	7.84630E-15	0.0	0.0	0.0
ALOH3	5.52250E-10	0.0	0.0	0.0
H3PO4	1.02251E-30	0.0	0.0	0.0
CAACET2	1.32729E-12	0.0	0.0	0.0
CAC2O4	1.54809E-12	0.0	0.0	0.0
CACL2	0.0	0.0	0.0	0.0
CACO3	6.35738E-10	0.0	0.0	0.0
CACOOH2	1.73559E-11	0.0	0.0	0.0
KACET	5.43770E-05	0.0	0.0	0.0
KCL	1.82712E-05	0.0	0.0	0.0
KCOOH	3.18105E-04	0.0	0.0	0.0
KGLYCOLAT	4.33042E-05	0.0	0.0	0.0
KHSO4	6.12659E-21	0.0	0.0	0.0
NAACET	0.0116962	0.0	0.0	0.0
NACOOH	0.049367	0.0	0.0	0.0
NAF	0.00305449	0.0	0.0	0.0
NAGLYCOLAT	0.00672207	0.0	0.0	0.0
NAHCO3	3.42769E-07	0.0	0.0	0.0
NANO3	0.0529507	0.0	0.0	0.0
CAGLYCOL2	1.23743E-12	0.0	0.0	0.0
NH4ACET	2.66535E-16	0.0	0.0	0.0
NH4NO3	4.16280E-14	0.0	0.0	0.0
NIACET2	1.42668E-24	0.0	0.0	0.0
NIC2O4	2.62820E-20	0.0	0.0	0.0
NICOOH2	7.62336E-23	0.0	0.0	0.0
NIGLYCOL2	1.17158E-23	0.0	0.0	0.0
NIOH2	6.61930E-13	0.0	0.0	0.0
NISO4	3.10787E-24	0.0	0.0	0.0
OXALAC	1.18607E-30	0.0	0.0	0.0
OHION	0.418907	0.0	0.0	0.0
ALEDTAION	5.92243E-26	0.0	0.0	0.0
ALF2ION	5.65317E-30	0.0	0.0	0.0
ALF4ION	5.82406E-28	0.0	0.0	0.0

ALF5ION	1.03608E-27	0.0	0.0	0.0
ALF6ION	1.70448E-27	0.0	0.0	0.0
ALFION	0.0	0.0	0.0	0.0
ALOH2ION	7.00299E-19	0.0	0.0	0.0
ALOH4ION	0.612438	0.0	0.0	0.0
ALOHCLION	8.39240E-28	0.0	0.0	0.0
ALOHION	2.04090E-28	0.0	0.0	0.0
CAACETION	3.31887E-11	0.0	0.0	0.0
CACLION	1.63893E-09	0.0	0.0	0.0
CACOOHION	3.17754E-10	0.0	0.0	0.0
CACTRTION	1.26781E-11	0.0	0.0	0.0
CAEDTAION	0.00119803	0.0	0.0	0.0
CAFION	4.68613E-14	0.0	0.0	0.0
CAGLYCOLION	7.36166E-11	0.0	0.0	0.0
CAH2PO4ION	1.21809E-25	0.0	0.0	0.0
CAHC2O4ION	1.02343E-23	0.0	0.0	0.0
CAHCO3ION	2.15348E-15	0.0	0.0	0.0
CAHEDTAION	2.14526E-16	0.0	0.0	0.0
CAION	7.36559E-10	0.0	0.0	0.0
CANO3ION	3.48156E-10	0.0	0.0	0.0
CANTA2ION	8.58620E-07	0.0	0.0	0.0
CANTAION	1.55582E-08	0.0	0.0	0.0
CAOHION	7.92946E-09	0.0	0.0	0.0
CAPO4ION	4.10733E-09	0.0	0.0	0.0
CITRATION	1.27452E-05	0.0	0.0	0.0
CLION	0.144218	0.0	0.0	0.0
CO3ION	0.333969	0.0	0.0	0.0
COOHION	0.0153314	0.0	0.0	0.0
CR2O7ION	1.01594E-20	0.0	0.0	0.0
CRO4ION	0.00951823	0.0	0.0	0.0
EDTAION	8.44589E-04	0.0	0.0	0.0
FION	0.0031959	0.0	0.0	0.0
GLYCOLATION	0.00437753	0.0	0.0	0.0
H2CITRATION	1.39121E-26	0.0	0.0	0.0
H2EDTAION	2.35328E-18	0.0	0.0	0.0
H2NTAION	3.20677E-24	0.0	0.0	0.0
H2PO4ION	8.95328E-17	0.0	0.0	0.0
H3EDTAION	0.0	0.0	0.0	0.0
HCITRATION	2.86810E-14	0.0	0.0	0.0
HCO3ION	5.21610E-07	0.0	0.0	0.0
HCRO4ION	6.44624E-13	0.0	0.0	0.0
HEDTAION	3.48477E-10	0.0	0.0	0.0
HF2ION	1.93311E-18	0.0	0.0	0.0
HION	1.35380E-16	0.0	0.0	0.0
HNTAION	4.55107E-10	0.0	0.0	0.0
HOXALATION	2.52902E-16	0.0	0.0	0.0
HP2O7ION	2.86531E-25	0.0	0.0	0.0
HPO4ION	4.20083E-07	0.0	0.0	0.0
HSO4ION	1.96937E-17	0.0	0.0	0.0
K1EDTAION	3.92912E-04	0.0	0.0	0.0
KCTRTION	1.07177E-05	0.0	0.0	0.0
KGLYCOL2ION	3.08877E-06	0.0	0.0	0.0
KION	0.0516137	0.0	0.0	0.0
KSO4ION	5.27405E-04	0.0	0.0	0.0
NA2FION	0.00189533	0.0	0.0	0.0
NACO3ION	0.132749	0.0	0.0	0.0

NACTRTION	0.00248706	0.0	0.0	0.0
NAEDTAION	0.00854657	0.0	0.0	0.0
NAION	5.18296	0.0	0.0	0.0
NANTAION	0.0146032	0.0	0.0	0.0
NASO4ION	0.0188402	0.0	0.0	0.0
NH2CO2ION	1.03495E-14	0.0	0.0	0.0
NH4ION	1.00056E-13	0.0	0.0	0.0
NH4SO4ION	2.10837E-15	0.0	0.0	0.0
NIACET3ION	1.54727E-24	0.0	0.0	0.0
NIACETION	6.74478E-23	0.0	0.0	0.0
NIC2O42ION	8.28041E-22	0.0	0.0	0.0
NICLION	5.14431E-24	0.0	0.0	0.0
NICOOHION	5.54796E-22	0.0	0.0	0.0
NICTRTION	5.78003E-22	0.0	0.0	0.0
NIEDTAION	6.57900E-08	0.0	0.0	0.0
NIFION	1.55138E-24	0.0	0.0	0.0
NIGLYCOLION	1.90330E-22	0.0	0.0	0.0
NIHEDTAION	1.22606E-20	0.0	0.0	0.0
NIION	2.51270E-21	0.0	0.0	0.0
NINH32ION	0.0	0.0	0.0	0.0
NINH3ION	2.51230E-26	0.0	0.0	0.0
NINO3ION	2.49546E-22	0.0	0.0	0.0
NINTA2ION	1.92533E-11	0.0	0.0	0.0
NINTAION	1.27876E-15	0.0	0.0	0.0
NIOH3ION	5.77254E-08	0.0	0.0	0.0
NIOHEDTAION	7.69835E-04	0.0	0.0	0.0
NIOHION	5.95553E-18	0.0	0.0	0.0
NO2ION	1.36902	0.0	0.0	0.0
NO3ION	1.59532	0.0	0.0	0.0
NTAION	2.32741E-05	0.0	0.0	0.0
ACETATEION	0.00705852	0.0	0.0	0.0
OXALATION	0.00159409	0.0	0.0	0.0
P2O7ION	9.26426E-17	0.0	0.0	0.0
PO4ION	0.040309	0.0	0.0	0.0
SO4ION	0.0170844	0.0	0.0	0.0
NA2C2O4	0.0	0.008596276	0.0	0.0
NAFPO4.19H2O	0.0	0.003527224	0.0	0.0
=====				
Total g/hr	871.2	3.66384	0.0	0.0
Volume, L/hr	0.627301	0.00126931	0.0	0.0
Enthalpy, cal/hr	-2.54272E+06	-11123.6	0.0	0.0
Density, g/L	1388.81	2886.48		
Vapor fraction	0.0	0.0	0.0	0.0
Solid fraction	0.0	1.	0.0	0.0
Organic fraction	0.0	0.0	0.0	0.0
Osmotic Pres, atm	476.781			
Redox Pot, volts	0.0			
E-Con, 1/ohm-cm	0.191966			
E-Con, cm2/ohm-mol	13.0205			
Abs Visc, cP	7.13488			
Rel Visc	6.77604			
Ionic Strength	12.575			

STREAM: Concentrate_9 (42% WVR)
 TO : Still_10
 FROM : Concentrate_9 Storage

Phases----->	Aqueous	Solid	Vapor	Organic
Temperature, C	18.	18.	18.	18.
Pressure, atm	1.	1.	1.	1.
pH	15.267			
Total mol/hr	32.69531	0.0355523	0.0	0.0
-----	mol/hr-----	mol/hr-----	mol/hr-----	mol/hr--
H2O	22.5354	0.0	0.0	0.0
ACETACID	6.61228E-14	0.0	0.0	0.0
CO2	4.62441E-17	0.0	0.0	0.0
HCL	1.06568E-23	0.0	0.0	0.0
HCOOH	1.99180E-14	0.0	0.0	0.0
HF	1.07075E-16	0.0	0.0	0.0
HNO2	1.32568E-13	0.0	0.0	0.0
HNO3	2.94027E-22	0.0	0.0	0.0
NH3	1.93164E-10	0.0	0.0	0.0
CAHCTRT	1.04810E-23	0.0	0.0	0.0
CAHPO4	2.39278E-17	0.0	0.0	0.0
CASO4	4.31074E-13	0.0	0.0	0.0
ALF3	2.87768E-29	0.0	0.0	0.0
GLYCOLACID	5.86729E-15	0.0	0.0	0.0
ALOH3	3.59716E-10	0.0	0.0	0.0
H3PO4	0.0	0.0	0.0	0.0
CAACET2	1.07550E-12	0.0	0.0	0.0
CAC2O4	5.89650E-13	0.0	0.0	0.0
CACL2	0.0	0.0	0.0	0.0
CACO3	4.38873E-10	0.0	0.0	0.0
CACOOH2	1.42943E-11	0.0	0.0	0.0
KACET	5.65630E-05	0.0	0.0	0.0
KCL	1.95122E-05	0.0	0.0	0.0
KCOOH	3.33598E-04	0.0	0.0	0.0
KGLYCOLAT	4.54408E-05	0.0	0.0	0.0
KHSO4	3.38162E-21	0.0	0.0	0.0
NAACET	0.0117051	0.0	0.0	0.0
NACOOH	0.0498083	0.0	0.0	0.0
NAF	0.0027597	0.0	0.0	0.0
NAGLYCOLAT	0.00678627	0.0	0.0	0.0
NAHCO3	3.15730E-07	0.0	0.0	0.0
NANO3	0.0459428	0.0	0.0	0.0
CAGLYCOL2	1.02038E-12	0.0	0.0	0.0
NH4ACET	1.27106E-17	0.0	0.0	0.0
NH4NO3	1.71017E-15	0.0	0.0	0.0
NIACET2	9.48677E-25	0.0	0.0	0.0
NIC2O4	8.21491E-21	0.0	0.0	0.0
NICOOH2	5.15239E-23	0.0	0.0	0.0
NIGLYCOL2	7.92794E-24	0.0	0.0	0.0
NIOH2	3.48143E-13	0.0	0.0	0.0
NISO4	1.01502E-24	0.0	0.0	0.0
OXALAC	0.0	0.0	0.0	0.0
OHION	0.418907	0.0	0.0	0.0
ALEDTAION	5.08724E-26	0.0	0.0	0.0
ALF2ION	4.26418E-30	0.0	0.0	0.0

ALF4ION	5.96762E-28	0.0	0.0	0.0
ALF5ION	1.27524E-27	0.0	0.0	0.0
ALF6ION	2.59483E-27	0.0	0.0	0.0
ALOH2ION	4.88977E-19	0.0	0.0	0.0
ALOH4ION	0.612438	0.0	0.0	0.0
ALOHCLION	7.28767E-28	0.0	0.0	0.0
ALOHION	9.82142E-29	0.0	0.0	0.0
CAACETION	2.73126E-11	0.0	0.0	0.0
CACLION	8.30515E-08	0.0	0.0	0.0
CACOOHION	2.63610E-10	0.0	0.0	0.0
CACTRTION	7.69905E-12	0.0	0.0	0.0
CAEDTAION	0.00119822	0.0	0.0	0.0
CAFION	3.48208E-14	0.0	0.0	0.0
CAGLYCOLION	6.11204E-11	0.0	0.0	0.0
CAH2PO4ION	4.78432E-26	0.0	0.0	0.0
CAHC2O4ION	4.27781E-24	0.0	0.0	0.0
CAHCO3ION	1.99856E-15	0.0	0.0	0.0
CAHEDTAION	1.74214E-16	0.0	0.0	0.0
CAION	4.06815E-10	0.0	0.0	0.0
CANO3ION	2.36172E-10	0.0	0.0	0.0
CANTA2ION	6.01531E-07	0.0	0.0	0.0
CANTAION	9.43480E-09	0.0	0.0	0.0
CAOHION	5.33464E-09	0.0	0.0	0.0
CAPO4ION	2.27592E-09	0.0	0.0	0.0
CITRATION	6.97759E-06	0.0	0.0	0.0
CLION	0.144217	0.0	0.0	0.0
CO3ION	0.42219	0.0	0.0	0.0
COOHION	0.0148746	0.0	0.0	0.0
CR2O7ION	1.00604E-20	0.0	0.0	0.0
CRO4ION	0.00951823	0.0	0.0	0.0
EDTAION	6.11069E-04	0.0	0.0	0.0
FION	0.00307536	0.0	0.0	0.0
GLYCOLATION	0.00430648	0.0	0.0	0.0
H2CITRATION	7.12444E-27	0.0	0.0	0.0
H2EDTAION	2.33602E-18	0.0	0.0	0.0
H2NTAION	1.64202E-24	0.0	0.0	0.0
H2PO4ION	4.84781E-17	0.0	0.0	0.0
H3EDTAION	0.0	0.0	0.0	0.0
HCITRATION	2.12900E-14	0.0	0.0	0.0
HCO3ION	5.94919E-07	0.0	0.0	0.0
HCRO4ION	4.98013E-13	0.0	0.0	0.0
HEDTAION	2.55126E-10	0.0	0.0	0.0
HF2ION	1.65999E-18	0.0	0.0	0.0
HION	8.77475E-17	0.0	0.0	0.0
HNTAION	3.37353E-10	0.0	0.0	0.0
HOXALATION	1.25247E-16	0.0	0.0	0.0
HP2O7ION	7.70823E-26	0.0	0.0	0.0
HPO4ION	2.95167E-07	0.0	0.0	0.0
HSO4ION	1.01909E-17	0.0	0.0	0.0
K1EDTAION	6.88097E-04	0.0	0.0	0.0
KCTRTION	1.11171E-05	0.0	0.0	0.0
KGLYCOL2ION	5.43939E-06	0.0	0.0	0.0
KION	0.0513738	0.0	0.0	0.0
KSO4ION	4.48262E-04	0.0	0.0	0.0
NA2FION	0.00256533	0.0	0.0	0.0
NACO3ION	0.0212943	0.0	0.0	0.0

NACTRTION	0.00249242	0.0	0.0	0.0
NAEDTAION	0.0084847	0.0	0.0	0.0
NAION	5.25198	0.0	0.0	0.0
NANTAION	0.0146142	0.0	0.0	0.0
NASO4ION	0.0211846	0.0	0.0	0.0
NH2CO2ION	6.22535E-16	0.0	0.0	0.0
NH4ION	4.96480E-15	0.0	0.0	0.0
NH4SO4ION	2.24484E-16	0.0	0.0	0.0
NIACET3ION	1.71382E-24	0.0	0.0	0.0
NIACETION	4.55499E-23	0.0	0.0	0.0
NIC2O42ION	2.69644E-22	0.0	0.0	0.0
NICLION	3.55382E-24	0.0	0.0	0.0
NICOOHION	3.77704E-22	0.0	0.0	0.0
NICTRTION	2.88044E-22	0.0	0.0	0.0
NIEDTAION	5.39976E-08	0.0	0.0	0.0
NIFION	9.46000E-25	0.0	0.0	0.0
NIGLYCOLION	1.29678E-22	0.0	0.0	0.0
NIHEDTAION	8.17077E-21	0.0	0.0	0.0
NIION	1.52034E-21	0.0	0.0	0.0
NINH3ION	8.59296E-28	0.0	0.0	0.0
NINO3ION	1.38928E-22	0.0	0.0	0.0
NINTA2ION	1.10690E-11	0.0	0.0	0.0
NINTAION	6.36367E-16	0.0	0.0	0.0
NIOH3ION	4.49780E-08	0.0	0.0	0.0
NIOHEDTAION	7.69860E-04	0.0	0.0	0.0
NIOHION	3.39802E-18	0.0	0.0	0.0
NO2ION	1.36902	0.0	0.0	0.0
NO3ION	1.60233	0.0	0.0	0.0
NTAION	1.27800E-05	0.0	0.0	0.0
ACETATEION	0.00704745	0.0	0.0	0.0
OXALATION	0.00114433	0.0	0.0	0.0
P2O7ION	2.47071E-17	0.0	0.0	0.0
PO4ION	0.0408184	0.0	0.0	0.0
SO4ION	0.014819	0.0	0.0	0.0
NA2C2O4	0.0	0.009046015	0.0	0.0
NA2CO3.1H2O	0.0	0.02323374	0.0	0.0
NAFPO4.19H2O	0.0	0.003272546	0.0	0.0
=====				
Total g/hr	815.73	6.42384	0.0	0.0
Volume, L/hr	0.580412	0.00252127	0.0	0.0
Enthalpy, cal/hr	-2.33453E+06	-18644.2	0.0	0.0
Density, g/L	1405.43	2547.86		
Vapor fraction	0.0	0.0	0.0	0.0
Solid fraction	0.0	1.	0.0	0.0
Organic fraction	0.0	0.0	0.0	0.0
Osmotic Pres, atm	527.12			
Redox Pot, volts	0.0			
E-Con, 1/ohm-cm	0.192035			
E-Con, cm2/ohm-mol	12.1044			
Abs Visc, cP	6.91433			
Rel Visc	6.56659			
Ionic Strength	14.6015			

STREAM: Concentrate_10 (45% WVR)
 TO : Still_11
 FROM : Concentrate_10 Storage

Phases----->	Aqueous	Solid	Vapor	Organic
Temperature, C	18.	18.	18.	18.
Pressure, atm	1.	1.	1.	1.
pH	15.3256			
Total mol/hr	30.64035	0.11958	0.0	0.0
-----	mol/hr-----	mol/hr-----	mol/hr-----	mol/hr--
H2O	20.7128	0.0	0.0	0.0
ACETACID	5.52453E-14	0.0	0.0	0.0
CO2	2.83658E-17	0.0	0.0	0.0
HCL	9.35652E-24	0.0	0.0	0.0
HCOOH	1.65540E-14	0.0	0.0	0.0
HF	8.14151E-17	0.0	0.0	0.0
HNO2	1.08322E-13	0.0	0.0	0.0
HNO3	2.36553E-22	0.0	0.0	0.0
NH3	1.11796E-11	0.0	0.0	0.0
CAHCTRT	6.78523E-24	0.0	0.0	0.0
CAHPO4	1.56370E-17	0.0	0.0	0.0
CASO4	3.38021E-13	0.0	0.0	0.0
ALF3	2.54897E-29	0.0	0.0	0.0
GLYCOLACID	4.92439E-15	0.0	0.0	0.0
ALOH3	2.96215E-10	0.0	0.0	0.0
H3PO4	0.0	0.0	0.0	0.0
CAACET2	9.82128E-13	0.0	0.0	0.0
CAC2O4	3.82673E-13	0.0	0.0	0.0
CACL2	0.0	0.0	0.0	0.0
CACO3	2.94164E-10	0.0	0.0	0.0
CACOOH2	1.29167E-11	0.0	0.0	0.0
KACET	5.74708E-05	0.0	0.0	0.0
KCL	2.08337E-05	0.0	0.0	0.0
KCOOH	3.37173E-04	0.0	0.0	0.0
KGLYCOLAT	4.63801E-05	0.0	0.0	0.0
KHSO4	2.85836E-21	0.0	0.0	0.0
NAACET	0.011974	0.0	0.0	0.0
NACOOH	0.0506849	0.0	0.0	0.0
NAF	0.00289082	0.0	0.0	0.0
NAGLYCOLAT	0.00697372	0.0	0.0	0.0
NAHCO3	2.29675E-07	0.0	0.0	0.0
NANO3	0.0446128	0.0	0.0	0.0
CAGLYCOL2	9.40292E-13	0.0	0.0	0.0
NH4ACET	7.12710E-19	0.0	0.0	0.0
NH4NO3	9.29246E-17	0.0	0.0	0.0
NIACET2	7.64452E-25	0.0	0.0	0.0
NIC2O4	4.70445E-21	0.0	0.0	0.0
NICOOH2	4.10837E-23	0.0	0.0	0.0
NIGLYCOL2	6.44663E-24	0.0	0.0	0.0
NIOH2	2.80199E-13	0.0	0.0	0.0
NISO4	7.02327E-25	0.0	0.0	0.0
OXALAC	0.0	0.0	0.0	0.0
OHION	0.418907	0.0	0.0	0.0
ALEDTAION	4.08879E-26	0.0	0.0	0.0
ALF2ION	3.47856E-30	0.0	0.0	0.0

ALF4ION	6.42511E-28	0.0	0.0	0.0
ALF5ION	1.58009E-27	0.0	0.0	0.0
ALF6ION	3.73367E-27	0.0	0.0	0.0
ALOH2ION	3.65010E-19	0.0	0.0	0.0
ALOH4ION	0.612438	0.0	0.0	0.0
ALOHCLION	6.09706E-28	0.0	0.0	0.0
ALOHION	5.23960E-29	0.0	0.0	0.0
CAACETION	2.38532E-11	0.0	0.0	0.0
CACLION	3.09098E-07	0.0	0.0	0.0
CACOOHION	2.29017E-10	0.0	0.0	0.0
CACTRTION	6.10680E-12	0.0	0.0	0.0
CAEDTAION	0.00119809	0.0	0.0	0.0
CAFION	3.11397E-14	0.0	0.0	0.0
CAGLYCOLION	5.36236E-11	0.0	0.0	0.0
CAH2PO4ION	2.88369E-26	0.0	0.0	0.0
CAHC2O4ION	2.57248E-24	0.0	0.0	0.0
CAHCO3ION	1.35212E-15	0.0	0.0	0.0
CAHEDTAION	1.50164E-16	0.0	0.0	0.0
CAION	2.91828E-10	0.0	0.0	0.0
CANO3ION	1.92622E-10	0.0	0.0	0.0
CANTA2ION	5.08696E-07	0.0	0.0	0.0
CANTAION	7.47965E-09	0.0	0.0	0.0
CAOHION	4.30483E-09	0.0	0.0	0.0
CAPO4ION	1.82231E-09	0.0	0.0	0.0
CITRATION	5.16678E-06	0.0	0.0	0.0
CLION	0.144215	0.0	0.0	0.0
CO3ION	0.353787	0.0	0.0	0.0
COOHION	0.0139944	0.0	0.0	0.0
CR2O7ION	9.30443E-21	0.0	0.0	0.0
CRO4ION	0.00951823	0.0	0.0	0.0
EDTAION	5.27907E-04	0.0	0.0	0.0
FION	0.00312005	0.0	0.0	0.0
GLYCOLATION	0.00411575	0.0	0.0	0.0
H2CITRATION	4.65535E-27	0.0	0.0	0.0
H2EDTAION	2.07505E-18	0.0	0.0	0.0
H2NTAION	1.07358E-24	0.0	0.0	0.0
H2PO4ION	3.41599E-17	0.0	0.0	0.0
H3EDTAION	0.0	0.0	0.0	0.0
HCITRATION	1.74029E-14	0.0	0.0	0.0
HCO3ION	4.49600E-07	0.0	0.0	0.0
HCRO4ION	4.18862E-13	0.0	0.0	0.0
HEDTAION	2.05294E-10	0.0	0.0	0.0
HF2ION	1.60435E-18	0.0	0.0	0.0
HION	6.46628E-17	0.0	0.0	0.0
HNTAION	2.75593E-10	0.0	0.0	0.0
HOXALATION	8.20431E-17	0.0	0.0	0.0
HP2O7ION	3.99561E-26	0.0	0.0	0.0
HPO4ION	2.48909E-07	0.0	0.0	0.0
HSO4ION	8.06574E-18	0.0	0.0	0.0
K1EDTAION	8.64870E-04	0.0	0.0	0.0
KCTRTION	1.10273E-05	0.0	0.0	0.0
KGLYCOL2ION	6.61278E-06	0.0	0.0	0.0
KION	0.0511738	0.0	0.0	0.0
KSO4ION	4.63722E-04	0.0	0.0	0.0
NA2FION	0.00307809	0.0	0.0	0.0
NACO3ION	0.00518834	0.0	0.0	0.0

NACTRTION	0.00249433	0.0	0.0	0.0
NAEDTAION	0.00839122	0.0	0.0	0.0
NAION	5.10248	0.0	0.0	0.0
NANTAION	0.0146177	0.0	0.0	0.0
NASO4ION	0.0211075	0.0	0.0	0.0
NH2CO2ION	2.92137E-17	0.0	0.0	0.0
NH4ION	2.68758E-16	0.0	0.0	0.0
NH4SO4ION	2.03094E-17	0.0	0.0	0.0
NIACET3ION	1.63929E-24	0.0	0.0	0.0
NIACETION	3.51029E-23	0.0	0.0	0.0
NIC2O42ION	1.46401E-22	0.0	0.0	0.0
NICLION	2.86878E-24	0.0	0.0	0.0
NICOOHION	2.89554E-22	0.0	0.0	0.0
NICTRTION	2.01608E-22	0.0	0.0	0.0
NIEDTAION	4.76431E-08	0.0	0.0	0.0
NIFION	7.46516E-25	0.0	0.0	0.0
NIGLYCOLION	1.00394E-22	0.0	0.0	0.0
NIHEDTAION	6.21469E-21	0.0	0.0	0.0
NIION	1.03477E-21	0.0	0.0	0.0
NINH3ION	3.92149E-29	0.0	0.0	0.0
NINO3ION	9.99836E-23	0.0	0.0	0.0
NINTA2ION	8.26004E-12	0.0	0.0	0.0
NINTAION	4.45173E-16	0.0	0.0	0.0
NIOH3ION	4.29445E-08	0.0	0.0	0.0
NIOHEDTAION	7.69868E-04	0.0	0.0	0.0
NIOHION	2.50218E-18	0.0	0.0	0.0
NO2ION	1.36902	0.0	0.0	0.0
NO3ION	1.60366	0.0	0.0	0.0
NTAION	9.49437E-06	0.0	0.0	0.0
ACETATEION	0.00677769	0.0	0.0	0.0
OXALATION	9.37714E-04	0.0	0.0	0.0
P2O7ION	1.37695E-17	0.0	0.0	0.0
PO4ION	0.0421956	0.0	0.0	0.0
SO4ION	0.0148807	0.0	0.0	0.0
NA2C2O4	0.0	0.009252652	0.0	0.0
NA2CO3.1H2O	0.0	0.1077434	0.0	0.0
NAFPO4.19H2O	0.0	0.002583979	0.0	0.0
=====				
Total g/hr	774.166	16.4407	0.0	0.0
Volume, L/hr	0.548221	0.00704203	0.0	0.0
Enthalpy, cal/hr	-2.18711E+06	-46113.4	0.0	0.0
Density, g/L	1412.14	2334.65		
Vapor fraction	0.0	0.0	0.0	0.0
Solid fraction	0.0	1.	0.0	0.0
Organic fraction	0.0	0.0	0.0	0.0
Osmotic Pres, atm	566.095			
Redox Pot, volts	0.0			
E-Con, 1/ohm-cm	0.193966			
E-Con, cm2/ohm-mol	11.5983			
Abs Visc, cP	7.05423			
Rel Visc	6.69945			
Ionic Strength	15.3132			

STREAM: Concentrate_11 (47% WVR)
 TO : Still_12
 FROM : Concentrate_11 Storage

Phases----->	Aqueous	Solid	Vapor	Organic
Temperature, C	18.	18.	18.	18.
Pressure, atm	1.	1.	1.	1.
pH	15.388			
Total mol/hr	29.28728	0.177328	0.0	0.0
-----	mol/hr-----	mol/hr-----	mol/hr-----	mol/hr--
H2O	19.5126	0.0	0.0	0.0
ACETACID	4.62290E-14	0.0	0.0	0.0
CO2	1.81228E-17	0.0	0.0	0.0
HCL	8.09411E-24	0.0	0.0	0.0
HCOOH	1.38111E-14	0.0	0.0	0.0
HF	6.47417E-17	0.0	0.0	0.0
HNO2	8.86668E-14	0.0	0.0	0.0
HNO3	1.90595E-22	0.0	0.0	0.0
NH3	6.03443E-12	0.0	0.0	0.0
CAHCTRT	4.68251E-24	0.0	0.0	0.0
CAHPO4	1.09219E-17	0.0	0.0	0.0
CASO4	2.81228E-13	0.0	0.0	0.0
ALF3	1.99206E-29	0.0	0.0	0.0
GLYCOLACID	4.13350E-15	0.0	0.0	0.0
ALOH3	2.41708E-10	0.0	0.0	0.0
H3PO4	0.0	0.0	0.0	0.0
CAACET2	9.16828E-13	0.0	0.0	0.0
CAC2O4	2.77569E-13	0.0	0.0	0.0
CACL2	0.0	0.0	0.0	0.0
CACO3	2.18620E-10	0.0	0.0	0.0
CACOOH2	1.19862E-11	0.0	0.0	0.0
KACET	5.82859E-05	0.0	0.0	0.0
KCL	2.18433E-05	0.0	0.0	0.0
KCOOH	3.40937E-04	0.0	0.0	0.0
KGLYCOLAT	4.71839E-05	0.0	0.0	0.0
KHSO4	2.41892E-21	0.0	0.0	0.0
NAACET	0.0121409	0.0	0.0	0.0
NACOOH	0.0512386	0.0	0.0	0.0
NAF	0.00301186	0.0	0.0	0.0
NAGLYCOLAT	0.00709291	0.0	0.0	0.0
NAHCO3	1.73581E-07	0.0	0.0	0.0
NANO3	0.0432137	0.01260351	0.0	0.0
CAGLYCOL2	8.83234E-13	0.0	0.0	0.0
NH4ACET	3.60177E-19	0.0	0.0	0.0
NH4NO3	4.53679E-17	0.0	0.0	0.0
NIACET2	6.22844E-25	0.0	0.0	0.0
NIC2O4	2.97826E-21	0.0	0.0	0.0
NICOOH2	3.32744E-23	0.0	0.0	0.0
NIGLYCOL2	5.28513E-24	0.0	0.0	0.0
NIOH2	2.48081E-13	0.0	0.0	0.0
NISO4	5.09992E-25	0.0	0.0	0.0
OXALAC	0.0	0.0	0.0	0.0
OHION	0.418907	0.0	0.0	0.0
ALEDTAION	2.88812E-26	0.0	0.0	0.0
ALF2ION	2.54301E-30	0.0	0.0	0.0

ALF4ION	5.89927E-28	0.0	0.0	0.0
ALF5ION	1.62801E-27	0.0	0.0	0.0
ALF6ION	4.34605E-27	0.0	0.0	0.0
ALOH2ION	2.67656E-19	0.0	0.0	0.0
ALOH4ION	0.612438	0.0	0.0	0.0
ALOHCLION	4.63011E-28	0.0	0.0	0.0
ALOHION	2.90584E-29	0.0	0.0	0.0
CAACETION	2.16273E-11	0.0	0.0	0.0
CACLION	7.57037E-07	0.0	0.0	0.0
CACOOHION	2.07029E-10	0.0	0.0	0.0
CACTRTION	5.14652E-12	0.0	0.0	0.0
CAEDTAION	0.0011977	0.0	0.0	0.0
CAFION	2.90109E-14	0.0	0.0	0.0
CAGLYCOLION	4.87720E-11	0.0	0.0	0.0
CAH2PO4ION	1.82437E-26	0.0	0.0	0.0
CAHC2O4ION	1.69687E-24	0.0	0.0	0.0
CAHCO3ION	9.76259E-16	0.0	0.0	0.0
CAHEDTAION	1.28696E-16	0.0	0.0	0.0
CAION	2.29309E-10	0.0	0.0	0.0
CANO3ION	1.64826E-10	0.0	0.0	0.0
CANTA2ION	4.49642E-07	0.0	0.0	0.0
CANTAION	6.30173E-09	0.0	0.0	0.0
CAOHION	3.85265E-09	0.0	0.0	0.0
CAPO4ION	1.55437E-09	0.0	0.0	0.0
CITRATION	4.12634E-06	0.0	0.0	0.0
CLION	0.144214	0.0	0.0	0.0
CO3ION	0.311846	0.0	0.0	0.0
COOHION	0.013437	0.0	0.0	0.0
CR2O7ION	8.03147E-21	0.0	0.0	0.0
CRO4ION	0.00951823	0.0	0.0	0.0
EDTAION	4.73751E-04	0.0	0.0	0.0
FION	0.00319729	0.0	0.0	0.0
GLYCOLATION	0.00399357	0.0	0.0	0.0
H2CITRATION	3.11678E-27	0.0	0.0	0.0
H2EDTAION	1.74233E-18	0.0	0.0	0.0
H2NTAION	7.19144E-25	0.0	0.0	0.0
H2PO4ION	2.43169E-17	0.0	0.0	0.0
HCITRATION	1.43690E-14	0.0	0.0	0.0
HCO3ION	3.52453E-07	0.0	0.0	0.0
HCRO4ION	3.52694E-13	0.0	0.0	0.0
HEDTAION	1.66731E-10	0.0	0.0	0.0
HF2ION	1.53412E-18	0.0	0.0	0.0
HION	4.94890E-17	0.0	0.0	0.0
HNTAION	2.27476E-10	0.0	0.0	0.0
HOXALATION	5.77332E-17	0.0	0.0	0.0
HP2O7ION	2.16974E-26	0.0	0.0	0.0
HPO4ION	2.11420E-07	0.0	0.0	0.0
HSO4ION	6.51026E-18	0.0	0.0	0.0
K1EDTAION	0.00102987	0.0	0.0	0.0
KCTRTION	1.10266E-05	0.0	0.0	0.0
KGLYCOL2ION	7.70945E-06	0.0	0.0	0.0
KION	0.0509861	0.0	0.0	0.0
KSO4ION	4.78849E-04	0.0	0.0	0.0
NA2FION	0.00355903	0.0	0.0	0.0
NACO3ION	0.00142982	0.0	0.0	0.0
NACTRTION	0.00249537	0.0	0.0	0.0

NAEDTAION	0.00828076	0.0	0.0	0.0
NAION	5.00619	0.0	0.0	0.0
NANTAION	0.0146197	0.0	0.0	0.0
NASO4ION	0.0212345	0.0	0.0	0.0
NH2CO2ION	1.30405E-17	0.0	0.0	0.0
NH4ION	1.32434E-16	0.0	0.0	0.0
NH4SO4ION	1.55863E-17	0.0	0.0	0.0
NIACET3ION	1.52709E-24	0.0	0.0	0.0
NIACETION	2.77784E-23	0.0	0.0	0.0
NIC2O42ION	8.99203E-23	0.0	0.0	0.0
NICLION	2.34131E-24	0.0	0.0	0.0
NICOOHION	2.28456E-22	0.0	0.0	0.0
NICTRTION	1.48292E-22	0.0	0.0	0.0
NIEDTAION	4.15690E-08	0.0	0.0	0.0
NIFION	6.07009E-25	0.0	0.0	0.0
NIGLYCOLION	7.96952E-23	0.0	0.0	0.0
NIHEDTAION	4.64864E-21	0.0	0.0	0.0
NIION	7.49732E-22	0.0	0.0	0.0
NINH3ION	1.70543E-29	0.0	0.0	0.0
NINO3ION	7.46715E-23	0.0	0.0	0.0
NINTA2ION	6.37236E-12	0.0	0.0	0.0
NINTAION	3.27353E-16	0.0	0.0	0.0
NIOH3ION	4.53173E-08	0.0	0.0	0.0
NIOHEDTAION	7.69872E-04	0.0	0.0	0.0
NIOHION	2.00346E-18	0.0	0.0	0.0
NO2ION	1.36902	0.0	0.0	0.0
NO3ION	1.59245	0.0	0.0	0.0
NTAION	7.60149E-06	0.0	0.0	0.0
ACETATEION	0.00660993	0.0	0.0	0.0
OXALATION	8.13777E-04	0.0	0.0	0.0
P2O7ION	8.27000E-18	0.0	0.0	0.0
PO4ION	0.0435541	0.0	0.0	0.0
SO4ION	0.0147386	0.0	0.0	0.0
NA2C2O4	0.0	0.00937657	0.0	0.0
NA2CO3.1H2O	0.0	0.1534432	0.0	0.0
NAFPO4.19H2O	0.0	0.001904752	0.0	0.0
=====				
Total g/hr	746.863	22.7118	0.0	0.0
Volume, L/hr	0.526818	0.00989581	0.0	0.0
Enthalpy, cal/hr	-2.09171E+06	-61627.4	0.0	0.0
Density, g/L	1417.69	2295.09		
Vapor fraction	0.0	0.0	0.0	0.0
Solid fraction	0.0	1.	0.0	0.0
Organic fraction	0.0	0.0	0.0	0.0
Osmotic Pres, atm	595.366			
Redox Pot, volts	0.0			
E-Con, 1/ohm-cm	0.195094			
E-Con, cm2/ohm-mol	11.3257			
Abs Visc, cP	7.30416			
Rel Visc	6.93681			
Ionic Strength	15.8731			

STREAM: Concentrate_12 (50% WVR)
 TO :
 FROM : Concentrate_12 Storage

Phases----->	Aqueous	Solid	Vapor	Organic
Temperature, C	18.	18.	18.	18.
Pressure, atm	1.	1.	1.	1.
pH	15.4562			
Total mol/hr	27.08708	0.441262	0.0	0.0
-----	mol/hr-----	mol/hr-----	mol/hr-----	mol/hr---
H2O	17.8909	0.0	0.0	0.0
ACETACID	3.78052E-14	0.0	0.0	0.0
CO2	1.08503E-17	0.0	0.0	0.0
HCL	6.83920E-24	0.0	0.0	0.0
HCOOH	1.12420E-14	0.0	0.0	0.0
HF	5.21947E-17	0.0	0.0	0.0
HNO2	7.24682E-14	0.0	0.0	0.0
HNO3	1.35569E-22	0.0	0.0	0.0
NH3	2.82022E-13	0.0	0.0	0.0
CAHCTRT	3.50263E-24	0.0	0.0	0.0
CAHPO4	8.19480E-18	0.0	0.0	0.0
CASO4	2.61058E-13	0.0	0.0	0.0
ALF3	1.07323E-29	0.0	0.0	0.0
GLYCOLACID	3.38534E-15	0.0	0.0	0.0
ALOH3	1.99067E-10	0.0	0.0	0.0
H3PO4	0.0	0.0	0.0	0.0
CAACET2	9.31223E-13	0.0	0.0	0.0
CAC2O4	2.11653E-13	0.0	0.0	0.0
CACL2	0.0	0.0	0.0	0.0
CACO3	1.70684E-10	0.0	0.0	0.0
CACOOH2	1.20615E-11	0.0	0.0	0.0
KACET	6.34272E-05	0.0	0.0	0.0
KCL	2.45600E-05	0.0	0.0	0.0
KCOOH	3.69286E-04	0.0	0.0	0.0
KGLYCOLAT	5.14224E-05	0.0	0.0	0.0
KHSO4	2.23888E-21	0.0	0.0	0.0
NAACET	0.0123129	0.0	0.0	0.0
NACOOH	0.0517231	0.0	0.0	0.0
NAF	0.00278276	0.0	0.0	0.0
NAGLYCOLAT	0.00720413	0.0	0.0	0.0
NAHCO3	1.25931E-07	0.0	0.0	0.0
NANO3	0.0383731	0.2254601	0.0	0.0
CAGLYCOL2	8.99776E-13	0.0	0.0	0.0
NH4ACET	1.56656E-20	0.0	0.0	0.0
NH4NO3	1.70971E-18	0.0	0.0	0.0
NIACET2	5.49098E-25	0.0	0.0	0.0
NIC2O4	1.97115E-21	0.0	0.0	0.0
NICOOH2	2.90625E-23	0.0	0.0	0.0
NIGLYCOL2	4.67325E-24	0.0	0.0	0.0
NIOH2	2.40881E-13	0.0	0.0	0.0
NISO4	4.10909E-25	0.0	0.0	0.0
OXALAC	0.0	0.0	0.0	0.0
OHION	0.418906	0.0	0.0	0.0
ALEDTAION	1.85058E-26	0.0	0.0	0.0
ALF2ION	1.40125E-30	0.0	0.0	0.0

ALF4ION	3.29500E-28	0.0	0.0	0.0
ALF5ION	9.06620E-28	0.0	0.0	0.0
ALF6ION	2.42148E-27	0.0	0.0	0.0
ALOH2ION	2.00828E-19	0.0	0.0	0.0
ALOH4ION	0.612438	0.0	0.0	0.0
ALOHCLION	3.43445E-28	0.0	0.0	0.0
ALOHION	1.87623E-29	0.0	0.0	0.0
CAACETION	2.08319E-11	0.0	0.0	0.0
CACLION	1.22293E-06	0.0	0.0	0.0
CACOOHION	1.98474E-10	0.0	0.0	0.0
CACTRTION	4.70740E-12	0.0	0.0	0.0
CAEDTAION	0.00119726	0.0	0.0	0.0
CAFION	2.54616E-14	0.0	0.0	0.0
CAGLYCOLION	4.70509E-11	0.0	0.0	0.0
CAH2PO4ION	1.20448E-26	0.0	0.0	0.0
CAHC2O4ION	1.14209E-24	0.0	0.0	0.0
CAHCO3ION	6.95864E-16	0.0	0.0	0.0
CAHEDTAION	1.09397E-16	0.0	0.0	0.0
CAION	1.93710E-10	0.0	0.0	0.0
CANO3ION	1.41778E-10	0.0	0.0	0.0
CANTA2ION	4.31215E-07	0.0	0.0	0.0
CANTAION	5.76492E-09	0.0	0.0	0.0
CAOHION	3.82315E-09	0.0	0.0	0.0
CAPO4ION	1.42608E-09	0.0	0.0	0.0
CITRATION	3.50846E-06	0.0	0.0	0.0
CLION	0.14421	0.0	0.0	0.0
CO3ION	0.262401	0.0	0.0	0.0
COOHION	0.0129241	0.0	0.0	0.0
CR2O7ION	6.73431E-21	0.0	0.0	0.0
CRO4ION	0.00951823	0.0	0.0	0.0
EDTAION	4.26659E-04	0.0	0.0	0.0
FION	0.0028701	0.0	0.0	0.0
GLYCOLATION	0.00387441	0.0	0.0	0.0
H2CITRATION	2.06937E-27	0.0	0.0	0.0
H2EDTAION	1.30575E-18	0.0	0.0	0.0
H2NTAION	4.78202E-25	0.0	0.0	0.0
H2PO4ION	1.66759E-17	0.0	0.0	0.0
HCITRATION	1.15873E-14	0.0	0.0	0.0
HCO3ION	2.56856E-07	0.0	0.0	0.0
HCRO4ION	2.96628E-13	0.0	0.0	0.0
HEDTAION	1.31748E-10	0.0	0.0	0.0
HF2ION	1.14789E-18	0.0	0.0	0.0
HION	3.64490E-17	0.0	0.0	0.0
HNTAION	1.83441E-10	0.0	0.0	0.0
HOXALATION	3.90746E-17	0.0	0.0	0.0
HP2O7ION	1.21161E-26	0.0	0.0	0.0
HPO4ION	1.72646E-07	0.0	0.0	0.0
HSO4ION	5.36404E-18	0.0	0.0	0.0
K1EDTAION	0.00120568	0.0	0.0	0.0
KCTRTION	1.18276E-05	0.0	0.0	0.0
KGLYCOL2ION	9.56235E-06	0.0	0.0	0.0
KION	0.0507049	0.0	0.0	0.0
KSO4ION	5.41202E-04	0.0	0.0	0.0
NA2FION	0.00364357	0.0	0.0	0.0
NACO3ION	4.14493E-04	0.0	0.0	0.0
NACTRTION	0.00249518	0.0	0.0	0.0

NAEDTAION	0.0081525	0.0	0.0	0.0
NAION	4.69284	0.0	0.0	0.0
NANTAION	0.0146209	0.0	0.0	0.0
NASO4ION	0.0224987	0.0	0.0	0.0
NH2CO2ION	4.92537E-19	0.0	0.0	0.0
NH4ION	5.38077E-18	0.0	0.0	0.0
NH4SO4ION	8.87455E-19	0.0	0.0	0.0
NIACET3ION	1.53204E-24	0.0	0.0	0.0
NIACETION	2.32241E-23	0.0	0.0	0.0
NIC2O42ION	5.56440E-23	0.0	0.0	0.0
NICLION	2.01432E-24	0.0	0.0	0.0
NICOOHION	1.90098E-22	0.0	0.0	0.0
NICTRTION	1.17731E-22	0.0	0.0	0.0
NIEDTAION	3.60672E-08	0.0	0.0	0.0
NIFION	4.62407E-25	0.0	0.0	0.0
NIGLYCOLION	6.67320E-23	0.0	0.0	0.0
NIHEDTAION	3.42983E-21	0.0	0.0	0.0
NIION	5.90071E-22	0.0	0.0	0.0
NINH3ION	0.0	0.0	0.0	0.0
NINO3ION	5.57506E-23	0.0	0.0	0.0
NINTA2ION	5.30435E-12	0.0	0.0	0.0
NINTAION	2.59929E-16	0.0	0.0	0.0
NIOH3ION	5.25504E-08	0.0	0.0	0.0
NIOHEDTAION	7.69870E-04	0.0	0.0	0.0
NIOHION	1.79794E-18	0.0	0.0	0.0
NO2ION	1.36902	0.0	0.0	0.0
NO3ION	1.38444	0.0	0.0	0.0
NTAION	6.49438E-06	0.0	0.0	0.0
ACETATEION	0.00643276	0.0	0.0	0.0
OXALATION	6.68958E-04	0.0	0.0	0.0
P2O7ION	5.27055E-18	0.0	0.0	0.0
PO4ION	0.0426106	0.0	0.0	0.0
SO4ION	0.0134121	0.0	0.0	0.0
NA2C2O4	0.0	0.009521383	0.0	0.0
NA2CO3.1H2O	0.0	0.2039041	0.0	0.0
NAFPO4.19H2O	0.0	0.002376501	0.0	0.0
=====				
Total g/hr	694.014	47.4163	0.0	0.0
Volume, L/hr	0.487809	0.0208034	0.0	0.0
Enthalpy, cal/hr	-1.94339E+06	-1.03559E+05	0.0	0.0
Density, g/L	1422.72	2279.26		
Vapor fraction	0.0	0.0	0.0	0.0
Solid fraction	0.0	1.	0.0	0.0
Organic fraction	0.0	0.0	0.0	0.0
Osmotic Pres, atm	625.976			
Redox Pot, volts	0.0			
E-Con, 1/ohm-cm	0.199117			
E-Con, cm2/ohm-mol	10.8404			
Abs Visc, cP	7.60853			
Rel Visc	7.22587			
Ionic Strength	16.1718			